

Role of Cell-specific Inducible Nitric Oxide Synthase in a Mouse Model of Chronic Intermittent Hypoxia

Inaugural Dissertation

Submitted to the

Faculty of Medicine

in partial fulfillment of the requirements for the

PhD-Degree

of the Faculties of Veterinary Medicine and Medicine

of the Justus Liebig University Giessen

by

Valadan, Mohsen

of

Shiraz, Iran

Giessen, 2021

From the Department of Internal Medicine II/V
Director / Chairman: Prof. Dr. Werner Seeger
of the Faculty of Medicine of the Justus Liebig University Giessen

First Supervisor and Committee Member: Prof. Dr. Norbert Weißmann

Second Supervisor and Committee Member: Prof. Dr. Christiane Herden

Committee Member: Prof. Dr. Martin Diener

Committee Member: Prof. Dr. Irene Lang

Date of Doctoral Defense: 04.08.2022

Declaration

I declare that I have completed this dissertation single-handedly without the unauthorized help of a second party and only with the assistance acknowledged therein. I have appropriately acknowledged and referenced all text passages that are derived literally from or are based on the content of published or unpublished work of others, and all information that relates to verbal communications. I have abided by the principles of good scientific conduct laid down in the charter of the Justus Liebig University of Giessen in carrying out the investigations described in the dissertation.

Mohsen Valadan

Giessen, Germany

I. Table of contents

1. Introduction	17
1.1. Pulmonary hypertension (PH)	17
1.1.1. Definition of PH.....	17
1.1.2. Importance of PH.....	17
1.1.3. Pulmonary vascular remodeling in PH	17
1.1.4. WHO classification of PH.....	18
1.1.5. Pathophysiology of different groups of PH	20
1.1.6. Diagnosis and treatment of PH	21
1.2. Systemic hypertension	22
1.2.1. Definition and importance	22
1.2.2. Classification of systemic hypertension.....	22
1.2.2.1. Classification based on etiology.....	22
1.2.2.2. Classification based on severity	22
1.2.3. Pathophysiology of systemic hypertension.....	23
1.2.3.1. Elevated total peripheral resistance	23
1.2.3.2. Left ventricular hypertrophy	23
1.2.3.3. Systolic and diastolic dysfunction	24
1.2.4. Treatment of systemic hypertension	24
1.3. Obstructive sleep apnea syndrome (OSAS)	24
1.3.1. Definition of sleep apnea	24
1.3.2. Forms of sleep apnea.....	24
1.3.3. Classification of the severity of OSAS	25
1.3.3.1. Correlation between ODI and AHI	25
1.3.4. Importance of sleep apnea.....	25
1.3.5. Risk factors of OSAS.....	26
1.3.6. Pathophysiology of OSAS	27
1.3.7. Pathogenesis of the OSAS	28
1.3.8. Signs and symptoms of OSAS	28
1.3.9. Importance of polysomnographic analysis as gold standard in diagnosis of OSAS.....	28
1.3.10. Treatment options for OSAS.....	28
1.3.10.1. Medications	29

1.3.10.2. Lifestyle changes.....	29
1.3.10.3. Oral appliances.....	29
1.3.10.4. CPAP.....	30
1.3.10.5. Surgical techniques.....	30
1.3.11. Medical conditions associated with OSAS.....	30
1.3.11.1. Associations between OSAS and PH.....	31
1.3.11.2. Associations and interactions between OSAS and systemic hypertension.....	32
1.4. Simulation of OSAS in animal models.....	32
1.4.1. Animal models with spontaneous OSA.....	33
1.4.2. Animal models with obstruction created by surgical or mechanical approaches.....	33
1.4.3. Sleep fragmentation animal models.....	33
1.4.4. Intermittent hypoxia animal models.....	33
1.4.5. Pulmonary and systemic hypertension in chronic intermittent hypoxia (CIH) animal model.....	33
1.5. Nitric oxide synthases (NOSs).....	34
1.5.1. Nitric oxide synthases and oxidative stress.....	35
1.5.2. Inducible nitric oxide synthase in cardiopulmonary diseases.....	35
1.5.3. Inducible nitric oxide synthase in OSA.....	35
1.5.4. iNOS knockout mice.....	36
1.6. Aim of the current study.....	36
2. Material and methods.....	37
2.1. Material.....	37
2.1.1. Medications and reagents.....	37
2.1.2. Devices, equipments, softwares.....	37
2.1.3. Consumables.....	39
2.1.4. Primers for genotyping.....	41
2.1.5. Materials, devices, consumables, softwares and macros for histology.....	41
2.1.6. Antibodies, reagents, solutions, and kits for immunohistochemistry staining.....	42
2.1.7. Animals.....	43
2.1.8. Regional council’s approvals for animal experiments.....	43
2.2. Methods.....	43
2.2.1. Bone marrow transplantation (BMT).....	44
2.2.2. Echocardiographic measurements.....	46

2.2.3. Telemetric blood pressure measurements	48
2.2.4. CIH protocol	49
2.2.5. Experimental animal groups	50
2.2.6. Measurement of hemodynamic parameters	50
2.2.7. Blood sample collection for measurement of hematocrit	52
2.2.8. Blood sample collection for superoxide anion measurement	52
2.2.9. Flushing and harvesting of the lung	52
2.2.10. Lung harvest for superoxide anion measurement	52
2.2.11. Preparation of lung samples for histology	52
2.2.12. Harvesting of the heart and assessment of heart ratios	53
2.2.13. Preparation of lung samples and histological assessment of the degree of muscularization of pulmonary arterial vessels	53
2.2.13.1. Embedding.....	53
2.2.13.2. Sectioning	53
2.2.13.3. Staining.....	54
2.2.13.4. Assessment of the degree of muscularization in pulmonary arterial vessels	56
2.2.14. Superoxide anion measurement by electron spin resonance (ESR) spectroscopy	57
2.2.15. Statistical evaluation	58
3. Results	60
3.1. Endpoint weight of chimeric mice after CIH exposure	60
3.2. Hematocrit level of chimeric mice after CIH exposure.....	62
3.3. Different heart ratios of chimeric mice after CIH exposure	64
3.3.1. Ratio of weight of right ventricle to left ventricle plus septum (Fulton index)	64
3.3.2. Ratio of right ventricle to tibia length	66
3.3.3. Ratio of left ventricle to tibia length	68
3.4. Final invasive hemodynamic measurements	70
3.4.1. Right ventricular systolic pressure (RVSP)	70
3.4.2. Left ventricular systolic pressure (LVSP).....	72
3.4.3. Mean arterial pressure (MAP).....	74
3.5. Telemetry blood pressure measurements.....	76
3.5.1. Mean arterial pressure measurements	76
3.5.1.1. Wild type mice with wild type bone marrow	76
3.5.1.2. Wild type mice with knock out bone marrow	78

3.5.1.3. Knock out mice with wild type bone marrow	80
3.5.1.4. Knock out mice with knock out bone marrow	82
3.5.2. Systolic blood pressure measurements	84
3.5.2.1. Wild type mice with wild type bone marrow	84
3.5.2.2. Wild type mice with knock out bone marrow	86
3.5.2.3. Knock out mice with wild type bone marrow	88
3.5.2.4. Knock out mice with knock out bone marrow	90
3.5.3. Diastolic blood pressure measurements	92
3.5.3.1. Wild type mice with wild type bone marrow	92
3.5.3.2. Wild type mice with knock out bone marrow	94
3.5.3.3. Knock out mice with wild type bone marrow	96
3.5.3.4. Knock out mice with knock out bone marrow	98
3.6. Histological assessment of the degree of muscularization in pulmonary vessels	100
3.7. Echocardiographic assessments.....	103
3.7.1. Left ventricular internal diameter at end-diastole (LVIDd).....	103
3.7.2. Left ventricular wall thickness at end-diastole (LVWTd)	105
3.7.3. Cardiac output and index	107
3.7.4. Left ventricular ejection fraction (LVEF).....	110
3.7.5. Right ventricular internal diameter at end-diastole (RVIDd)	112
3.7.6. Right ventricular wall thickness at end-diastole (RVWTd).....	114
3.7.7. Tricuspid annular plane systolic excursion (TAPSE).....	116
3.7.8. Pulmonary acceleration time/pulmonary ejection time (PAT/PET)	118
3.8. Superoxide anion measurement by electron spin resonance spectroscopy	120
3.8.1. Blood samples	120
3.8.2. Lung samples	122
4. Discussion	124
4.1. Mouse model	124
4.2. Bone marrow transplantation.....	124
4.2.1. Effect of irradiation, BMT, and bone marrow-derived stem cells on OSA	125
4.3. Simulation of OSAS with CIH exposure of chimeric mice.....	125
4.3.1. Limitations and criticisms of the CIH animal model	126
4.4. Final weight of chimeric mice following CIH exposure	126
4.5. Hematocrit level in chimeric mice after CIH exposure	126

4.6. Assessments of pulmonary hypertension and right ventricular hypertrophy in chimeric mice.....	127
4.7. Assessments of systemic hypertension and left ventricular hypertrophy in chimeric mice	128
4.8. Histological assessment of the degree of muscularization in pulmonary vessels of chimeric mice.....	129
4.9. Echocardiographic readouts in chimeric mice.....	129
4.10. Superoxide anion measurement by electron spin resonance spectroscopy	131
4.11. Conclusion	132
5. Summary	134
6. Zusammenfassung	136
7. References	138
8. Acknowledgments	157

II. List of tables

Table 1	WHO clinical classification of PH
Table 2	Classification of clinical blood pressure level in adults
Table 3	Classification of sleep apnea syndrome according to ICD-10
Table 4	Risk factors of OSAS
Table 5	Conditions associated with OSAS in different medical fields

III. List of figures

Figure 1	Endpoint body weight of different chimeric mice in the CIH
Figure 2	Hematocrit of different chimeric mice in the CIH
Figure 3	Fulton index (RV/(LV+S)) of different chimeric mice in the CIH
Figure 4	Ratio of weight of right ventricle to length of tibia of different chimeric mice in the CIH
Figure 5	Ratio of weight of left ventricle to length of tibia of different chimeric mice in the CIH
Figure 6	Right ventricular systolic pressure (RVSP) of different chimeric mice in the CIH
Figure 7	Left ventricular systolic pressure (LVSP) of different chimeric mice in the CIH
Figure 8	Mean arterial pressure (MAP) of different chimeric mice in the CIH
Figure 9	Mean arterial pressure (MAP) of WT(WT) mice in the CIH
Figure 10	Mean arterial pressure (MAP) of WT(KO) mice in the CIH
Figure 11	Mean arterial pressure (MAP) of KO(WT) mice in the CIH
Figure 12	Mean arterial pressure (MAP) of KO(KO) mice in the CIH
Figure 13	Systolic blood pressure (SBP) of WT(WT) mice in the CIH
Figure 14	Systolic blood pressure (SBP) of WT(KO) mice in the CIH
Figure 15	Systolic blood pressure (SBP) of KO(WT) mice in the CIH
Figure 16	Systolic blood pressure (SBP) of KO(KO) mice in the CIH
Figure 17	Diastolic blood pressure (DBP) of WT(WT) mice in the CIH
Figure 18	Diastolic blood pressure (DBP) of WT(KO) mice in the CIH
Figure 19	Diastolic blood pressure (DBP) of KO(WT) mice in the CIH
Figure 20	Diastolic blood pressure (DBP) of KO(KO) mice in the CIH
Figure 21	Quantification of vascular remodeling as degree of muscularization in small pulmonary arterial vessels (20-70 μm of diameter) of different chimeric mice in the CIH
Figure 22	Quantification of vascular remodeling as degree of muscularization in medium pulmonary arterial vessels (70-150 μm of diameter) of different chimeric mice in the CIH

Figure 23	Endpoint left ventricular internal diameter at end-diastole (LVIDd) of different chimeric mice in the CIH
Figure 24	Endpoint left ventricular wall thickness at end-diastole (LVWTd) of different chimeric mice in the CIH
Figure 25	Endpoint cardiac output (CO) of different chimeric mice in the CIH
Figure 26	Endpoint cardiac index (CI) of different chimeric mice in the CIH
Figure 27	Endpoint left ventricular ejection fraction (LVEF) of different chimeric mice in the CIH
Figure 28	Endpoint right ventricular internal diameter at end-diastole (RVIDd) of different chimeric mice in the CIH
Figure 29	Endpoint right ventricular wall thickness at end-diastole (RVWTd) of different chimeric mice in the CIH
Figure 30	Endpoint tricuspid annular plane systolic excursion (TAPSE) of different chimeric mice in the CIH
Figure 31	Endpoint pulmonary acceleration time/pulmonary ejection time (PAT/PET) of different chimeric mice in the CIH
Figure 32	Superoxide anion in blood samples of different chimeric mice in the CIH
Figure 33	Superoxide anion in lung homogenate samples of different chimeric mice in the CIH

IV. List of abbreviations

°C	Degree celsius
AHI	Apnea-hypopnea index
ApoE	Apolipoprotein E
ARDS	Acute respiratory distress syndrome
a.u.	Arbitrary unit
BH4	Tetrahydrobiopterin
BMT	Bone marrow transplantation
bp	Base pair
BSA	Bovine serum albumin
BW	Body weight
CI	Cardiac index
CIH	Chronic intermittent hypoxia
cm	Centimeter
CMH	1-hydroxy-3-methoxycarbonyl-2,2,5,5-tetramethyl-pyrrolidine
CNS	Central nervous system
CO	Cardiac output
Co	Cobalt
CO ₂	Carbon dioxide
COPD	Chronic obstructive pulmonary disease
CPAP	Continuous positive airway pressure
CTEPH	Chronic thromboembolic pulmonary hypertension
DBP	Diastolic blood pressure
DNA	Deoxyribonucleic acid
ECG	Electrocardiography
ECMO	Extracorporeal membrane oxygenation
EDS	Excessive daytime sleepiness
EDTA	Ethylenediaminetetraacetic acid
EDV	End-diastolic volume

EEG	Electroencephalography
EF	Ejection fraction
EMG	Electromyography
eNOS	Endothelial nitric oxide synthase
ESR	Electron spin resonance
ESV	End-systolic volume
FAD	Flavin adenine dinucleotide
FCS	Fetal calf serum
Fig.	Figure
FMN	Flavin mononucleotide
FTBI	Fractionated total body irradiation
g	Gram
<i>g</i>	g-force unit
G	Gauge
GERD	Gastroesophageal reflux disease
H ₂ O ₂	Hydrogen peroxide
HCl	Hydrogen chloride
Hox	Hypoxia
HPV	Hypoxic pulmonary vasoconstriction
HR	Heart rate
HRP	Horseradish peroxidase
i.p.	Intraperitoneal
ICD	International classification of diseases
IH	Intermittent hypoxia
iNOS	Inducible nitric oxide synthase
IPAH	Idiopathic pulmonary arterial hypertension
IU	International unit
IVC	Individually ventilated cage
KCl	Potassium chloride
kg	Kilogram

KH ₂ PO ₄	Monopotassium phosphate
KO	Knockout
KO(KO)	Knock out mice transplanted with knock out bone marrow
KO(WT)	Knock out mice transplanted with wild type bone marrow
l	Liter
LV	Left ventricle
LVID	Left ventricular internal diameter
LVIDd	Left ventricular internal diameter at end-diastole
LVOT	Left ventricular outflow tract
LVSP	Left ventricular systolic pressure
LVWT	Left ventricular wall thickness
LVWTd	Left ventricular wall thickness at end-diastole
m	Meter
M	Molar
MAA	Mandibular advancement appliance
MAD	Mandibular advancement device
MAP	Mean arterial pressure
MAS	Mandibular advancement splint
MCP-1	Monocyte chemoattractant protein-1
mg	Milligram
min	Minute
ml	Milliliter
mM	Millimolar
mm	Millimeter
MMA	Maxillomandibular advancement
mmHg	Millimeter of mercury
mPAP	Mean pulmonary artery pressure
n	Quantity number
Na ₂ HPO ₄ x 2 H ₂ O	Sodium phosphate dibasic dihydrate
NaCl	Sodium chloride

NADPH	Nicotinamide adenine dinucleotide phosphate hydrogen
NF- κ B	Nuclear factor kappa-light-chain-enhancer of activated B cells
nm	Nanometer
nNOS	Neuronal nitric oxide synthase
NO	Nitric oxide
no.	Number
NOS	Nitric oxide synthase
NOS2	Nitric oxide synthase 2
NOX	Normoxia
O ₂	Oxygen
O ₂ ⁻	Superoxide anion
ODI	Oxygen desaturation index
ONOO ⁻	Peroxynitrite
OSA	Obstructive sleep apnea
OSAS	Obstructive sleep apnea syndrome
P	P-value
PAH	Pulmonary arterial hypertension
PAP	Pulmonary artery pressure
PAT/PET	Pulmonary acceleration time/pulmonary ejection time
PBS	Phosphate buffered saline
PC	Personal computer
pCO ₂	Carbon dioxide partial pressure
PCR	Polymerase chain reaction
PH	Pulmonary hypertension
pO ₂	Oxygen partial pressure
pSOD	Polyethylen-glycol conjugated superoxide dismutase
PVR	Pulmonary vascular resistance
PWV	Pulse wave velocity
RHC	Right heart catheterization
RHF	Right heart failure

ROS	Reactive oxygen species
RV	Right ventricle
RVID	Right ventricular internal diameter
RVIDd	Right ventricular internal diameter at end-diastole
RVSP	Right ventricular systolic pressure
RVWT	Right ventricular wall thickness
RVWTd	Right ventricular wall thickness at end-diastole
S	Septum
s.c.	Subcutaneous
SBP	Systolic blood pressure
SEM	Standard error of the mean
SF	Sleep fragmentation
SMC	Smooth muscle cell
SOD	Superoxide dismutase
STAT	Signal transducer and activator of transcription
SV	Stroke volume
TAC	Transverse aortic constriction
TAPSE	Tricuspid annular plane systolic excursion
TNF- α	Tumor necrosis factor-alpha
UPPP	Uvulopalatopharyngoplasty
vs.	Versus
VTI	Velocity time integral
WHO	World Health Organization
WT	Wild type
WT(KO)	Wild type mice transplanted with knock out bone marrow
WT(WT)	Wild type mice transplanted with wild type bone marrow
μ g	Microgram
μ l	Microliter
μ m	Micrometer
μ M	Micromolar

1. Introduction

1.1. Pulmonary hypertension (PH)

1.1.1. Definition of PH

PH is defined as mean pulmonary artery pressure (mPAP) of ≥ 20 mmHg during rest (Simonneau et al., 2019). For diagnosis of PH, the right heart catheterization (RHC) is performed to measure mPAP. However, this invasive procedure must be standardized in order to avoid mismeasurement (Rosenkranz and Preston, 2015).

1.1.2. Importance of PH

PH may cause hypertrophy and/or dilatation of the right heart (cor pulmonale) due to the increased right ventricular afterload. Eventually, PH can lead to right heart failure (RHF) (Weitzenblum and Chaouat, 2009). Moreover, PH is considered a prevalent disease as well, and it is speculated that around 1% of the global population are affected by PH. The prevalence of PH is supposed to be around 10% in the population who are older than 65 years (Hoeper et al., 2016).

1.1.3. Pulmonary vascular remodeling in PH

The depiction of PH is complex and includes vascular remodeling, vasoconstriction, and thrombosis in the pulmonary vessels (Humbert et al., 2004). These changes ultimately lead to reduced compliance of pulmonary vessels, and also increased pulmonary vascular resistance (PVR), which in turn lead to augmented afterload of the right ventricle and can affect the right heart function adversely (Stenmark et al., 2006b) (Schermuly et al., 2011).

Vascular remodeling is a crucial modification in PH and leads to structural and functional changes in all layers of the pulmonary vessel wall (*tunica intima*, *tunica media*, and *tunica adventitia*). The *tunica intima* becomes thicker by different processes e.g. proliferation of endothelial-like cells, and increased extracellular matrix deposition. These in turn can lead to formation of plexiform lesions which are glomeruloid-like lesions in the lungs of PAH patients (Tuder, 2017). Medial muscular layer of the pulmonary arteries become thicker by hypertrophy of the pulmonary smooth muscle cells (SMC), reduced apoptosis and increased proliferation of SMC and also possible migration of fibroblasts from the *tunica adventitia* (Rabinovitch, 2012) (Mandegar et al., 2004) (Schermuly et al., 2011) (Stenmark et al., 2006a). The *tunica adventitia* becomes thicker during remodeling through different processes like proliferation of fibroblasts, matrix protein deposition, and neovascularization in the *vasa vasorum* (Humbert et al., 2004). Furthermore, the *tunica adventitia*

may act as a reservoir for bone marrow derived progenitor cells that may stimulate or influence remodeling processes in the pulmonary vasculature (Davie et al., 2004).

1.1.4. WHO classification of PH

In table 1, the WHO classification of PH is shown. In this regard, PH is divided into five main groups.

Table 1: WHO clinical classification of PH, modified from (Simonneau et al., 2019)

1	Pulmonary arterial hypertension (PAH)
1.1	Idiopathic PAH (IPAH)
1.2	Heritable PAH
1.3	Drugs and toxins induced
1.4	Associated with:
1.4.1	Connective tissue diseases
1.4.2	Human immunodeficiency virus (HIV) infection
1.4.3	Portal hypertension
1.4.4	Congenital heart disease
1.4.5	Schistosomiasis
1.5	PAH long-term responders to calcium channel blockers
1.6	Pulmonary veno-occlusive disease (PVOD) and/or pulmonary capillary haemangiomatosis (PCH)
1.7	Persistent pulmonary hypertension of the newborn (PPHN)
2	Pulmonary hypertension due to left heart disease
2.1	PH due to heart failure with preserved left ventricular ejection fraction (LVEF)
2.2	PH due to heart failure with reduced left ventricular ejection fraction (LVEF)
2.3	Valvular heart disease
2.4	Congenital/acquired cardiovascular conditions leading to post-capillary PH
3	Pulmonary hypertension due to lung diseases and/or hypoxia
3.1	Chronic obstructive pulmonary disease (COPD)
3.2	Restrictive lung disease
3.3	Other lung disease with mixed restrictive/obstructive pattern
3.4	Hypoxia without lung disease
3.5	Developmental lung disorders
4	Chronic thromboembolic pulmonary hypertension (CTEPH)
5	PH with unclear and/or multifactorial mechanisms

1.1.5. Pathophysiology of different groups of PH

As it can be noticed in table 1, PH can be caused by different pathologies. In this part, different WHO groups of PH are described briefly.

In group 1, the pathogenesis of pulmonary arterial hypertension (PAH) involves the reduction of pulmonary vessels lumen diameter. There are different molecular and cellular mechanisms suggested to be involved in the narrowing process of the pulmonary vessels e.g. reduced apoptosis in the vessel walls, excessive cellular proliferation, dysregulation of vasoconstriction, and inflammation (Schermuly et al., 2011). Gradually, the resistance increases in affected pulmonary vessels which are narrower and thicker. The increased resistance makes it more difficult for the right heart to pump blood through the lung vessels and RHF can follow as a consequence (Vonk-Noordegraaf et al., 2013).

In subgroup 1.6 (PVOD), pulmonary blood vessel remodeling occurs specially in post-capillary pulmonary venules (Montani et al., 2016).

In group 2, due to left heart disease, left ventricle fails to pump blood efficiently in the systemic circulation. This leads to congestion of blood in the pulmonary circulation and increased pressure in the pulmonary vessels. If the insufficiency of left heart is severe, pulmonary edema and pleural effusion can be caused by left heart disease (Guazzi and Galie, 2012).

In group 3, as a result of low oxygen level in the alveoli (because of lung diseases and/or hypoxia), pulmonary arterioles constrict. This phenomenon is termed hypoxic pulmonary vasoconstriction (HPV) and it is originally a protective reaction to stop abundant blood flow to lung parts which are not well ventilated or damaged and do not contain adequate oxygen. In other words, pulmonary precapillary vasoconstriction is a physiological adaptation mechanism that diverts the blood circulation from poorly ventilated areas of the lung to healthy and well-ventilated regions to ensure the best possible oxygen uptake in the pulmonary circulation. In occurrence of widespread and prolonged alveolar hypoxia, which can happen in different conditions including sleep apnea, the hypoxia-mediated vasoconstriction in the pulmonary vascular bed can lead to PH (Sommer et al., 2008). It has been suggested that hypoxia-induced pulmonary vascular remodeling is site specific and the remodeling processes in the large vessels and the small vessels have different cellular and molecular mechanisms. This can be explained by different cellular composition and local environment of vessels at each specific site (Stenmark et al., 2006b).

In group 4 (CTEPH), the unresolved thromboemboli in blood cause narrowing and blockage of the pulmonary vessels and ultimately can lead to increased pulmonary blood pressure. In this group the increase in the resistance in pulmonary circulation and increased pulmonary pressure is due to combination of vessel obstruction and vascular remodeling (McNeil and Dunning, 2007) (Hoepfer et al., 2006). Different medical conditions have been associated with increased risk of CTEPH. These risk factors include history of splenectomy, inflammatory bowel disease, and osteomyelitis (Bonderman et al., 2005). In another study elevated levels of blood clotting factor VIII has been reported in CTEPH patients (Bonderman et al., 2003).

1.1.6. Diagnosis and treatment of PH

The identification of category of PH in each patient determines the treatment choices. Echocardiography for diagnosis of the PH is considered a valuable noninvasive method that can be used in early stages of the disease before confirmation with invasive RHC (Dunlap and Weyer, 2016).

In PAH patients, a precise evaluation of the disease is suggested to be performed before initiation of vasodilator or other therapies (Taichman et al., 2014). Pharmacologic treatment options include calcium-channel blockers (relaxation of smooth muscle cells and dilatation of vessels), endothelin receptor antagonist (reduction of vasoconstriction), phosphodiesterase type 5 inhibitor (inhibition of degradation of cyclic guanosine monophosphate and vasodilation), soluble guanylate cyclase stimulator (vasodilation), and prostanoids (vasodilation) (Chaumais et al., 2013) (Humbert, 2008) (Rosenkranz, 2007). Although there are pharmacological treatments for the PAH, because of progressive right ventricular dysfunction in severe forms, it can lead to death of the patient. Therefore, in these severely ill patients, lung or heart-lung transplantation should be considered for treatment. Balloon atrial septostomy and using extracorporeal membrane oxygenation (ECMO) can give the patients time until transplantation (Bartolome et al., 2017) (Sultan et al., 2018).

In patients with PH due to left heart disease, controlling of underlying left heart failure or correction of heart valve disease should be considered before specific treatment for PH. Nonspecific vasodilators as well as diuretic therapy for fluid volume correction should be considered, however under constant monitoring (Vachier et al., 2013) (McMurray et al., 2012).

Similarly, in patients with PH due lung disease the management and treatment of underlying disease should be considered in the first line of treatment (Seeger et al., 2013).

In patients with chronic thromboembolic pulmonary hypertension (CTEPH) who are capable of undergoing operation, pulmonary endarterectomy (surgical removal of an organized obstructing thrombus) can be considered the best choice of treatment. Patients who are not surgical candidates can be considered for targeted pharmacological therapies which are used for treatment of PAH. Furthermore, CTEPH patients should receive enduring anticoagulation therapy if these drugs are not contraindicated in these patients (Kim et al., 2013).

1.2. Systemic hypertension

1.2.1. Definition and importance

Systemic hypertension is a condition characterized by a chronic increase of blood pressure to values ≥ 130 mmHg (systolic) and ≥ 80 mmHg (diastolic) (Whelton et al., 2018).

Systemic hypertension is a common and chronic disorder which is considered to be one of the most important cardiovascular risk factor in the general population (Staessen et al., 2003). Systemic hypertension can damage different organs and cause cerebrovascular diseases (e.g. hemorrhagic stroke and retinopathy), heart diseases (e.g. myocardial infarction, coronary heart disease, and heart failure), nephropathies (proteinuria and renal failure), and vasculopathies (e.g. atherosclerotic stenosis and aneurysms) (Schmieder, 2010) (Escobar, 2002).

1.2.2. Classification of systemic hypertension

1.2.2.1. Classification based on etiology

Systemic hypertension can be divided into two categories based on the cause of hypertension. Primary (essential) hypertension occurs when hypertension does not have any clear underlying etiology. On the other hand, if the disease leading to hypertension is known, this hypertension is named secondary hypertension e.g. hypertension caused by obstructive sleep apnea, hyperaldosteronism, Cushing's syndrome, thyroid disease, coarctation of the aorta, renal disease, and usage of some medications (Charles et al., 2017).

1.2.2.2. Classification based on severity

In table 2, the different categories of blood pressure levels in adults are shown with their respective systolic and diastolic blood pressure.

Table 2: Classification of clinical blood pressure level in adults (When a patient’s systolic and diastolic blood pressure levels fall into different categories, the higher blood pressure category should be chosen.) (Whelton et al., 2018)

Blood pressure category	Systolic (mmHg)	Diastolic (mmHg)
Normal	<120	<80
Elevated	120–129	<80
Hypertension (Stage 1)	130–139	80–89
Hypertension (Stage 2)	≥140	≥90

1.2.3. Pathophysiology of systemic hypertension

1.2.3.1. Elevated total peripheral resistance

Increased peripheral resistance is playing an important role in systemic hypertension. Elevated peripheral resistance is mainly associated with increased activity of the renin-angiotensin-aldosterone system and disorders of the renal salt and water homeostasis (Navar, 2010). The other mechanisms which can be involved in elevated peripheral resistance and systemic hypertension are vascular inflammation and endothelial dysfunction (Agita and Alsagaff, 2017) (Versari et al., 2009) as well as chronic activation of the sympathetic nervous system (Esler et al., 2010).

1.2.3.2. Left ventricular hypertrophy

The increased peripheral resistance and consequent hypertension as well as the increased afterload and workload of the heart leads to functional and structural changes of the heart (e.g. elevated heart rate and hypertrophy of heart) (Courand and Lantelme, 2014) (Lovic et al., 2017). The left ventricular hypertrophy in patients with systemic hypertension is associated with increased risk of cardiovascular events (Garg et al., 2015).

Electrocardiography (ECG) is a valuable tool for assessment of left ventricular hypertrophy (Verdecchia et al., 1998) (Verdecchia et al., 2007). It has also been suggested that aortic vascular stiffness which can be evaluated by pulse wave velocity (PWV) is correlated with left ventricular hypertrophy (Rabkin and Chan, 2012).

1.2.3.3. Systolic and diastolic dysfunction

Uncontrolled high blood pressure and left ventricular hypertrophy can eventually lead to systolic and/or diastolic heart failure (Prisant, 2005).

1.2.4. Treatment of systemic hypertension

Multifactorial approaches must be used to control blood pressure. Lifestyle alterations (e.g. physical activity, diet modifications, weight reduction, sodium intake reduction, and moderating alcohol consumption) as well as antihypertensive medications are usually recommended (Go et al., 2014).

There are different recommendations for different hypertensive patients. For instance, in the population aged ≥ 60 years with hypertension, it is recommended to initiate pharmacologic treatment to reduce blood pressure to a goal systolic blood pressure (SBP) < 150 mmHg and goal diastolic blood pressure (DBP) < 90 mmHg. Additionally, concurrent diseases of the patients (e.g. diabetes) should be considered before selecting treatment approach (James et al., 2014). In the treatment of patients with secondary hypertension, treatment of underlying disease should be considered (Charles et al., 2017).

1.3. Obstructive sleep apnea syndrome (OSAS)

1.3.1. Definition of sleep apnea

An episode of sleep apnea is defined as the lack of inspiratory airflow for at least 10 seconds during sleep. A hypopnea is defined as a decrease in airflow, which lasts at least 10 seconds, and is connected to a decrease in arterial oxygen saturation ($\geq 3\%$) and/or an arousal detected by electroencephalography (Javaheri et al., 2017) (Berry et al., 2012).

1.3.2. Forms of sleep apnea

The sleep apnea syndrome in humans can be divided into two categories, the less frequent form, central sleep apnea syndrome (CSAS) is due to decreased respiratory drive of central nervous system (CNS), whereas the prevalent form, obstructive sleep apnea syndrome (OSAS) is characterized by a partial or complete closure of the upper respiratory tract during sleep due to its structural conditions (Banno and Kryger, 2007). OSAS is a widespread, chronic, and the most frequent sleep-related disorder (Sankri-Tarbichi, 2012). In table 3, the ICD codes of sleep apnea are shown.

Table 3: Classification of sleep apnea syndrome according to ICD-10 (International Classification of Diseases, Tenth Revision) (Thorpy, 2012)

ICD code	Sleep disorders
G47	Organic sleep disorders
G47.30	Sleep apnea/sleep related breathing disorder, unspecified
G47.31	Primary central sleep apnea
G47.33	Obstructive sleep apnea (adult) (pediatric)
G47.39	Other sleep apnea

1.3.3. Classification of the severity of OSAS

Different indexes are used to classify the severity of OSAS. Apnea-hypopnea index (AHI) is defined as the total number of apnea or hypopnea events per hour of sleep. The $AHI < 5$ is considered normal. OSAS with an $AHI \geq 5$ is typical accompanied by clinical symptoms (e.g. daytime sleepiness, fatigue, and concentration difficulties). AHI categories are, mild ($AHI = 5-14$), moderate ($AHI = 15-30$), and severe ($AHI > 30$) (Hudgel, 2016) (AASM, 1999).

The oxygen desaturation index (ODI) is another index to classify the severity of OSAS. This index indicates the average number of oxygen desaturation episodes (which are $\geq 4\%$ for longer than 10 seconds) per hour of sleep (Temirbekov et al., 2018).

1.3.3.1. Correlation between ODI and AHI

It has been shown that ODI correlates with AHI. In a study it was observed that, with accuracy of 86%, an $ODI > 5$ was predictor of $AHI > 5$, with accuracy of 86%, an $ODI > 15$ was predictor of an $AHI > 15$, and with accuracy of 94%, an $ODI > 30$ was predictor of an $AHI > 30$ (Chung et al., 2012).

1.3.4. Importance of sleep apnea

Sleep apnea is associated with cardiovascular diseases (e.g. ischemic heart disease, heart failure, and hypertension), metabolic diseases (e.g. diabetes, hyperlipidemia), pulmonary diseases, psychiatric diseases, and traffic collisions (Saaresranta et al., 2016) (Maekawa et al., 1998).

Sleep-disordered breathing is considered a prevalent disease which can remain undiagnosed in patients (Young et al., 1993). A study comparing the prevalence of disordered breathing during sleep in the Wisconsin Sleep Cohort Study with an interval of 20 years, showed a substantial

increase in prevalence. The results obtained in 1988-1994 showed that the prevalence of moderate to severe sleep-disordered breathing ($AHI \geq 15$) was 8.8% among 30-70-year-old men and 3.9% among 30-70-year-old women. Whereas the results obtained in 2007-2010 indicated that, 13% among 30-70-year-old men and 5.6% among 30-70-year-old women demonstrated an $AHI \geq 15$ (Peppard et al., 2013).

Polysomnographic investigations in United States, India, China, and Korea showed that the prevalence of OSAS in general population is 3.9-7.5% in men and 1.2-4.5% in women (Punjabi, 2008). In another study carried out in Europe, sleep-related data from 13057 individuals (15-100-year-old) were collected by telephone interviews. Prevalence of OSAS was estimated 1.8% in Germany, 1.1% in Italy, and 1.9% in United Kingdom (Ohayon et al., 2000).

Different prevalence results have been observed in different studies that have assessed the prevalence of obstructive sleep apnea (OSA). These differences are consequences of differences in sampling, recording and/or scoring techniques and methods, and also the described cutoff AHI score for diagnosis of sleep apnea (Sarkar et al., 2018) (Punjabi, 2008).

1.3.5. Risk factors of OSAS

In table 4, different predisposing factors of OSAS are shown.

Table 4: Risk factors of OSAS

Risk factors contributing to OSAS	Explanations or examples	References
Gender	Men are affected more often	(Young et al., 1993)
Obesity	Higher prevalence in obese people	(Young et al., 2002a)
Smoking cigarettes	Higher prevalence in smokers	(Wetter et al., 1994)
Consumption of muscle relaxants	Sedatives Alcohol	(Weatherspoon et al., 2016) (Taveira et al., 2018)
Age	Higher prevalence in older people	(Young et al., 2002b)
Endocrine disorder	Acromegaly	(Vouzouneraki et al., 2018)
Genetic	Heritable factors	(Mukherjee et al., 2018)
Anatomical predisposition	Larger neck circumference Craniofacial familial abnormalities	(Davies et al., 1992) (Guilleminault et al., 1995)
Menopause	Higher prevalence and severity in postmenopausal women	(Dancey et al., 2001)

1.3.6. Pathophysiology of OSAS

In OSAS patients, the obstruction in the upper airways during sleep and inadequate ventilation leads to apnea and/or hypopnea, hypoxemia (decrease of the pO_2 in the blood), and hypercapnia (increase of the pCO_2). The obstruction of the respiratory tract is mainly due to the relaxation of the pharyngeal musculature during sleep and recurrent narrowing and/or complete closure of the pharynx. The abnormal anatomical features in the upper airways of the patient can be considered another main cause of OSAS (Somers et al., 2008). These processes and deterioration of blood gas profile activate chemoreceptors and the sympathetic nervous system which eventually lead to an arousal. The arousal increases the activity of the pharyngeal dilator muscles, and opens the airways, which allows the normalization of ventilation, respiration, and blood gas profile. These cycles of airway obstruction and opening (and the subsequent hypoxia and reoxygenation) can repeat more than 40 times per hour of sleep ($AHI > 40$) in severe cases (Bonsignore et al., 1994).

1.3.7. Pathogenesis of the OSAS

The pathogenesis of the OSAS has been suggested to involve increased oxidative stress (Passali et al., 2015), selective stimulation of inflammatory pathways (de Lima et al., 2016), and endothelial dysfunction (Duchna et al., 2006).

1.3.8. Signs and symptoms of OSAS

The key sign of OSAS is excessive daytime sleepiness (EDS) (Kryger, 2000). OSAS patient also suffer from cognitive disturbance e.g. concentration and memory problems (Vaessen et al., 2015). One of the frequent symptoms of OSAS is witnessed apneas which can be observed by another person who has the opportunity to see the patient while sleeping (Gibson, 2004). Snoring is also considered to be a sign of OSAS (Morris et al., 2008).

1.3.9. Importance of polysomnographic analysis as gold standard in diagnosis of OSAS

Apart from clinical symptoms, polysomnography and assessment of documented abnormal breathing during sleep is necessary for the diagnosis of OSAS (McNicholas, 2008) (Kryger, 2000). It has been shown that regular polysomnographic data can recognize changes (e.g. arousal, hypopnea, hypoxia, and etc.) that can be helpful to assess the risk of cardiovascular events (Zinchuk et al., 2018).

However, it has been suggested that only one sleep study may be insufficient to diagnose the severity of OSAS, as the severity of OSAS may differ substantially in each sleep (Stoberl et al., 2017).

1.3.10. Treatment options for OSAS

In a review of the literature on OSAS from 1980 to 2014 it has been concluded that there is no common view for the best treatment option. The best option for therapy must be based on the cause and severity of OSAS and a multidisciplinary treatment is suggested in most of the articles (Maspero et al., 2015). Appropriate treatment methods for different patients should be selected to achieve an effective treatment. Different factors such as weight, age, sex, the exact site of narrowing or collapse of the upper airway, craniofacial and dental abnormalities, positional-dependency of obstruction, and acceptance of the treatment method (and treatment adherence) by the patient should be assessed before the final decision for treatment procedure is made (Boudewyns et al., 2007).

As OSAS is considered a cardiovascular risk factor, it has been suggested that before anesthesia and surgery a pre-operative screening is performed to identify the undiagnosed OSAS, and if applicable, OSAS treatment (e.g. continuous positive airway pressure) is considered peri-operatively (Verbraecken et al., 2017).

1.3.10.1. Medications

Although some studies have reported reduction of AHI after use of some medications, evidences are not adequate to recommend a certain medication therapy for treatment of OSAS (Mason et al., 2013).

If sleep apnea is due to another underlying disease (e.g. primary aldosteronism, acromegaly, or hypothyroidism) medication therapy of the underlying disease is useful for the management of OSAS. However this does not always completely resolve the OSAS (Wolley et al., 2017) (Zhang et al., 2016) (Ceccato et al., 2015) (Veasey et al., 2006).

1.3.10.2. Lifestyle changes

As obesity is an important risk factor for the OSAS, weight reduction (even through bariatric surgery) is an important option for treatment of OSAS (Tuomilehto et al., 2013) (Buchwald et al., 2004) (Schwartz et al., 2008).

It has also been suggested that quitting smoking can have positive effects for prevention and treatment of OSAS (Wetter et al., 1994).

1.3.10.3. Oral appliances

Patients with a mild or moderate form of OSAS can benefit from the mandibular advancement splint (MAS) also called mandibular advancement device (MAD) and mandibular advancement appliance (MAA) (Serra-Torres et al., 2016) (Chan et al., 2008). The task of the splint is to fix the mandible as front as possible, to prevent the tongue and muscle structures narrowing or blocking the pharynx, so that the upper airways are kept open during sleep (Kostrzewa-Janicka et al., 2017). Although MADs are associated with some side effects on temporomandibular joint when used over long time, these side effects can be reduced with cautious selection and later control of the MADs (Knappe et al., 2017). Nevertheless, oral appliances are not as effective and predictable as continuous positive airway pressure (CPAP) therapy in treatment of OSA (Ng and Yow, 2019) (Ferguson et al., 2006).

1.3.10.4. CPAP

CPAP is the gold standard treatment for patients with all severity categories of OSAS. CPAP is able to eliminate OSAS by acting as a pneumatic splint that retains the upper airway open during sleep (Kushida et al., 2006). In other words, pressurized room air is pumped through a face or nose mask to keep the upper respiratory tract open (Prabhat et al., 2012). As using a mask with pressurized air during sleep is undesirable for patients, CPAP is not accepted or tolerated by all patients (Somers et al., 2008).

CPAP therapy is recommended in OSAS patients as it reduces daytime sleepiness (Patel et al., 2003), and also decreases blood pressure in hypertensive OSAS patients (Kushida et al., 2006). It has been shown that CPAP treatment reduces the car accident risk (George, 2001).

1.3.10.5. Surgical techniques

As treatment options for patients with OSAS, there are surgical techniques which can be performed on the upper airways. These surgical procedures are usually for those who previously mentioned treatments (e.g. CPAP therapy and oral appliances) have been unsuccessful to control their OSAS or for the patients who cannot tolerate these treatments. Surgical treatment for OSAS needs to be individualized to eliminate the exact anatomical site of obstruction. Tonsillectomy, adenoidectomy, and uvulopalatopharyngoplasty (UPPP) can be used to eliminate pharyngeal obstruction restore normal air flow (Spicuzza et al., 2015) (Won et al., 2008). It has been reported that the risk of OSA related depression can be decreased following UPPP (Cho et al., 2019). In another study UPPP showed significantly lower success rate in reducing apnea index compared to the dental appliance (Walker-Engstrom et al., 2002).

As another surgical treatment, soft palate implants can be used to harden the soft palate and reduce OSAS (Spicuzza et al., 2015). Maxillomandibular advancement (MMA) can be used as another surgical treatment option for OSAS (Prinsell, 2002) (Boudewyns et al., 2007). Tracheostomy can be used as another surgical option for OSAS patients if other treatment options have failed to control their OSAS (Tan et al., 2016) (Epstein et al., 2009).

1.3.11. Medical conditions associated with OSAS

In table 5, some of the important conditions associated with OSAS in diverse medical fields are listed.

Table 5: Conditions associated with OSAS in different medical fields (Gibson, 2004) (Schlosshan and Elliott, 2004) (Orr et al., 2004)

Medical field	Associated disorders
Cardiology	Systemic hypertension, arrhythmia, ischemic heart disease, cardiac failure
Respirology	Respiratory failure, PH, cor pulmonale
Endocrinology	Diabetes mellitus, insulin resistance, metabolic syndrome, hypothyroidism, acromegaly
Neurology	Impaired memory and concentration
Psychiatry	Depression
Gastroenterology	Gastroesophageal reflux disease (GERD)
Urology	Nocturia, impotence, decreased sexual function
Otorhinolaryngology	Enlarged tonsils, nasal obstruction
Dentistry and orthodontics	Retrognathia, Micrognathia
Hematology	Polycythemia

1.3.11.1. Associations between OSAS and PH

PH in OSA patients is considered to be a consequence of vasoconstriction and remodeling of pulmonary arterioles, diastolic dysfunction of left ventricle, and dilation of left atrium (Sajkov and McEvoy, 2009).

In OSA patients, the prevalence of PH is considered between 17% and 53% (Wong et al., 2017). In another study it has been reported that PH (evaluated by pulmonary artery catheterization) is observed in 16% of the severe OSAS patients, and it has been concluded that PH correlated to the severity of the OSAS (Hawrylkiewicz et al., 2004). On the contrary, in a study it has been doubted if only nocturnal apnea/hypopnea events per se (without any other lung and heart disease) can cause daytime PH. It has been concluded that AHI (an indicator of OSAS severity) was not playing a decisive role in PH (Kessler et al., 1996). However, in another study it was concluded that some OSAS patients with normal lung function developed PH (Sajkov et al., 1999).

CPAP therapy has shown to reduce pulmonary blood pressure in OSAS patients (Wong et al., 2017) (Alchanatis et al., 2001) (Sajkov et al., 2002).

1.3.11.2. Associations and interactions between OSAS and systemic hypertension

It has been shown that there is an association between OSAS and systemic hypertension independent of confounding factors like gender, age, weight, and ethnic backgrounds. Furthermore, it has been concluded that this association follows dose-response relationship, meaning that OSAS with higher severity is associated with higher prevalence of systemic hypertension (Young et al., 1997) (Nieto et al., 2000) (Carlson et al., 1994) (Peppard et al., 2000). Similarly, in a 15-year-long prospective cohort study, it has been shown that OSA was associated with increased risk of cumulative incidence of systemic hypertension (Marin et al., 2012).

OSAS has been shown to be the most prevalent (64%) secondary cause of resistant systemic hypertension (Pedrosa et al., 2011). Resistant systemic hypertension is defined as high blood pressure despite simultaneous treatment with three antihypertensive medications of different classes including a diuretic agent. 20% to 30% of the systemic hypertension patients suffer from resistant systemic hypertension (Calhoun et al., 2008). In another study, prevalence of OSAS (with AHI ≥ 10 per hour of sleep) in resistant systemic hypertension patient was estimated 83% (Logan et al., 2001).

Both systemic hypertension and OSAS involve common systems of the body and are considered to have complex connections with each other. These complex interactions are through involvement of the CNS, the pulmonary system, the cardiovascular system, the endocrine system, and the renal system (Konecny et al., 2014). Suggested mechanisms involved in both diseases include sympathetic nervous system hyperactivity, endothelial dysfunction, activation of inflammatory pathways, coagulation disorders, oxidative stress, and metabolic disturbances (McNicholas, 2007) (Zhang and Si, 2012). In another study performed on patients with the combination of sleep apnea and an acute cardiovascular event, a significant increased serum levels of different inflammatory biomarkers was observed (Testelmans et al., 2013).

CPAP therapy can decrease systemic hypertension and cardiovascular risk in OSAS patients (Pack and Gislason, 2009) (Bazzano et al., 2007).

1.4. Simulation of OSAS in animal models

In order to simulate OSAS, animal models have been used to promote the knowledge about its pathogenesis, effects on different body systems (e.g. cardiovascular, metabolic, and etc.), and treatment options. There are different animal models used to simulate OSAS, including animals

with spontaneous OSAS, obstruction created by surgical or mechanical approaches, sleep fragmentation, and intermittent hypoxia (Chopra et al., 2016) (Jun and Polotsky, 2007).

1.4.1. Animal models with spontaneous OSA

There are some animals with spontaneous OSA that can serve as animal model. English bulldog breed with its special anatomical features (narrow oropharynx and oversized soft palate) can be used to study this disease (Hendricks et al., 1987). Obese Yucatan miniature pigs can also be used as spontaneous OSAS model (Lonergan et al., 1998). It has also been reported that obese Zucker rats showed a reduced pharyngeal airway size (Brennick et al., 2006).

1.4.2. Animal models with obstruction created by surgical or mechanical approaches

Different surgical and mechanical methods have been used for occlusion of the upper airway in a variety of different species, including rats (Nacher et al., 2007) (Farre et al., 2003), dogs (Brooks et al., 1997) (Kimoff et al., 1994), lambs (Fewell et al., 1988), pigs (Launois et al., 2001) (Pinto et al., 1993) (Chen et al., 2000), baboons (White et al., 1995), and monkeys (Philip et al., 2005).

1.4.3. Sleep fragmentation animal models

Another method of simulating OSAS in animal models is sleep fragmentation (SF), in which different devices (e.g. rotating disk, treadmill, high-flow air blasts, and etc.) have been used to interrupt sleep in mice (Trammell et al., 2014) (Polotsky et al., 2006) and rats (Bergmann et al., 1989) (McCoy et al., 2007).

1.4.4. Intermittent hypoxia animal models

Intermittent hypoxia (IH) is one of the main consequences of the OSA (Mesarwi et al., 2015). Different IH protocols for rodent models have been used to simulate OSA (Foster et al., 2007). In this models, the animals can be exposed to IH regardless of their awake/sleep phase (Schulz et al., 2014), or only during their sleep phase by using electroencephalography (EEG) or electromyography (EMG) (Hamrahi et al., 2001) (Tagaito et al., 2001).

1.4.5. Pulmonary and systemic hypertension in chronic intermittent hypoxia (CIH) animal model

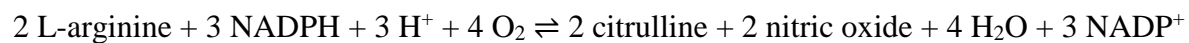
Cardiovascular and pulmonary consequences due to CIH exposure in rodents have been associated with consequences of OSAS in humans (Savransky et al., 2007) (Jun et al., 2010) (Campen et al., 2005) (Dematteis et al., 2009).

It has been reported that exposure to CIH in rats increased the mean arterial pressure (MAP) (Li et al., 2018) which decreased to starting values two days after discontinuation of CIH (Knight et al., 2011). Similarly, it has been reported that CIH increased diastolic blood pressure and also systolic blood pressure in rats (Diogo et al., 2015).

Moreover, it has been shown that CIH exposure of mice significantly elevated their systemic blood pressure (Elliot-Portal et al., 2018) (Schulz et al., 2014). Other studies reported CIH-induced PH in mice (Nisbet et al., 2009) (Fagan, 2001). Similarly, in another study performed on CIH-exposed mice it was shown that CIH resulted in systemic hypertension, PH, and left and right ventricular hypertrophy (Campen et al., 2005).

1.5. Nitric oxide synthases (NOSs)

NOSs catalyze the production of nitric oxide (NO) through the following reaction (Knowles and Moncada, 1994):



NOSs need cofactors for this reaction including calmodulin, flavin adenine dinucleotide (FAD), flavin mononucleotide (FMN), heme, and tetrahydrobiopterin (BH₄). There are three isoforms of NOS, which are coded by different genes on different chromosomes. These three isoforms are regulated differently, with different catalytic properties, and different sensitivity to inhibitors (Alderton et al., 2001). The isoenzymes eNOS (endothelial NOS) and nNOS (neuronal NOS) are constitutively expressed and are regulated by intracellular calcium ion (Ca²⁺) concentration. These two isoenzymes produce small amount of NO and are involved in physiological functions and processes. The inducible isoform (iNOS) functions independent of intracellular Ca²⁺ and produce relatively large amount of NO upon stimulation by endotoxins, cytokines (e.g. tumor necrosis factor-alpha (TNF- α), interleukin-1, interleukin-2, and interferon- γ), or other proinflammatory stimuli. NO produced by iNOS is involved in inflammation, immune responses, and immune defense mechanism in infections (Campbell et al., 2014) (Hill et al., 2010) (Kone et al., 2003).

It has been shown that different pathways are controlling iNOS expression. Regulation of iNOS expression can be via transcription factors (e.g. STAT1 α and NF- κ B), and by means of post-transcriptional mechanisms (Kleinert et al., 2004).

NOSs can also produce superoxide anion specially in absence of their required cofactor or substrate (i.e. uncoupled NOSs) (Luo et al., 2014).

1.5.1. Nitric oxide synthases and oxidative stress

Reactive oxygen species (ROS) have many physiological functions (e.g. immune system, cellular signaling, and etc.). Oxidative stress (i.e. increased generation of ROS) has been associated with different pathological conditions, including cardiovascular diseases (e.g. hypertension and atherosclerosis), metabolic disorders, and renal diseases. Superoxide anion (a potent ROS) can be produced by electron transport chain in mitochondria, NADPH oxidases, cyclooxygenase, lipoxygenase, xanthine oxidase, and also uncoupled NOS (Paravicini and Touyz, 2008). NO produced by NOSs can react with the superoxide anion and form peroxynitrite, which can cause DNA, protein, and lipid damage (Schiffrin, 2008) (Hill et al., 2010).

1.5.2. Inducible nitric oxide synthase in cardiopulmonary diseases

It has been shown that iNOS plays an important role in the pathogenesis of lung diseases e.g. acute respiratory distress syndrome (ARDS) (Dias-Junior et al., 2008). Moreover, it has been reported that in chronic transverse aortic constriction (TAC) mouse model, iNOS has an important role in ventricular hypertrophy and dysfunction (Zhang et al., 2007).

NO produced by iNOS in the myocardial ischemic reperfusion injury has shown to have complex dual effect which can be both harmful and cardioprotective. These paradoxical observations has been suggested to be because of the importance of the amount of NO and peroxynitrite and the balance between them (Yu et al., 2018).

1.5.3. Inducible nitric oxide synthase in OSA

Oxidative stress and NOSs have been suggested to play an important role in the pathogenesis of OSA (Zhang and Veasey, 2012). Furthermore, it has been shown that CIH exposure activates NF- κ B and also increases downstream products of NF- κ B e.g. TNF- α , monocyte chemoattractant protein-1 (MCP-1), interleukin-6, and iNOS (Liu et al., 2018) (Lee et al., 2016) (Greenberg et al., 2006).

In 2000, two independent studies showed that OSA patients have a lower amounts of serum nitrites and nitrates (derived from circulating NO) and after CPAP, serum NO was significantly increased (Ip et al., 2000) (Schulz et al., 2000). Another study performed on harvested venous endothelial cell from recently diagnosed OSA patients who did not have history of cardiovascular disease in the previous 10 years, showed that iNOS expression was higher in OSA patients than in control subjects. CPAP therapy significantly decreased iNOS expression (Jelic et al., 2008).

It has been reported that iNOS has an important role in oxidative damage, peroxidation of lipids, and proinflammatory reactions in some brain regions in CIH-exposed mice (Zhan et al., 2005).

1.5.4. iNOS knockout mice

In this project different chimeric mice were examined. These chimeric mice were generated by using bone marrow transplantation technique from wild type (WT) and iNOS knockout (KO) mice. iNOS^{-/-} mice with C57BL/6J background (B6.129P2-Nos2^{tm1Lau/J}) do not show any gross and histological noticeable differences from WT mice. These mice are viable and fertile (Laubach et al., 1995).

1.6. Aim of the current study

The role of iNOS in a mouse model of CIH has been previously studied by using iNOS^{-/-} mice and it has been shown that iNOS plays an important role in the pathogenesis of this OSAS model. The mice lacking iNOS showed less systemic hypertension, pulmonary vascular remodeling, and PH compared to WT mice in the CIH model (Kraut, 2014). The aim of the present work was to further investigate the pathogenesis of systemic and pulmonary hypertension in this model. The experiments were designed to clarify whether the iNOS involved in pathogenesis of OSAS is originating from bone marrow cells or non-bone marrow-derived cells. For this purpose, mice (WT and iNOS^{-/-}) were irradiated at the beginning of the experiment until complete bone marrow depression, and afterwards transplanted with either WT or iNOS^{-/-} bone marrow cells. After bone marrow reconstitution the mice were exposed to CIH or normoxia (NOX). The experiments on generated chimeric mice in CIH model of OSAS were thought to shed light on the pathogenesis of systemic and pulmonary hypertension associated with the OSAS.

2. Material and methods

2.1. Material

2.1.1. Medications and reagents

1-hydroxy-3-methoxycarbonyl-2,2,5,5-tetramethyl-pyrrolidine (spin probe CMH)	Noxygen, Elzach, Germany
50% 2-propanol / 1% Povidone-iodine solution, Braunoderm [®]	B. Braun Melsungen AG, Melsungen, Germany
Buprenorphine, Temgesic [®]	Essex Pharma, Munich, Germany
Dulbecco's Phosphate-buffered Saline (DPBS)	Sigma-Aldrich, St. Louis, USA
Enrofloxacin, Baytril [®] 2.5%	Bayer, Leverkusen, Germany
Ethylenediaminetetraacetic acid (EDTA)	Sigma-Aldrich, St. Louis, USA
Eye and nasal ointment, Bepanthen [®]	Bayer Vital, Leverkusen, Germany
Heparin, Ratiopharm [®]	Ratiopharm GmbH, Ulm, Germany
Isoflurane, Baxter [®]	Baxter Deutschland GmbH, Unterschleissheim, Germany
Polyethylene-glycol conjugated superoxide dismutase (pSOD)	Sigma-Aldrich, St. Louis, USA
Protease inhibitor cocktail	Sigma-Aldrich, St. Louis, USA
Ringer Solution, Ringer-Solution Ecoflac plus	B. Braun Melsungen AG, Melsungen, Germany
RPMI 1640 Medium, Gibco [™]	Invitrogen, Karlsruhe, Germany
Sodium chloride solution 0.9% Diaco [®]	Serag-Wiessner KG, Naila, Germany
Sodium chloride solution, for rinsing and moisten	B. Braun Melsungen AG, Melsungen, Germany

2.1.2. Devices, equipments, softwares

16 Port Gigabit Switch	Cisco Systems, San Jose, USA
------------------------	------------------------------

Bio Amp ML136 amplifier (for ECG)	ADInstruments, Oxford, United Kingdom
Chronic intermittent hypoxia chamber	Biospherix, Parish, NY, USA
EMXmicro Electron Spin Resonance (ESR) spectrometer	Bruker Biospin GmbH, Rheinstetten, Germany
Gas detector, X-am 2000	Drägerwerk AG & Co. KGaA, Lübeck, Germany
Heating Plate, 21,5x11cm, HP-1M	AgnTho AB, Lidingö, Sweden
Hematocrit centrifuge, hematocrit 210	Hettich, Tuttlingen, Germany
Homeothermic Controller (Animal Temperature Control System), TCAT-2LV	AgnTho AB, Lidingö, Sweden
Irrigation cannula	Hugo Sachs Elektronik-Harvard Apparatus GmbH March-Hugstetten, Germany
Isoflurane Evaporator, Vet Equip	KF Technology, Rome, Italy
LabChart software	ADInstruments, Oxford, United Kingdom
Millar catheter, SPR-671 Mikro-Tip [®] mouse pressure catheter	Millar Instruments Inc., Houston, USA
MPVS Ultra [®] pressure-volume loop system	Millar Instruments Inc., Houston, USA
Needle Electrodes for Animal Bio Amp (3 pk) MLA1213	ADInstruments, Oxford, United Kingdom
Nitrogen generator, NGM44-LC/MS	cmc Instruments GmbH, Eschborn, Germany
OxyCycler, A84XOV, dynamic O ₂ controller	Biospherix, Parish, USA
Ponemah Version 6.11 software	Data Science International, St. Paul, USA
PowerLab 8/30 amplifier	ADInstruments, Oxford, United Kingdom
Rectal Thermometer	Indus Instruments, Houston, USA
Routine stereomicroscopes (Magnifier), M50	Leica Microsystems, Wetzlar, Germany
Surgical instruments	Fine science tools GmbH, Heidelberg, Germany
Telemetry ambient pressure reference APR-1	Data Science International, St. Paul, USA
Telemetry data converter, data exchange matrix [™]	Data Science International, St. Paul, USA

Telemetry receiver, PhysioTel [®] RPC-1	Data Science International, St. Paul, USA
Telemetry transmitter, TA11PA-C10	Data Science International, St. Paul, USA
Tissue homogenizer, Bullet Blender [®]	Next Advance Inc., New York, USA
Tripod	For holding syringes for flushing procedure
Ultrasound machine, Vevo [®] 2100 high frequency imaging platform	VisualSonics Inc., Toronto, Canada
Vascular clamp, S&T, for femoral artery	Fine science tools GmbH, Heidelberg, Germany
Ventilation pump, MiniVent Type 845	Hugo Sachs Elektronik-Harvard Apparatus GmbH, March-Hugstetten, Germany
Vevo 770, ECG table	VisualSonics Inc., Toronto, Ontario, Canada
Vevo [®] LAB software, for analyzing ultrasound and photoacoustic data	VisualSonics Inc., Toronto, Ontario, Canada

2.1.3. Consumables

100 µm Cell Strainer, BD Falcon	BD GmbH, Heidelberg, Germany
Adhesive tape, Durapore [®] 3M [™]	3M, St. Paul, USA
BD Microlance 3 [™] needles 24 G (0.55 mm x 25 mm) 26 G (0.9 mm x 25 mm) 30 G (0.3 mm x 25 mm)	Becton Dickinson, Heidelberg, Germany
Blood lancet, Romed [®] Holland	Oostveen Medical B.V. Van, Wilnis, Netherlands
Cellulose swabs, 4 x 5 cm, Pur-Zellin [®]	Paul Hartmann AG, Heidenheim, Germany
Disposable gloves, Vasco [®] Nitrile white	B. Braun Melsungen AG, Melsungen, Germany
Disposable micro-hematocrit capillary tube, Hirschmann [®] , sodium heparinized	Hirschmann Laborgeräte GmbH & Co. KG, Eberstadt, Germany
Disposable surgical blades with plastic handle 10, 11, 20, Feather [®]	Pfm medical AG, Köln, Germany

Disposable syringe, Inject Luer [®] , 1 ml, 2 ml, 5 ml, 10 ml, 20 ml	B. Braun Melsungen AG, Melsungen, Germany
Disposable syringe, Original Perfusor [®] , 50 ml	B. Braun Melsungen AG, Melsungen, Germany
DNeasy Blood and Tissue Kit	Qiagen, Hilden, Germany
Embedding cassettes, Tissue Tek [®] III Uni-Cassette [®]	Sakura Finetek Europe B.V, Zoeterwoude, Netherlands
Eppendorf Tubes, 0.5 ml, 1.5 ml	Sarstedt AG & Co, Nuembrecht, Germany
Falcon tube, Cellstar [®] , 15 ml, 50 ml	Greiner Bio-One GmbH, Frickenhausen, Germany
Glutaraldehyde solution, 25% in H ₂ O	Sigma-Aldrich, St. Louis, USA
Hair removal cream, VEET [®]	Reckitt Benckiser Germany GmbH, Heidelberg, Germany
Hematocrit sealing compound, BRAND [®]	Brand GmbH & Co KG, Wertheim, Germany
IV catheter, 20 G (1.1 mm x 33 mm), Vasofix [®] Safety	B. Braun Melsungen AG, Melsungen, Germany
PARAFILM [®] M	American National Can Company, Menasha, USA
PCR kit, GoTaq [®] G2 Hot Start Master Mixes	Promega, Madison, USA
Perfusor tubing, 150 cm	B. Braun Melsungen AG, Melsungen, Germany
Polypropylene suture material 6-0, Prolene [®]	Ethicon GmbH, Norderstedt, Germany
Rodent cage bedding, Alpha-dri [®]	Shepherd Specialty Papers, Tennessee, USA
Screw cap freezer tube, Cryo.s [™] , 2 ml	Greiner Bio-One GmbH, Frickenhausen, Germany
Three-way stopcock, Discifix [®]	B. Braun Melsungen AG, Melsungen, Germany
Tissue adhesive, 3M Vetbond [™]	3M Animal Care Products, St. Paul, USA
Ultrasound gel, Aquagel [®]	Parker Laboratories Inc., Fairfield, USA

2.1.4. Primers for genotyping

The sequence of primers (suggested by the Jackson Laboratory) used for genotyping was as follows:

<https://www.jax.org/Protocol?stockNumber=002609&protocolID=24473>

Common	TCACCACCAGCAGTAGTTGC
Mutant Forward	CCTTCTATCGCCTTCTTGACG
Wild type Forward	TCCGATTTAGAGTCTTGGTGA

Length of the amplified fragment was approximately 640 bp for the WT allele and approximately 200 bp for the disrupted allele in iNOS knockout mice (QIAxcel[®], Qiagen, Germany).

2.1.5. Materials, devices, consumables, softwares and macros for histology

Computer, Q 550 IW	Leica Biosystems, Nussloch, Germany
Cooling plate, EG 1150C	Leica Biosystems, Nussloch, Germany
Cover glasses 24 x 36mm	R. Langenbrinck, Emmendingen, Germany
Digital camera, DC 300F	Leica Biosystems, Nussloch, Germany
Fully motorized rotary microtome, RM 2165	Leica Biosystems, Nussloch, Germany
Heated embedding module, EG 1140H	Leica Biosystems, Nussloch, Germany
Incubator	Memmert GmbH & Co KG Schwabach, Germany
Macro for assessment of degree of muscularization	Developed by Mr. Christoph Frank (computer scientist), Leica Biosystems, Nussloch, Germany
Microscope slide, Superfrost Plus [®]	R. Langenbrinck, Emmendingen, Germany
Microtome Blades S 35, Feather [®]	Pfm medical AG, Köln, Germany
Motorized transmitted light microscope, DMLA	Leica Microsystems, Wetzlar, Germany

Mounting medium, Pertex [®]	Medite GmbH, Burgdorf, Germany
Paraffin tissue embedding medium, Paraplast Plus [®]	Sigma-Aldrich, St. Louis, USA
Q Win V3, software	Leica Biosystems, Nussloch, Germany
Tissue processor, TP1050	Leica Biosystems, Nussloch, Germany
Water bath for paraffin sections, HI1210	Leica Biosystems, Nussloch, Germany

2.1.6. Antibodies, reagents, solutions, and kits for immunohistochemistry staining

Anti-alpha smooth muscle actin, clone 1A4 monoclonal, mouse anti-human, Dilution 1: 800 in 10% BSA	Sigma-Aldrich, St. Louis, USA
Anti-von Willebrand factor, polyclonal, rabbit anti-human, Dilution 1: 1100 in 10% BSA	Dako Cytomation Hamburg, Germany
Bovine serum albumin	Serva Electrophoresis GmbH, Heidelberg, Germany
DAB Peroxidase Substrat Kit	Vector / Linaris, Wertheim-Bettingen, Germany
Disodium hydrogen phosphate dihydrate (Na ₂ HPO ₄ x 2 H ₂ O)	Merck, Darmstadt, Germany
Ethanol 70%, 96%, 99.6%	Fischer, Saarbrücken, Germany
Formaldehyde solution 3.5 - 3.7%, neutral buffered stabilized with methanol	Otto Fischar GmbH & Co. KG, Saarbrücken, Germany
Hydrochloric acid (HCl)	Carl Roth GmbH Karlsruhe, Germany
Hydrogen peroxide 30%	Merck, Darmstadt, Germany
ImmPRESSTM Reagent, Anti-Rabbit Ig	Vector / Linaris, Wertheim-Bettingen, Germany
Isopropanol (99, 8%)	Fluka chemistry, Buchs, Switzerland
Methanol, pure	Fluka chemistry, Buchs, Switzerland
Methyl green	Vector / Linaris, Wertheim-Bettingen, Germany

Potassium chloride (KCl)	Carl Roth GmbH, Karlsruhe, Germany
Potassium hydrogen phosphate (KH ₂ PO ₄)	Merck, Darmstadt, Germany
R.T.U. Normal horse serum 2.5%	Vector / Linaris, Wertheim-Bettingen, Germany
Sodium chloride (NaCl)	Carl Roth GmbH, Karlsruhe, Germany
Trypsin, Digest-All 2 [®]	Zytomed, Berlin, Germany
Vector VIP [®] Substrate kit	Vector / Linaris, Wertheim-Bettingen, Germany
Xylol	Carl Roth GmbH, Karlsruhe, Germany

2.1.7. Animals

Adult male C57BL/6J and iNOS KO (line B6.129P2-Nos2^{tm1Lau/J}) mice at a weight of 20-30 g and an age of 12 weeks (Charles River Germany GmbH, Sulzfeld) were used in this work. After bone marrow transplantation the mice were individually housed during the experimental period under constant monitoring of the animal caretakers of the animal facility. Each mouse was kept separately in individually ventilated cages (IVC), at a room temperature of 22 ± 2 °C, on a 14:10 hour light-dark cycle and provided access to food and water *ad libitum* (Altromin[®] standard diet food) and water.

2.1.8. Regional council's approvals for animal experiments

The experiment was approved by Regional board (Regierungspräsidium Giessen, Hesse, Germany; A2 V54-19c 2015 h 01 GI 20/10 Nr. 22/2015) in accordance with the German animal welfare law and the European legislation for the protection of animals used for scientific purposes (2010/63/EU). Under the name:

„Rolle der zelltypspezifischen iNOS im Mausmodell der CIH zur Nachstellung des OSA“

English translation: role of cell specific iNOS in the mouse model of CIH for investigation of OSA

2.2. Methods

According to the design of the experiments, on day 0, recipient mice were irradiated and bone marrow transplantation was performed after isolation of bone marrow cells from donor mice. On

day 42, peripheral blood samples were taken for verification of successful transplantation by PCR. On day 63, baseline echocardiographic measurements were performed. On day 64, a telemetry transmitter was implanted into each of the chimeric mice. On day 71, CIH or NOX exposure was started for 6 weeks and during these 6 weeks blood pressure measurement was performed by a telemetric system. On day 113, endpoint echocardiographic measurements were performed. On day 114, terminal hemodynamic measurements and organ harvest were performed. Moreover, blood and lung homogenates samples were prepared to measure superoxide anion.

Day 0	Bone marrow transplantation
Day 42	Verification of successful bone marrow transplantation
Day 63	Baseline echocardiographic measurements
Day 64	Implantation of telemetry transmitter
Day 71	Initiation of CIH or NOX exposure
Day 113	Endpoint echocardiographic measurements
Day 114	Terminal hemodynamic measurements and organ harvest

2.2.1. Bone marrow transplantation (BMT)

In order to generate chimeric mice, the BMT technique was used. BMT was performed as already described and used in previous investigations (Voswinckel et al., 2003) (Seimetz et al., 2011). Bone marrow of the recipient mice (12 weeks old) was suppressed by fractionated total body irradiation (FTBI) with Co-60 irradiation. FTBI protocol with 11 Gray (twice 5.5 Gray irradiations with interval of 2 hours between the irradiations) was performed by Dr. Dirk Krambrich in the irradiation facility of Justus-Liebig-University Giessen. The irradiated mice were bone marrow transplanted on the same day and kept individually in IVC cages till the end of the experiment (day 114).

Donor mice, either WT or iNOS KO, (12 weeks old) were injected with 500 IU heparin i.p. and after 10 minutes and complete distribution of heparin, the mice were anesthetized by isoflurane and then euthanized by cervical dislocation. After immersing distal parts of the mouse body in ethanol 70%, skin of the legs and all the muscles covering the femora and tibiae were removed. The femora and tibiae were put into ice cold DPBS buffer and kept on ice. From this step until injection of the bone marrow cells, all the steps of the bone marrow cell isolation and transport was done on ice

and centrifugation was performed at 4 °C. 1% fetal calf serum (FCS), 100 U/ml penicillin, and 1000 U/ml streptomycin were added to RPMI 1640 medium. In a laminar flow hood, bone ends were separated with a scalpel and the bone shafts were flushed with a needle on a 5 ml syringe with RPMI 1640 medium into 15 ml Falcon tube. The isolated bone marrow (from femora and tibiae of the mouse) was centrifuged at 400 g for 5 minutes. The supernatant was cautiously discarded and the pellet was carefully suspended within 1 ml RPMI 1640 medium by several cautious pipetting. The cell suspension was passed through a 100 µm cell strainer and collected in a new 15 ml falcon tube which was placed below the cell strainer. The cell strainer was washed with 1 ml of medium, trying to pass the cell remaining on the cell strainer. Afterwards, the suspension was centrifuged at 400 g for 5 minutes, the supernatant was carefully discarded and the pellet was gently resuspended with 1 ml medium by repeated pipetting. Approximately 2.5×10^7 nucleated cells were isolated from each donor mouse. These cells were used for transplantation to 4-5 recipient mice. Approximately 4-5 hours after the end of irradiation, 200 µl medium containing 5×10^6 donor bone marrow cells was injected into the lateral tail vein of each recipient mouse. The recipient mice were warmed before injection of bone marrow cell suspension, so that tail vein was dilated. Enrofloxacin (with dosage of 10 mg/kg body weight) was added in drinking water of the transplanted chimeric mice for 2 weeks to avoid infection.

Performing BMT technique on WT and KO mice led to generation of four different groups of chimeric mice. In this project, irradiated WT mice that received bone marrow cells from WT mice are abbreviated as WT(WT), and irradiated iNOS^{-/-} mice that received bone marrow cells from iNOS^{-/-} mice are named as KO(KO). Irradiated WT mice that received bone marrow cells from iNOS^{-/-} mice are termed as WT(KO), and *vice versa*, irradiated iNOS^{-/-} mice that received bone marrow cells from WT mice are termed as KO(WT).

42 days after BMT, peripheral blood samples were collected and genomic DNA was isolated by DNeasy Blood and Tissue Kit (Qiagen, Germany) according to the manufacturer's protocol from blood cells and success of BMT was tested by PCR with primers suggested by the Jackson Laboratory (<https://www.jax.org/Protocol?stockNumber=002609&protocolID=24473>). 100 µl blood was obtained by phlebotomy from superficial temporal vein of the chimeric mice and put directly and immediately into a 0.5 ml Eppendorf tube, which contained 20 µl of 10 mM EDTA. The tube was gently shaken so that blood and EDTA are mixed. Blood samples were stored at -20 °C until PCR time.

PCR was performed in final reaction mixture volume of 15 µl. The mixture contained 6.05 µl H₂O, 0.3 µl dNTP mix, 3 µl FlexiBuffer, 1.2 µl MgCl₂, 0.75 µl of each primer, 0.2 µl GoTaq-Polymerase, and 2 µl DNA. The initial denaturing temperature was 94 °C for 5 minutes, and the cycling parameters were 94 °C for 30 s, 65 °C (-0,5 °C per cycle) for 30 s, and 68 °C for 30 s (11 cycles), and afterwards next cycling parameters were 94 °C for 30 s, 60 °C for 30 s, and 72 °C for 30 s (29 cycles), and finally 72 °C for 7 minutes.

2.2.2. Echocardiographic measurements

Echocardiography is a non-invasive imaging tool which enables the operator to have repeatable evaluation of the cardiovascular system in laboratory rodents. In this project echocardiography was performed by Dr. Simone Kraut and Mr. Nils Schupp before and after CIH exposure to check the effects of CIH. The first time point was one day before telemetry transmitter implantation (day 63) and the second time point was one day before the end of the experiment (day 113). The echocardiographic measurements were performed by means of a Vevo[®] 2100 high-resolution imaging system with a 40-MHz linear-array transducer.

Before performing the echocardiographic evaluation, to induce the anesthesia with isoflurane, the mouse was put in a transparent chamber with 3% isoflurane in 100% oxygen at a flow rate of 3 l/min. Subsequently, the mouse was placed in supine position on a regulated heating pad with all four limbs attached to ECG electrodes for monitoring heart rate. A mask was used to maintain anesthesia with 1.5-3.0% isoflurane added in 100% oxygen. A rectal thermometer was used to keep body temperature at 37 °C by regulated heating pad. Bepanthen[®] eye ointment was applied on the eyes of the mouse to protect the cornea from drying during the anesthesia. In order to increase the quality of the echocardiographic measurements, the chest and cranial abdominal area were shaved and a preheated and bubble free ultrasound gel was applied on the skin.

The whole echocardiography procedure took about 30 minutes. The Vevo[®] LAB software was used to calculate echocardiographic parameters. After echocardiographic evaluation, ultrasound gel was removed from the chest of the mouse. Afterwards, the mouse was returned to the cage and observed until complete recovery from anesthesia.

Different echocardiographic parameters were used to evaluate the phenotype and systolic function of the right and left ventricles as already described (Kraut, 2014):

Cardiac output (CO)

CO is defined as the volume of the blood, which is pumped out of the heart via the ascending aorta into the bloodstream in one minute. The CO is calculated using the formula, $CO = \text{stroke volume (SV)} \times \text{heart rate (HR)}$. Left ventricular outflow tract (LVOT) and velocity time integral (VTI) can be determined to calculate stroke volume ($SV = LVOT \times VTI$). VTI is the integral of the flow rate within the aorta during the systole. A decrease in CO shows a deterioration of the pumping function of the heart. The unit for CO is milliliters per minute. In this project the right ventricular CO has been calculated.

Cardiac index (CI)

In human medicine CI is a parameter that associates the CO to body surface area, in other words, this parameter relates heart performance to the size of the person's body. The unit of CI is liters per minute per body surface area in square meters (Saugel et al., 2015). In this project the CI has been calculated in accordance with the formula, $CI = CO / BW$ (g). The unit is milliliter per minute per body weight (BW) in grams.

Ejection fraction (EF)

EF is a parameter of the systolic function of the left ventricle and indicates the percentage of ejected blood during one contraction of the ventricle. This parameter can be calculated by end-systolic volume (ESV) and end-diastolic volume (EDV) as follows:

$$EF = [(EDV - ESV) / EDV] \times 100$$

Left ventricular internal diameter (LVID)

Left ventricular wall thickness (LVWT)

Pulmonary acceleration time/pulmonary ejection time (PAT/PET)

PAT is the time from the initial onset of pulmonary artery flow to peak pulmonary artery velocity and PET is the total duration of flow through the pulmonary artery. In the PH assessment, PAT and PET can be used to estimate pulmonary artery pressure (Kohut et al., 2016).

Tricuspid annular plane systolic excursion (TAPSE)

TAPSE is a parameter showing the right ventricular systolic function and is described as the distance that the tricuspid ring moves between end-diastole and end-systole. It is measured in mm and is associated with the right ventricular ejection fraction. This parameter also serves as an important prognostic factor for the survival of patients suffering from PH. A decreased TAPSE

indicates reduced contraction and thus impaired systolic function of the RV (Howard, 2011) (Vonk Noordegraaf and Galie, 2011).

Right ventricular internal diameter (RVID)

Right ventricular wall thickness (RVWT)

2.2.3. Telemetric blood pressure measurements

DSI radiotelemetry system was used to continuously record systemic blood pressure of the mice during nights. Catheter part of TA11PA-C10 implant was inserted into the abdominal aorta through the femoral artery. The transmitter part was placed subcutaneously and remained under skin for the duration of the experiment (7 weeks).

The implantation surgery was performed under isoflurane inhalation anesthesia. After induction of anesthesia (3-5% isoflurane in 100% oxygen at a flow rate of 3 l/min) in a transparent chamber, the mouse was put in supine position and the muzzle was put into the mask for maintenance of anesthesia (1.5-2.5% isoflurane in 100% oxygen at a flow rate of 1 l/min). Bepanthen[®] eye ointment was applied on the animal's eyes to protect the cornea from drying. Buprenorphine (with dosage of 0.1 mg/kg BW) as analgesic pre-treatment of the mice was injected s.c. after induction of anesthesia. ECG electrodes were attached for monitoring the heart rate. During the surgery the mouse was placed on a heating pad with regulated temperature via a rectal probe, to maintain physiological temperature (37 °C). The left leg was fixed and the surgical site, which was shaved thoroughly the day before surgery, was disinfected with disinfectant solution containing 1% povidone-iodine. A 1.5 cm long skin incision was made on the left inguinal part by means of a pair of scissors and the exposed connective tissue was bluntly dissected. A subcutaneous tunnel was made from the incision site towards the back of the mouse for the placement of the transmitter. For ligation and stabilization of femoral artery a polyester thread was put around femoral artery and vein distal to the incision site on femoral artery which also allowed further manipulation and stretching of the artery that facilitates catheter implantation. Thereafter, the femoral artery was clamped and separated bluntly from the femoral vein. Another polyester thread was put around the femoral artery to fix the catheter in the vessel following catheter implantation. A very small incision was made in the femoral artery by means of a pair of scissors below the clamped site. The catheter part of the implant was inserted into the femoral artery. Afterwards, the clamp was removed and the catheter was advanced approximately 1.5 cm into the vessel, so that the catheter tip was located

in the abdominal aorta. The polyester thread around the femoral artery was then tightened and knotted around the catheter inside the vessel. A very small amount of tissue adhesive (3M Vetbond™) was applied on the knot and the catheter-artery junction for further fixation of catheter and avoiding loosening of the knot and migration of the catheter. The transmitter part of the implant was placed in the already prepared subcutaneous tunnel and the skin was closed with single interrupted pattern by suture material (6.0 Prolene®). The mice were put in cage with Alpha-dri® bedding and monitored to wake up.

The animals were treated 3 days after operation with buprenorphine 3 times daily with the previously mentioned dosage and Enrofloxacin with dosage of 10 mg/kg BW subcutaneously. In addition, the mice received Enrofloxacin orally for further 3 days (5-10 mg/kg BW) in drinking water.

The transmitter implanted mice were given one-week time for recovery from the implantation surgery. With start of CIH/NOX during days, over the periods in which the mice were not under CIH or NOX (about 14 hours a day) blood pressure was measured. Systemic blood pressures (including MAP, SBP, and DBP) were measured during 10 seconds sampling periods (sampling rate of 500 Hz) with 60 seconds of not recording interval. The daily average of measured values was obtained by the Ponemah 6.11 software. Signals from implants were measured at atmospheric pressure before implantation of the transmitter to quantify and correct any signal drift before starting the experiments.

The implanted transmitter emits the blood pressure signals and the telemetry receiver (model RPC-1 DSI, USA) which was placed under the mouse cage received the transmitted signals. The receiver was attached to a personal computer (PC) via a data converter (Data Exchange Matrix™ DSI, USA) and a switch (16 Port Gigabit Switch, Cisco Systems, San Jose, California, United States). In order to prevent influence of ambient pressure, which can be different on different periods of measurement, a barometer (ambient pressure reference Model APR-1 DSI, USA) was designed in the setup.

2.2.4. CIH protocol

The current work was designed according to the previous investigations in our research group (Kraut, 2014), therefore the mouse model of CIH was used with similar conditions. After bone marrow reconstitution and telemetry transmitter implantation, each of the mentioned four chimeric

groups was randomly divided into two groups, either controls which were exposed to normoxia-normoxia cycles or hypoxic groups which were exposed to CIH.

One week after implantation, chimeric mice were individually housed in assigned custom-made cages for CIH. Thereafter, mice were exposed to CIH for 8 hours a day, 5 days per week, for 6 weeks. The O₂ concentration in the chambers was regulated using the Biospherix oxycycler. In the CIH chamber O₂ concentration was reduced from 21% (room air) to 7% and then returned to 21% in 2 minutes. In other words, each complete cycle took 2 minutes, allowing 30 cycles/hour. The O₂ concentration was monitored via an oxygen sensor inside the chamber during all CIH exposures and all the recordings were saved on the server of Justus Liebig University, Giessen. Moreover, the O₂ concentration inside the chamber was confirmed by another portable oxygen sensor (Dräger X-am 2000). The control mice were exposed to normoxia-normoxia cycles in which O₂ concentration of chambers were maintained at 21%. Control animals were housed in similar cages in the same room and were exposed to the same conditions, environmental stress, and ambient noise as mice exposed to CIH.

2.2.5. Experimental animal groups

Groups	Abbreviation of chimeric group	Recipient	Donor (Bone marrow cells)	Exposure
1	WT(WT)	C57BL/6J	C57BL/6J	NOX
2				CIH
3	WT(KO)	C57BL/6J	iNOS KO	NOX
4				CIH
5	KO(WT)	iNOS KO	C57BL/6J	NOX
6				CIH
7	KO(KO)	iNOS KO	iNOS KO	NOX
8				CIH

2.2.6. Measurement of hemodynamic parameters

After 6 weeks of exposure to CIH or normoxia-normoxia cycles the hemodynamic measurements of the chimeric mice was performed by Ms. Karin Quanz. Hemodynamic measurements included

right ventricular systolic pressure (RVSP), left ventricular systolic pressure (LVSP), and systemic blood pressure.

Before initiation of hemodynamic measurements, the measuring system was prepared. The Mikro-Tip® catheter was preheated to 37 °C about 30 minutes before the start of the measurement. Afterwards, the catheter was calibrated. The mouse was anesthetized in a transparent chamber by 3% isoflurane. After reaching the appropriate depth of anesthesia (loss of paw withdrawal reflex), the mouse was put in supine position on a heating pad with regulated temperature via rectal probe, to maintain physiological temperature (37 °C) during measurements. The anesthesia was maintained by 1.5-3.0% isoflurane. Electrocardiograph of the mouse was recorded and monitored during measurements. To avoid fur contamination over the surgical field, the fur of the neck area was moistened with disinfectant solution containing 1% povidone-iodine so that the fur stick to the skin. Approximately 2 cm of skin on the midline was removed by a pair of scissors and then connective tissue and the mandibular glands were bluntly dissected. The muscles that are located along and over the trachea were put aside so that a thread could be passed from below the trachea and a ligature could be placed loosely. Through a small incision of the ventral part of tracheal wall between ring cartilages and below the larynx, a tube (self-made from Vasofix® Safety 20 G) was inserted into the trachea. The ligature around the trachea was tightened to fix the tube and the animals was ventilated with a frequency of 150 breaths per minute and a tidal volume of 10 µl per gram of BW. A positive-end expiratory pressure of 1 cm water column was used to avoid collapse of the alveoli during mechanical expiration by the ventilator.

In order to perform RVSP measurements, the right jugular vein was dissected bluntly, fixed, and stretched with two threads. The cranial thread was ligated to stretch the vessel cranially, and the caudal thread was stretched caudally. After calibration, the pressure measuring catheter was entered in the jugular vein from an incision between the two threads, the catheter was advanced caudally approximately 5 mm into the vein and fixed with the caudal thread. Subsequently, the catheter was advanced into the right ventricle and the RVSP was recorded. For measuring LVSP and systemic pressure the same procedure was performed on the left carotid artery. The pressure was recorded when the catheter tip was inside the ascending aorta (systemic pressure) and also when it was advanced further into the left ventricle (LVSP).

The whole procedure of the hemodynamic parameters measurement took about 30 minutes for each mouse.

2.2.7. Blood sample collection for measurement of hematocrit

Hematocrit of the mice was measured after the hemodynamic measurements. The blood was directly collected from the heart with a capillary tube. The capillary tube was sealed on one end with hematocrit sealing compound, centrifuged at 16060 g for 5 minutes at room temperature, and the hematocrit was measured.

2.2.8. Blood sample collection for superoxide anion measurement

After completion of hemodynamic measurements, the skin of the thorax and the abdomen was excised with a pair of scissors on midline. The abdominal wall muscles were cut and the diaphragm was incised carefully in a way that the lungs and heart were not damaged. Parallel to midline, all ribs were cut by a pair of scissors, the thorax was opened, and the ribs were fixed laterally to the pad beneath the mouse with pins. Blood was taken from right ventricle by means of a 1 ml syringe which was attached to 24 G needle. The blood was used for superoxide anion measurements.

2.2.9. Flushing and harvesting of the lung

After the ribcage was opened, while the lungs were mechanically ventilated, both ventricles were incised with a small and sharp pair of scissors. A rinsing cannula was inserted through the right ventricle into the pulmonary artery. The irrigation of lungs was done with 0.9% saline (isotonic saline) at a pressure of 22 cm water column to flush the lungs from blood. The saline was entered from pulmonary artery and drained from the cut already made in the left ventricle. To avoid the collapse of the alveoli during flushing, the tracheal tube was removed and an irrigation cannula (self-made from Vasofix[®] Safety 20 G) was introduced into the trachea. Through this catheter isotonic saline solution with pressure of 10 cm water column was infused until the lung was distended. After complete irrigation of lungs from blood, the irrigation cannulas were removed and the lung was harvested.

2.2.10. Lung harvest for superoxide anion measurement

After the lungs were flushed, a small part of right lung (approximately 30 mg) was harvested to be used for superoxide measurement.

2.2.11. Preparation of lung samples for histology

The left lung lobe was used for histological analysis and immediately after flushing was fixed in formaldehyde for 24 hours at room temperature. After fixation, left lung was placed in embedding cassettes and kept for 24 hours in phosphate-buffered saline (PBS) at 4 °C and stored for another

24 hours in 50% ethanol. Eventually the left lung was in 70% ethanol and stored at 4 °C and finally dehydration was performed overnight with dehydration machine. The lungs were imbedded in paraffin immediately afterwards.

The 10x concentrated PBS was prepared by dissolving 80 g of NaCl, 2 g KCl, 11.5 g Na₂HPO₄ × 2 H₂O, 2.0 g KH₂PO₄ in 900 ml distilled water, and finally the volume was adjusted to 1 liter. This solution was diluted 1:10 and the pH was adjusted to 7.4 if needed with NaOH or HCl.

2.2.12. Harvesting of the heart and assessment of heart ratios

After harvesting the lung, the heart was separated from the thoracic cavity and surrounding connective tissue and the atria were removed. In order to measure different heart ratios ventricles were separated and weighed.

The weights of the ventricles were used to determine different heart ratios. Heart ratios were used to evaluate heart hypertrophy as a result of CIH in any of the chimeric groups and also to assess the degree of hypertrophy.

The following ratios were calculated:

- Right ventricle (mg) to left ventricle plus septum (mg) (Fulton index)
- Right ventricle (mg) to tibia length (mm)
- Left ventricle (mg) to tibia length (mm)

2.2.13. Preparation of lung samples and histological assessment of the degree of muscularization of pulmonary arterial vessels

2.2.13.1. Embedding

For embedding the lung samples in paraffin, the left lung was placed in casting mold and the labeled part of embedding cassette was put on top of the casting mold. Then melted paraffin was poured to completely fill the casting mold in a way that the labeled part of the embedding cassette was attached to the paraffin block at the end of embedding. Immediately afterwards, the casting mold was placed on a cooling plate until the paraffin was hardened and the paraffin block could easily be separated from the casting mold.

2.2.13.2. Sectioning

In this project lungs were cut by microtome with a thickness of 3 µm. The cut paraffin sections were mounted on the slides and put on a hot plate for drying.

2.2.13.3. Staining

Immunohistochemistry staining of the lung sections with antibodies against alpha smooth muscle actin and von Willebrand factor was performed as follows:

no.	Incubation time	Reagent	Note
1	60 minutes	Incubation in 58 °C	Melting paraffin
2	3 x 10 minutes	Xylol	Always fresh
3	2 x 5 minutes	Ethanol 99.6% (absolute)	Rehydration
4	5 minutes	Ethanol 96%	Rehydration
5	5 minutes	Ethanol 70%	Rehydration
6	20 minutes	H ₂ O ₂ 3% in methanol (180 ml Methanol + 20 ml H ₂ O ₂ 30 %)	To avoid unspecific binding and block endogenous peroxidases (always fresh)
7	2 x 5 minutes	Wash with aqua dest. (Millipore)	
8	2 x 5 minutes	Wash with PBS	
9	15 minutes	Trypsin (Proteolytic unmasking)	1 : 3 dilution, In the dark box, 38 °C
10	4 x 5 minutes	Wash with PBS	
11	20 minutes	Bovine Serum Albumin (BSA) 10%	Block unspecific binding
12	3 x 5 minutes	Wash with PBS	
13	30 minutes	Rodent Block M (MM HRP Plymer Kit)	Block of nonspecific bonding and endogenous mouse IgG
14	3 x 5 minutes	Wash with PBS	

15	30 minutes	Primary antibody, anti-alpha smooth muscle actin	1 : 800 dilution with antibody diluent
16	4 x 5 minutes	Wash with PBS	
17	20 minutes	MM HPR Polymer	Binds to AB
18	3 x 5 minutes	Wash with PBS	
19	About 1-4 minutes	Vector VIP [®] Substrate kit	Violet staining of SMC
20	5 minutes	Wash with faucet water	
21	2 x 5 minutes	Wash with PBS	
22	20 minutes	BSA 10%	
23	3 x 5 minutes	Wash with PBS	
24	20 minutes	Serum block I	2,5% normal horse Serum ImmPRESS Kit Anti-Rabbit Ig
25	30 minutes	Primary antibody, anti-von Willebrand factor	Dilution 1 : 1100, 37 °C
26	4 x 5 minutes	Wash with PBS	
27	30 minutes	Secondary antibody	ImmPRESS Kit Anti-Rabbit Ig, Peroxidase
28	4 x 5 minutes	Wash with PBS	
29	1 – 40 seconds	DAB substrate kit	Brown staining of Endothelial cells
30	5 minutes	Wash with faucet water	
31	2-3 minutes	Methyl green	On the hotplate 60 °C, Staining of cell nuclei

32	1 minute	Wash with aqua dest. (Millipore)	
33	2 x 30 seconds	Ethanol 96%	
34	2 x 30 seconds	Isopropyl alcohol	
35	3 x 2 minutes	Xylol	
36	60 minutes	Pertex and cover lid	Let to be dry

2.2.13.4. Assessment of the degree of muscularization in pulmonary arterial vessels

After immunohistochemistry staining, the sections were assessed by a computer-assisted picture analysis software. The degree of muscularization of all small vessels (diameter of 20-70 μm) and medium vessels (diameter of 70-150 μm) in each lung section were analyzed. The muscularized parts of the vessel wall were stained violet when VIP substrate interacted with the secondary antibody which was bound to the anti-alpha smooth muscle actin. The endothelium of the vessels was stained brown when DAB substrate interacted with the secondary antibody which was attached to anti-von Willebrand factor.

To determine the degree of muscularization, the vessels were manually marked and their lumen area was detected automatically by the software. After confirming the marked lumen, muscularized proportion of the vessel wall (violet part) was determined automatically by a colorimetric spectrometric measurement. Subsequently, the measured values of vessel muscularization were automatically transferred to a Microsoft excel-file.

All the small vessels and medium vessels in each lung section were analyzed. To categorize these vessels, the percentage of violet stained part of the vessel to the total circumference of the vessel was determined.

The cutoff values between the categories were classified as follows:

- Non-muscularized: $\leq 5\%$ of violet-stained area of vascular circumference
- Partial-muscularized: $> 5 - \leq 70\%$ of violet-stained area of vascular circumference
- Full-muscularized: $> 70\%$ of violet-stained area of vascular circumference

2.2.14. Superoxide anion measurement by electron spin resonance (ESR) spectroscopy

The spin probe 1-hydroxy-3-methoxycarbonyl-2,2,5,5-tetramethyl-pyrrolidine (CMH) was used for the superoxide anion ($O_2^{\cdot-}$) measurements by ESR spectroscopy in this project as already described in our laboratory (Sommer et al., 2017). By using polyethylen-glycol conjugated superoxide dismutase (pSOD) which converts $O_2^{\cdot-}$ into either O_2 or H_2O_2 , it can be calculated that how much of the total free radicals in the sample (detected by CMH) has been superoxide with the following formula:

$$\text{Superoxide} = \text{CMH signal} - (\text{pSOD} + \text{CMH}) \text{ signal}$$

The concentration of CMH solution used in the experiments was 5 mM and the concentration of pSOD solution was 1000 U/ml. The prepared samples or controls had the final volume of 300 μ l in which final concentration of CMH was 0.5 mM and the final concentration of pSOD was 50 U/ml.

For preparation of 1 liter of ESR buffer (Krebs-Hepes buffer) 5.786 g NaCl, 0.350 g KCl, 0.368 g $CaCl_2 \times 2 H_2O$, 0.296 g $MgSO_4 \times 7 H_2O$, 2.1 g $NaHCO_3$, 0.142 g KH_2PO_4 , 1.009 g D-glucose, 5.206 g Na-HEPES was used. All the mentioned ingredients were ultra-pure chemicals (Sigma-Aldrich, St. Louis, USA) and the used water was double-distilled. The buffer was filtered by a 0.22 μ m filter, and stored in $-20^\circ C$. The ESR buffer pH was adjusted to 7.4 before each use.

A small part of the right lung (approximately 30 mg) was used for superoxide anion measurement. This small part was immediately put on ice after separation from the flushed lungs. For homogenization of lung samples 500 μ l cold ESR buffer and 1 μ l protease inhibitor cocktail (Sigma-Aldrich, St. Louis, USA) were added to a 1.5 ml Eppendorf tube containing beads and the lung tissue. The tubes were kept on ice. The tissue was homogenized by homogenization machine (Bullet Blender[®] Homogenizer) for 2 minutes. After homogenization the tubes were centrifuged at $4^\circ C$, 13000 RPM, for 5 minutes. Tubes were put back on ice immediately after centrifugation.

Similarly, immediately after taking blood samples, the blood samples were poured in 1.5 ml Eppendorf tubes and kept on ice (without homogenization).

ESR samples were prepared from the blood samples or the lung homogenate as following:

Steps	1	2	3	4	5	6
Tubes	ESR Buffer	Lung homogenate / Blood	pSOD	Incubation time in 37 °C	CMH	Incubation time in 37 °C
Sample CMH	170 µl	100 µl	-	60 minutes	30 µl	30 minutes
Sample CMH + SOD	155 µl	100 µl	15 µl	60 minutes	30 µl	30 minutes
Control ESR Buffer	300 µl	-	-	60 minutes	-	30 minutes
Control CMH	270 µl	-	-	60 minutes	30 µl	30 minutes
Control SOD	255 µl	-	15 µl	60 minutes	30 µl	30 minutes

All the samples and controls were prepared in duplicate. In the first step, the above-mentioned volume of ice cold ESR buffer was added to each dedicated 1.5 ml tube. In the second step 100 µl of either lung homogenate or blood was added to the tubes. In the third step 15 µl of pSOD was added to the tubes mentioned in the above table. The contents of the tubes were mixed and incubated for 60 minutes in 37 °C with open lids. In the fifth step 30 µl of CMH was added to the tubes according to the above table. The contents of the tubes were mixed again and incubated for 30 minutes at 37 °C with open lids. Afterwards, the tubes were immediately put on ice and then the content of each tube was poured in the already prepared and labeled 1 ml syringes and snap frozen in liquid nitrogen in order to form a cylindrical frozen ESR sample. The syringes were kept in -80 °C until ESR spectroscopy measurement. Finally, Dr. Susan Scheibe and Mr. Nils Schupp measured CMH signal in the frozen samples by ESR spectrometer and the amount of superoxide anion in the samples was calculated.

CMH signal the lung samples were normalized to the protein concentration of lung homogenates (µg/µl). The protein concentration of lung homogenates was determined by Bio-Rad protein assays following the standard protocol (Bradford method) using Microplate Reader (Tecan Infinite M200, Grödig, Austria) measuring the absorption at 750 nm.

2.2.15. Statistical evaluation

The graphs presented in this work were prepared using the GraphPad PRISM Version 8.0.1 (GraphPad Software, California, USA) and this software was also used for statistical analysis of

the results. All data were depicted as mean values \pm standard error of the mean (SEM). Unless stated otherwise, the data were primarily analyzed by three-way ANOVA to determine the three-way interaction of the independent variables (genotype of non-bone marrow-derived cells, genotype of bone marrow-derived cells, and exposure) to address the main question “if the data demonstrate that the CIH response depends on the iNOS genotype combination of non-bone marrow-derived cells and bone marrow-derived cells”. In other words, three-way ANOVA was used to study the influence of interaction among the three independent variables on each readout. Moreover, Sidak's multiple comparisons test was performed to determine the effect of CIH in each of chimeric groups compared to the respective control NOX-exposed mice.

Afterwards, the effect of CIH in WT(WT) group on each readout was compared to effect of CIH in other chimeric groups. For this, in order to determine two-way interaction of genotype of the mice and exposure (two variables), two-way ANOVA was used to compare separately “WT(WT) NOX and CIH vs. WT(KO) NOX and CIH”, “WT(WT) NOX and CIH vs. KO(WT) NOX and CIH”, and “WT(WT) NOX and CIH vs. KO(KO) NOX and CIH”.

3. Results

3.1. Endpoint weight of chimeric mice after CIH exposure

The body weights of the mice at the end of experiment (on day 114) were compared in the chimeric groups. The three-way interaction was not significant ($P = 0.7526$). None of the two-way interactions were significant. The CIH-exposed mice in none of the chimeric groups showed significant different weight compared to the respective control NOX-exposed mice (Fig. 1).

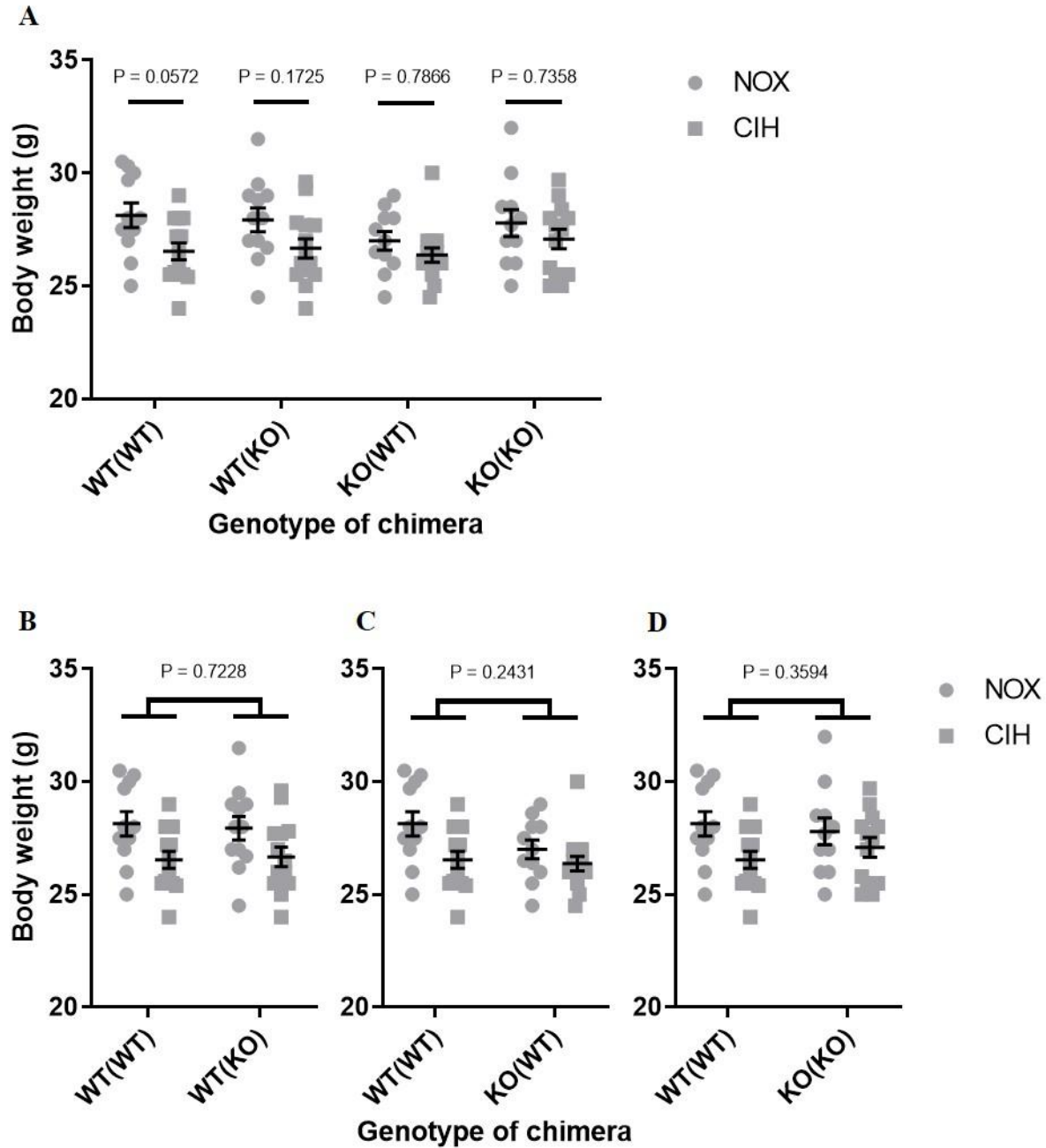


Figure 1: Endpoint body weight of different chimeric mice in the CIH

WT(WT) = WT mice transplanted with WT bone marrow, WT(KO) = WT mice transplanted with KO bone marrow, KO(WT) = KO mice transplanted with WT bone marrow, KO(KO) = KO mice transplanted with KO bone marrow, NOX = normoxia, CIH = chronic intermittent hypoxia, WT = C57BL/6J, KO = *iNOS*^{-/-}, g = gram, values are depicted as mean ± SEM, (A) analysis by three-way ANOVA and Sidak's multiple comparisons test, (B-D) analyses by two-way ANOVA (n = 11-15 each group)

3.2. Hematocrit level of chimeric mice after CIH exposure

The hematocrit of the mice at the end of experiment (on day 114) were compared in each chimeric group. The three-way interaction was not significant ($P = 0.2416$). None of the two-way interactions were significant. No statistically significant change was observed in hematocrit of different CIH-exposed chimeric mice compared to their respective NOX-exposed chimeric mice (Fig. 2).

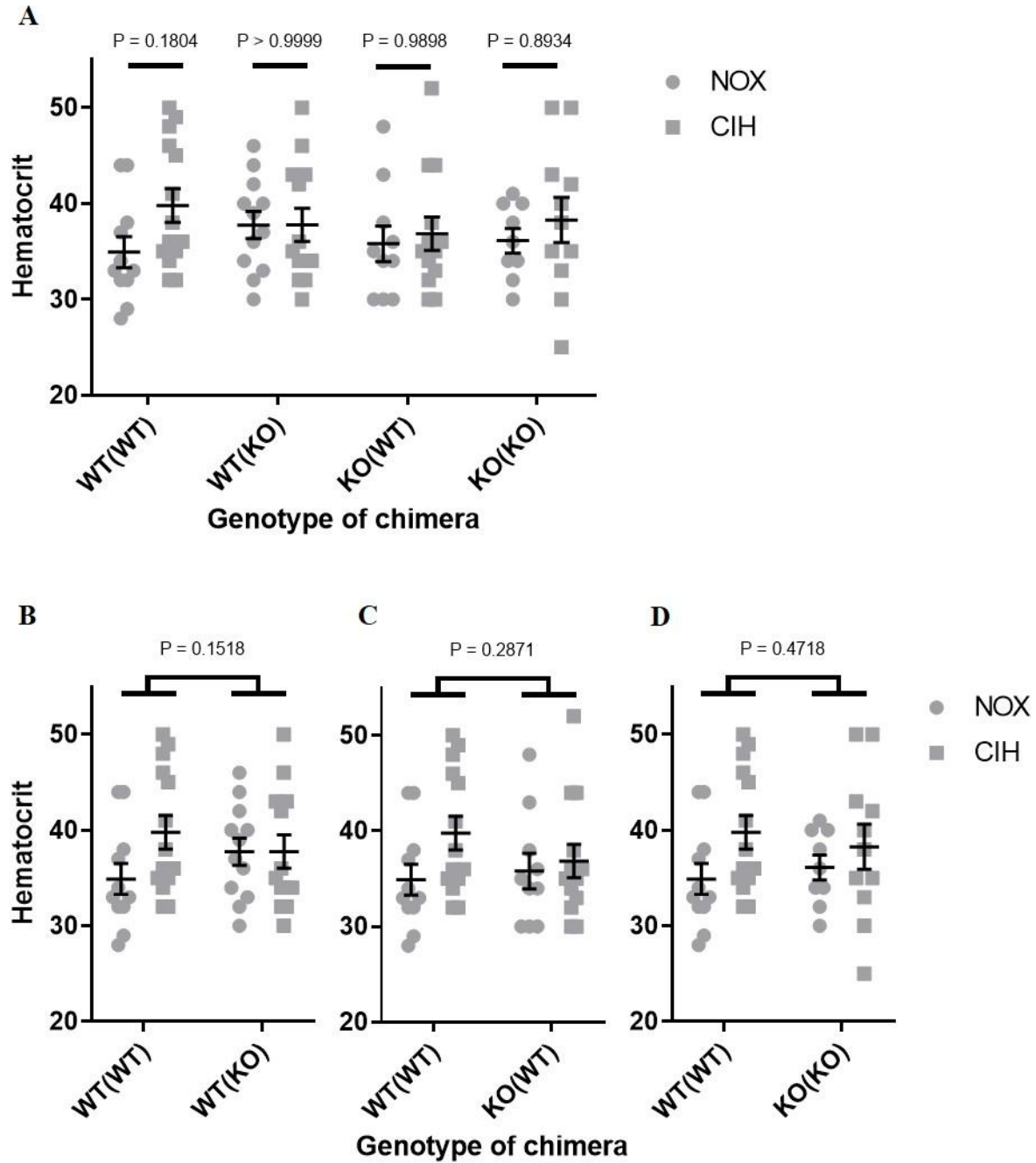


Figure 2: Hematocrit of different chimeric mice in the CIH

WT(WT) = WT mice transplanted with WT bone marrow, WT(KO) = WT mice transplanted with KO bone marrow, KO(WT) = KO mice transplanted with WT bone marrow, KO(KO) = KO mice transplanted with KO bone marrow, NOX = normoxia, CIH = chronic intermittent hypoxia, WT = C57BL/6J, KO = *iNOS*^{-/-}, values are depicted as mean \pm SEM, (A) analysis by three-way ANOVA and Sidak's multiple comparisons test, (B-D) analyses by two-way ANOVA, (n = 10-14 each group)

3.3. Different heart ratios of chimeric mice after CIH exposure

3.3.1. Ratio of weight of right ventricle to left ventricle plus septum (Fulton index)

Ratio of wet weight of right ventricle to weight of left ventricle plus septum ($RV/(LV+S)$) was used to determine the degree of right ventricular hypertrophy. The three-way interaction was not significant ($P = 0.6590$). None of the two-way interactions were significant. No statistically significant changes were observed in this ratio in the CIH-exposed mice compared to NOX-exposed mice in any of the groups (Fig. 3).

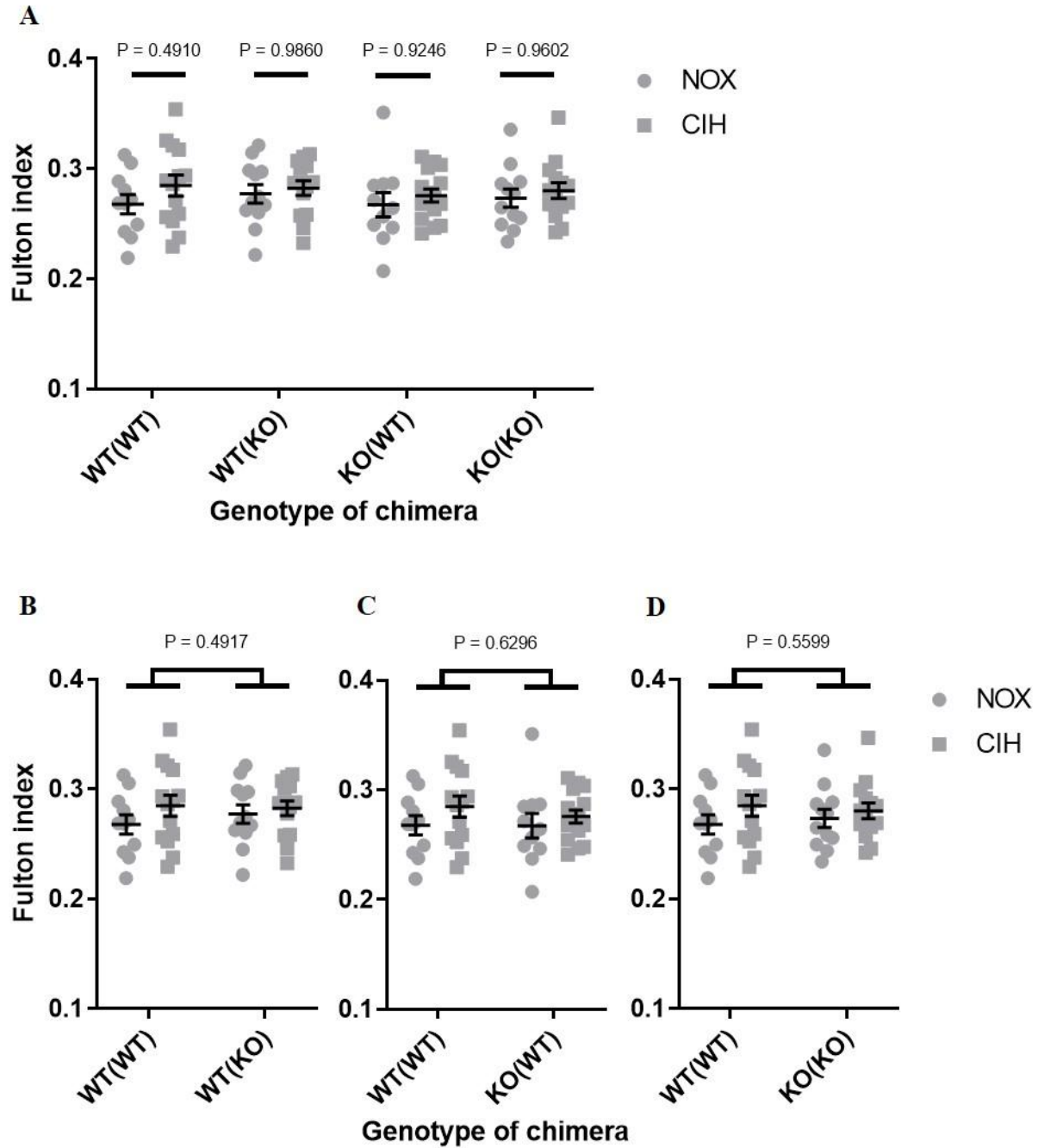


Figure 3: Fulton index (RV/(LV+S)) of different chimeric mice in the CIH

WT(WT) = WT mice transplanted with WT bone marrow, WT(KO) = WT mice transplanted with KO bone marrow, KO(WT) = KO mice transplanted with WT bone marrow, KO(KO) = KO mice transplanted with KO bone marrow, RV/(LV+S) = ratio of weight of right ventricle to weight of left ventricle plus septum, NOX = normoxia, CIH = chronic intermittent hypoxia, WT = C57BL/6J, KO = *iNOS*^{-/-}, values are depicted

as mean \pm SEM, **(A)** analysis by three-way ANOVA and Sidak's multiple comparisons test, **(B-D)** analyses by two-way ANOVA, (n = 11-15 each group)

3.3.2. Ratio of right ventricle to tibia length

Ratio of wet weight of right ventricle to the length of tibia (RV/tibia) was used as another parameter to determine the degree of right ventricular hypertrophy. The three-way interaction was not significant (P = 0.5804). None of the two-way interactions were significant. This parameter did not show any statistically significant changes in the CIH-exposed mice compared to NOX-exposed mice in any of the chimeric groups (Fig. 4).

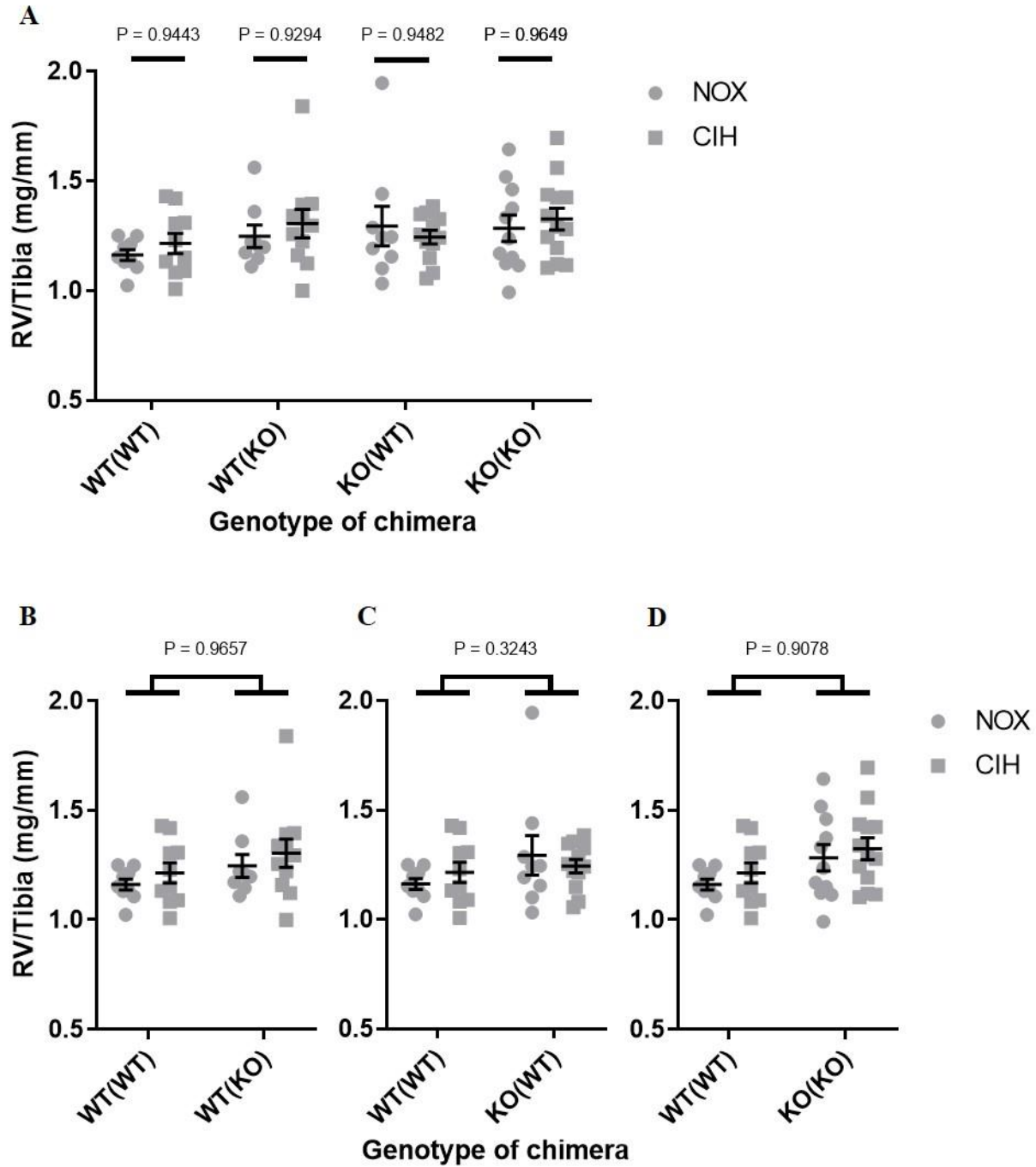


Figure 4: Ratio of weight of right ventricle to length of tibia of different chimeric mice in the CIH

WT(WT) = WT mice transplanted with WT bone marrow, WT(KO) = WT mice transplanted with KO bone marrow, KO(WT) = KO mice transplanted with WT bone marrow, KO(KO) = KO mice transplanted with KO bone marrow, NOX = normoxia, CIH = chronic intermittent hypoxia, WT = C57BL/6J, KO = iNOS^{-/-}, mg = milligram, mm = millimeter, values are depicted as mean ± SEM, (A) analysis by three-way ANOVA and Sidak's multiple comparisons test, (B-D) analyses by two-way ANOVA, (n = 8-13 each group)

3.3.3. Ratio of left ventricle to tibia length

The ratio of the wet weight of left ventricle to the length of tibia (RV/tibia) was used to determine the left ventricular hypertrophy. The three-way interaction was not significant ($P = 0.4612$). None of the two-way interactions were significant. NOX- and CIH-exposed mice in different chimeric groups showed no statistically significant difference in this ratio (Fig. 5).

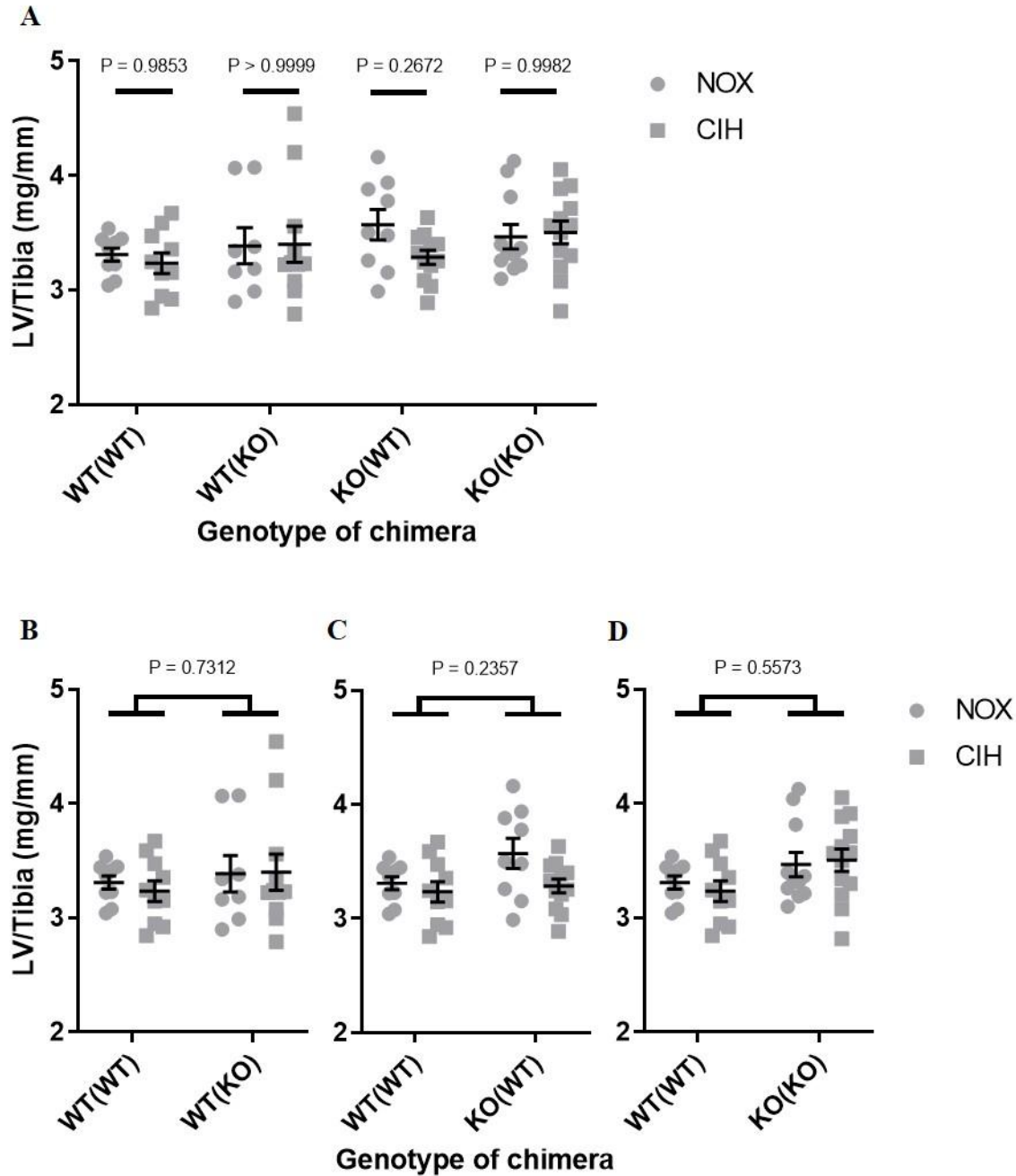


Figure 5: Ratio of weight of left ventricle to length of tibia of different chimeric mice in the CIH

WT(WT) = WT mice transplanted with WT bone marrow, WT(KO) = WT mice transplanted with KO bone marrow, KO(WT) = KO mice transplanted with WT bone marrow, KO(KO) = KO mice transplanted with KO bone marrow, NOX = normoxia, CIH = chronic intermittent hypoxia, WT = C57BL/6J, KO = iNOS^{-/-}, mg = milligram, mm = millimeter, values are depicted as mean ± SEM, (A) analysis by three-way ANOVA and Sidak's multiple comparisons test, (B-D) analyses by two-way ANOVA, (n = 8-13 each group)

3.4. Final invasive hemodynamic measurements

3.4.1. Right ventricular systolic pressure (RVSP)

RVSP was measured in final invasive hemodynamic measurements to determine whether the chimeric mice have developed PH due to CIH. The three-way interaction was not significant ($P = 0.9533$). None of the two-way interactions were significant. The CIH-exposed WT(WT) and WT(KO) mice showed significant higher RVSP compared to NOX-exposed mice in these chimeric groups, whereas KO(WT) and KO(KO) chimeric groups did not show significant different RVSP in the CIH-exposed mice compared to NOX-exposed mice (Fig. 6).

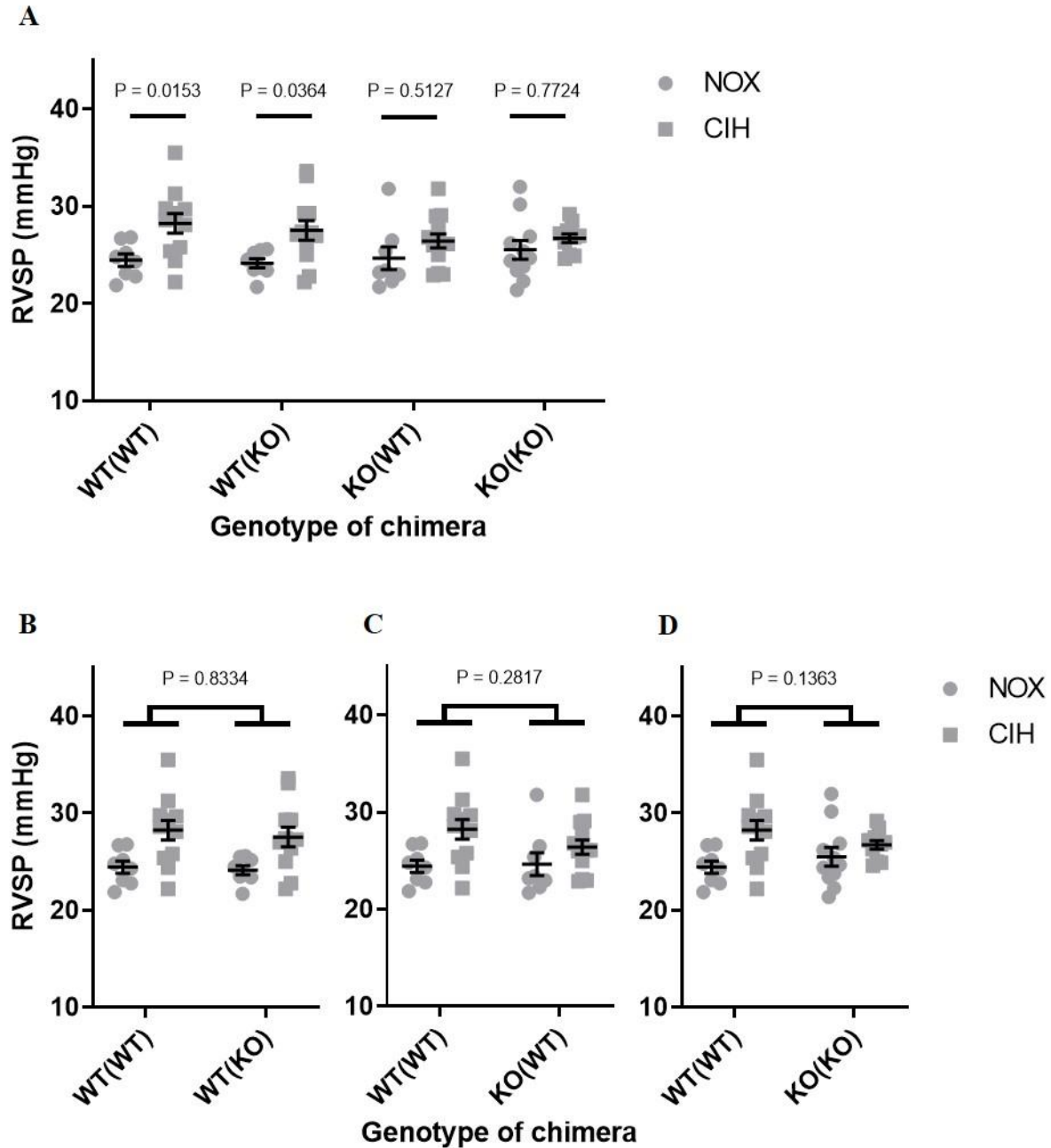


Figure 6: Right ventricular systolic pressure (RVSP) of different chimeric mice in the CIH

WT(WT) = WT mice transplanted with WT bone marrow, WT(KO) = WT mice transplanted with KO bone marrow, KO(WT) = KO mice transplanted with WT bone marrow, KO(KO) = KO mice transplanted with KO bone marrow, NOX = normoxia, CIH = chronic intermittent hypoxia, WT = C57BL/6J, KO = iNOS^{-/-}, mmHg = millimeter of mercury, values are depicted as mean ± SEM, (A) analysis by three-way ANOVA and Sidak's multiple comparisons test, (B-D) analyses by two-way ANOVA, (n = 8-13 each group)

3.4.2. Left ventricular systolic pressure (LVSP)

LVSP was measured in final hemodynamic measurements as an index of left ventricular function in the chimeric mice. The three-way interaction was not significant ($P = 0.9758$). None of the two-way interactions were significant. The CIH-exposed mice showed no statistically significant change in LVSP compared to NOX-exposed mice in any of the chimeric groups (Fig. 7).

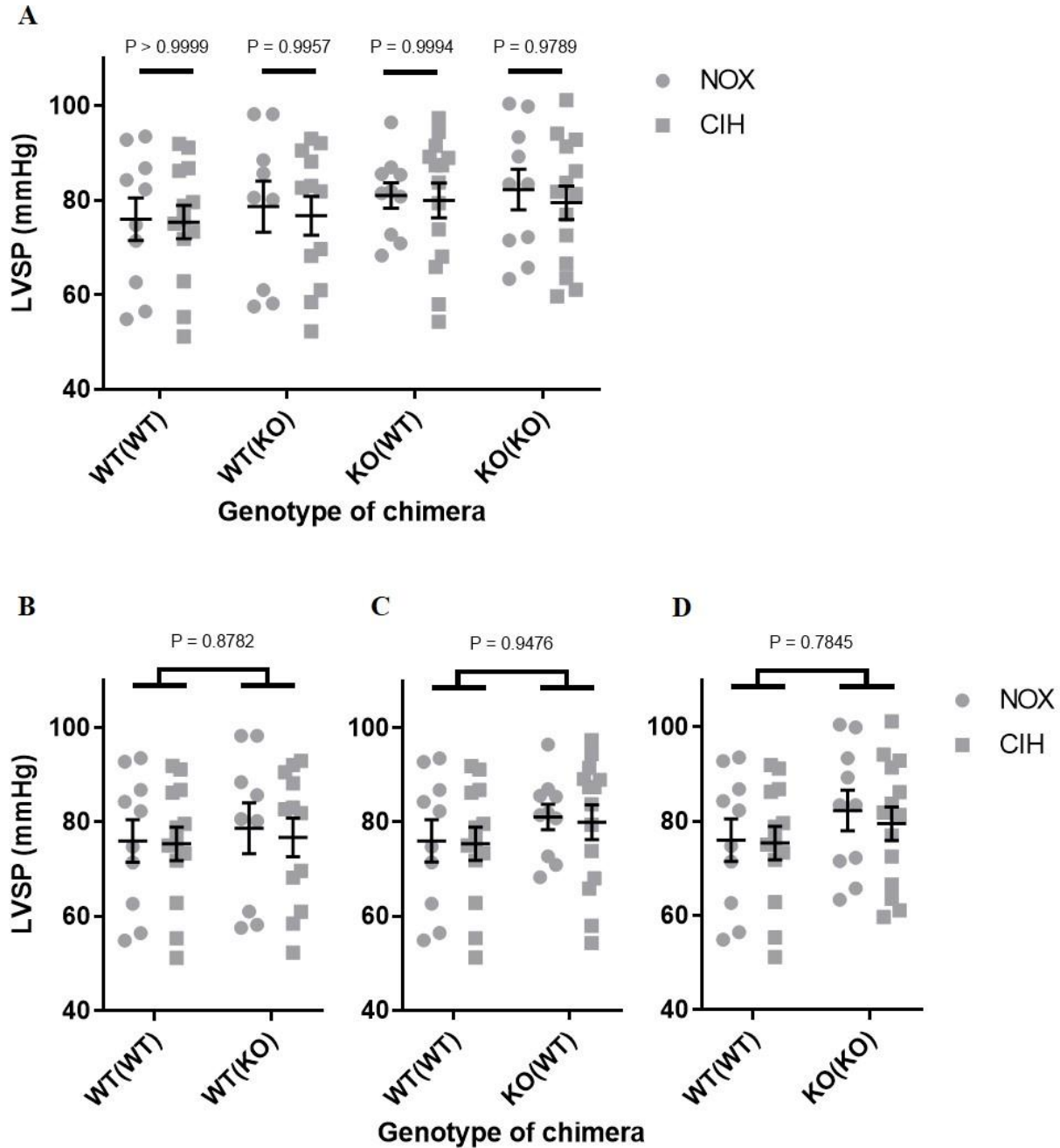


Figure 7: Left ventricular systolic pressure (LVSP) of different chimeric mice in the CIH

WT(WT) = WT mice transplanted with WT bone marrow, WT(KO) = WT mice transplanted with KO bone marrow, KO(WT) = KO mice transplanted with WT bone marrow, KO(KO) = KO mice transplanted with KO bone marrow, NOX = normoxia, CIH = chronic intermittent hypoxia, WT = C57BL/6J, KO = *iNOS*^{-/-}, mmHg = millimeter of mercury, values are depicted as mean \pm SEM, (A) analysis by three-way ANOVA and Sidak's multiple comparisons test, (B-D) analyses by two-way ANOVA, (n = 9-14 each group)

3.4.3. Mean arterial pressure (MAP)

MAP was measured in final invasive hemodynamic measurements to determine whether the chimeric mice have developed systemic hypertension due to CIH. The three-way interaction was not significant ($P = 0.2862$). None of the two-way interactions were significant. The CIH-exposed mice showed no statistically significant change compared to NOX-exposed mice in any of the chimeric groups (Fig. 8).

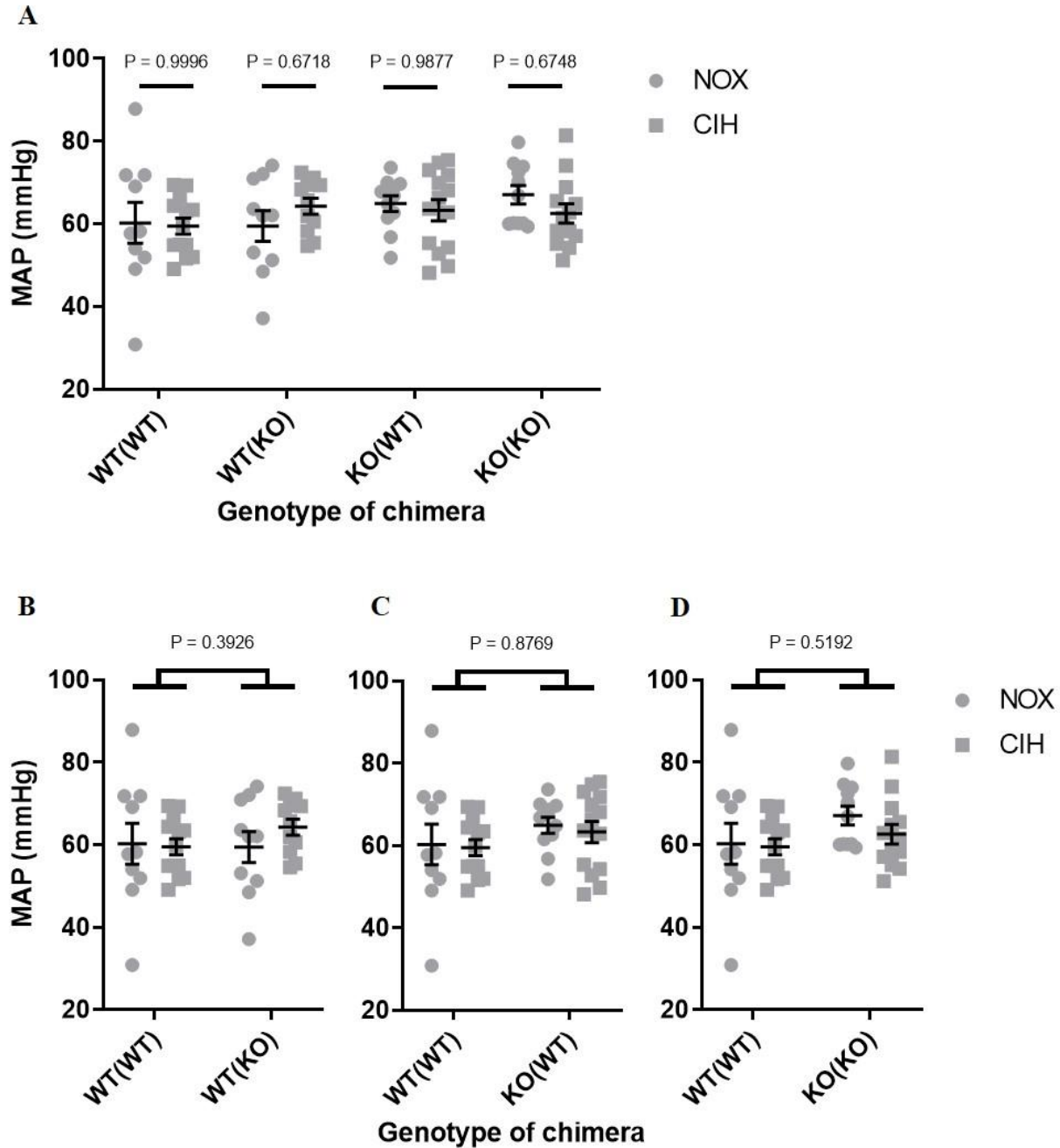


Figure 8: Mean arterial pressure (MAP) of different chimeric mice in the CIH

WT(WT) = WT mice transplanted with WT bone marrow, WT(KO) = WT mice transplanted with KO bone marrow, KO(WT) = KO mice transplanted with WT bone marrow, KO(KO) = KO mice transplanted with KO bone marrow, NOX = normoxia, CIH = chronic intermittent hypoxia, WT = C57BL/6J, KO = *iNOS*^{-/-}, mmHg = millimeter of mercury, values are depicted as mean \pm SEM, (A) analysis by three-way ANOVA and Sidak's multiple comparisons test, (B-D) analyses by two-way ANOVA, (n = 10-14 each group)

3.5. Telemetry blood pressure measurements

The measurement of MAP and also systolic and diastolic blood pressure was performed between days 70 and 114 of the experiment in the period of time in which the mice were not exposed to CIH or NOX. To evaluate the systolic blood pressure, diastolic blood pressure, or MAP on each day the average of all recorded pressures of a mouse in that day was used. The initial value of each chimeric mouse blood pressure was used as the baseline blood pressure before exposure of the chimeric mice to CIH or NOX.

3.5.1. Mean arterial pressure measurements

3.5.1.1. Wild type mice with wild type bone marrow

The mean arterial pressure of the WT(WT) mice was measured by the telemetric system. Two-way interaction was not significant for the changes of MAP between first and sixth week of exposure for NOX- vs. CIH-exposed mice (Fig. 9).

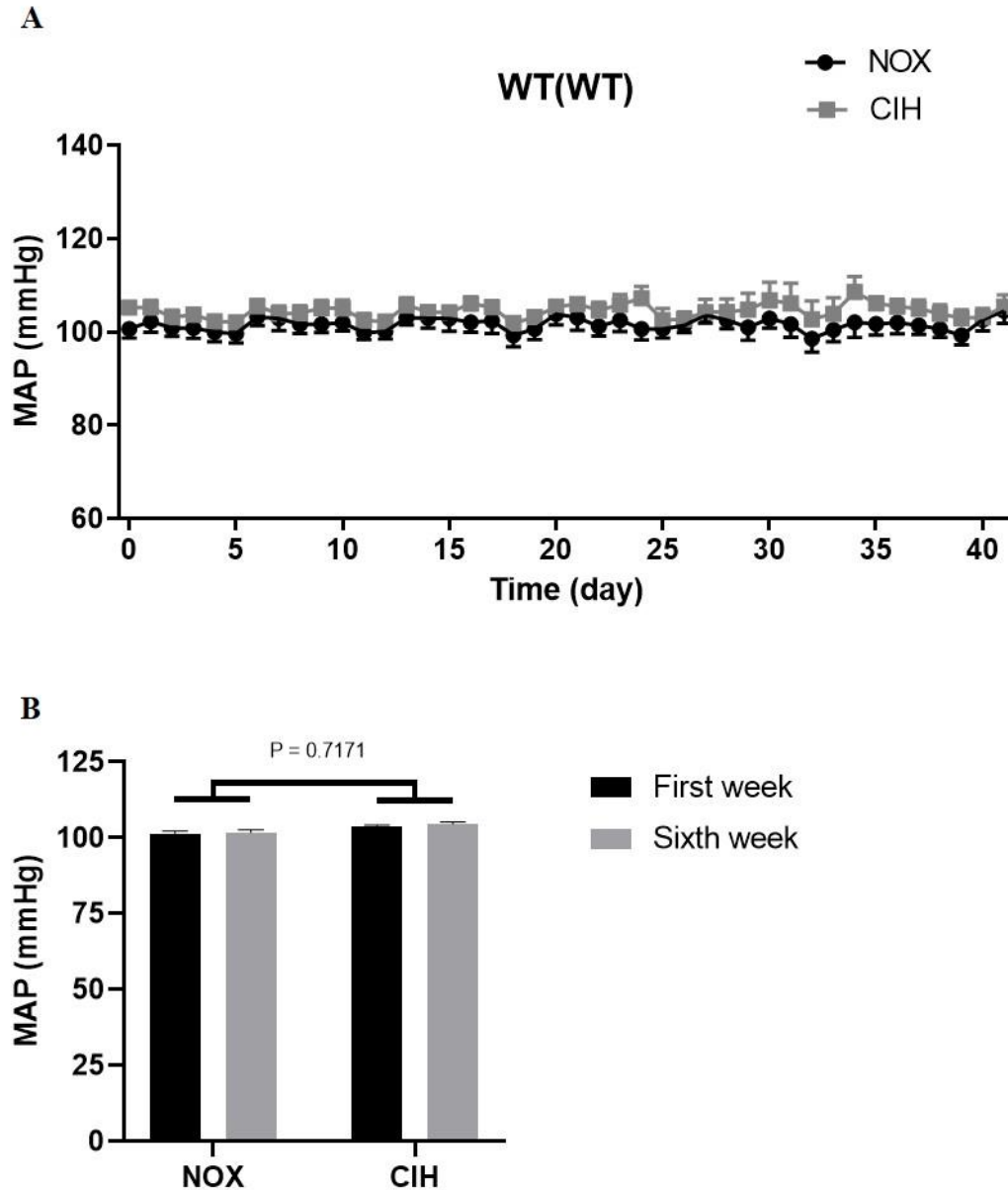


Figure 9: Mean arterial pressure (MAP) of WT(WT) mice in the CIH

WT(WT) = WT mice transplanted with WT bone marrow, NOX = normoxia, CIH = chronic intermittent hypoxia, WT = C57BL/6J, mmHg = millimeter of mercury, values are depicted as mean \pm SEM, (A) mean arterial pressure (daily), (B) mean arterial pressure (first week vs. sixth week), analysis by two-way ANOVA, (NOX n = 9, CIH n = 12)

3.5.1.2. Wild type mice with knock out bone marrow

The mean arterial pressure of the WT(KO) mice was measured by the telemetric system. Two-way interaction was not significant for the changes of MAP between first and sixth week of exposure for NOX- vs. CIH-exposed mice (Fig. 10).

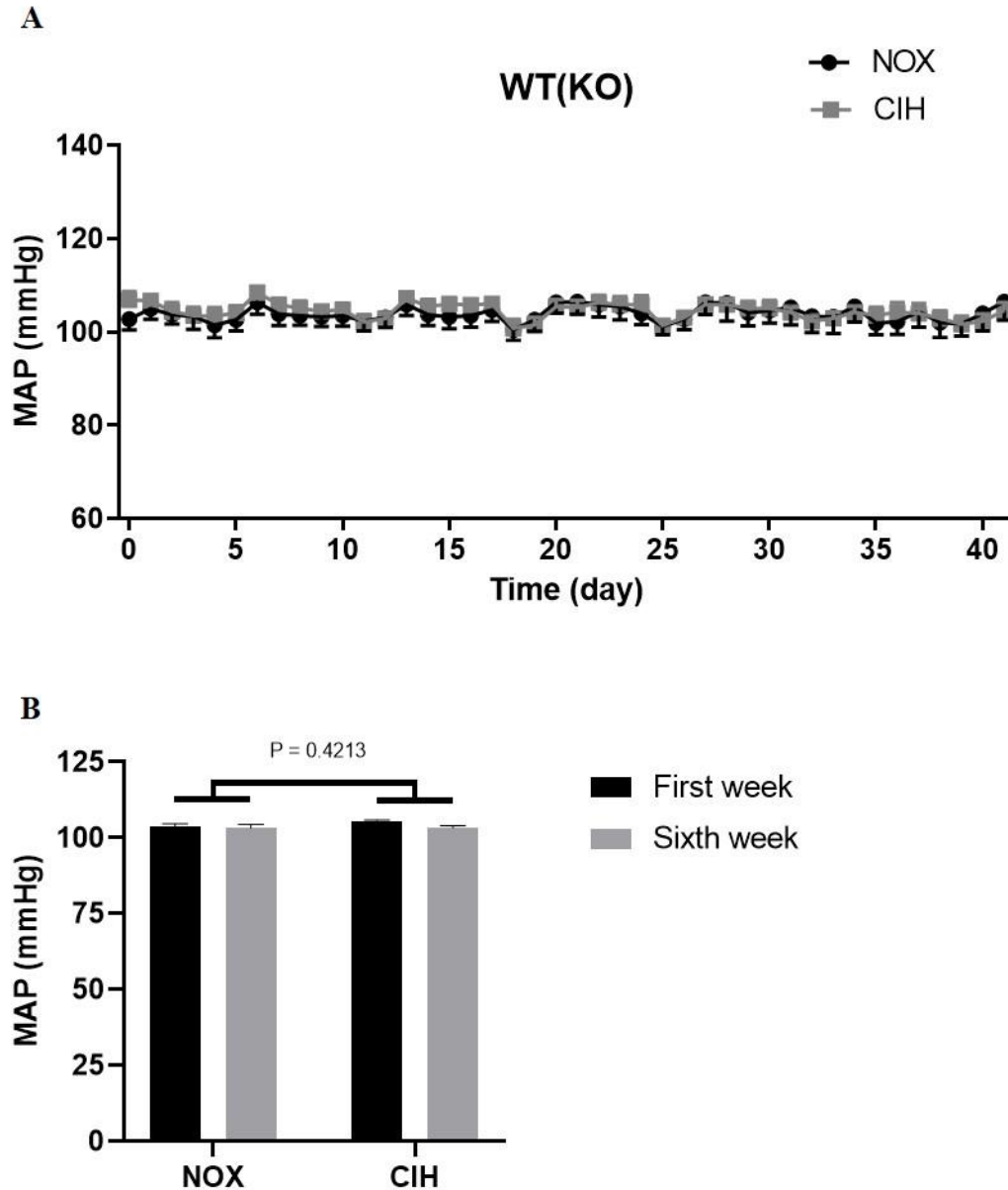


Figure 10: Mean arterial pressure (MAP) of WT(KO) mice in the CIH

WT(KO) = WT mice transplanted with KO bone marrow, NOX = normoxia, CIH = chronic intermittent hypoxia, WT = C57BL/6J, KO = *iNOS*^{-/-}, mmHg = millimeter of mercury, values are depicted as mean ± SEM, (A) mean arterial pressure (daily), (B) mean arterial pressure (first week vs. sixth week), analysis by two-way ANOVA, (NOX n = 8, CIH n = 10)

3.5.1.3. Knock out mice with wild type bone marrow

The mean arterial pressure of the KO(WT) mice was measured by the telemetric system. Two-way interaction was not significant for the changes of MAP between first and sixth week of exposure for NOX- vs. CIH-exposed mice (Fig. 11).

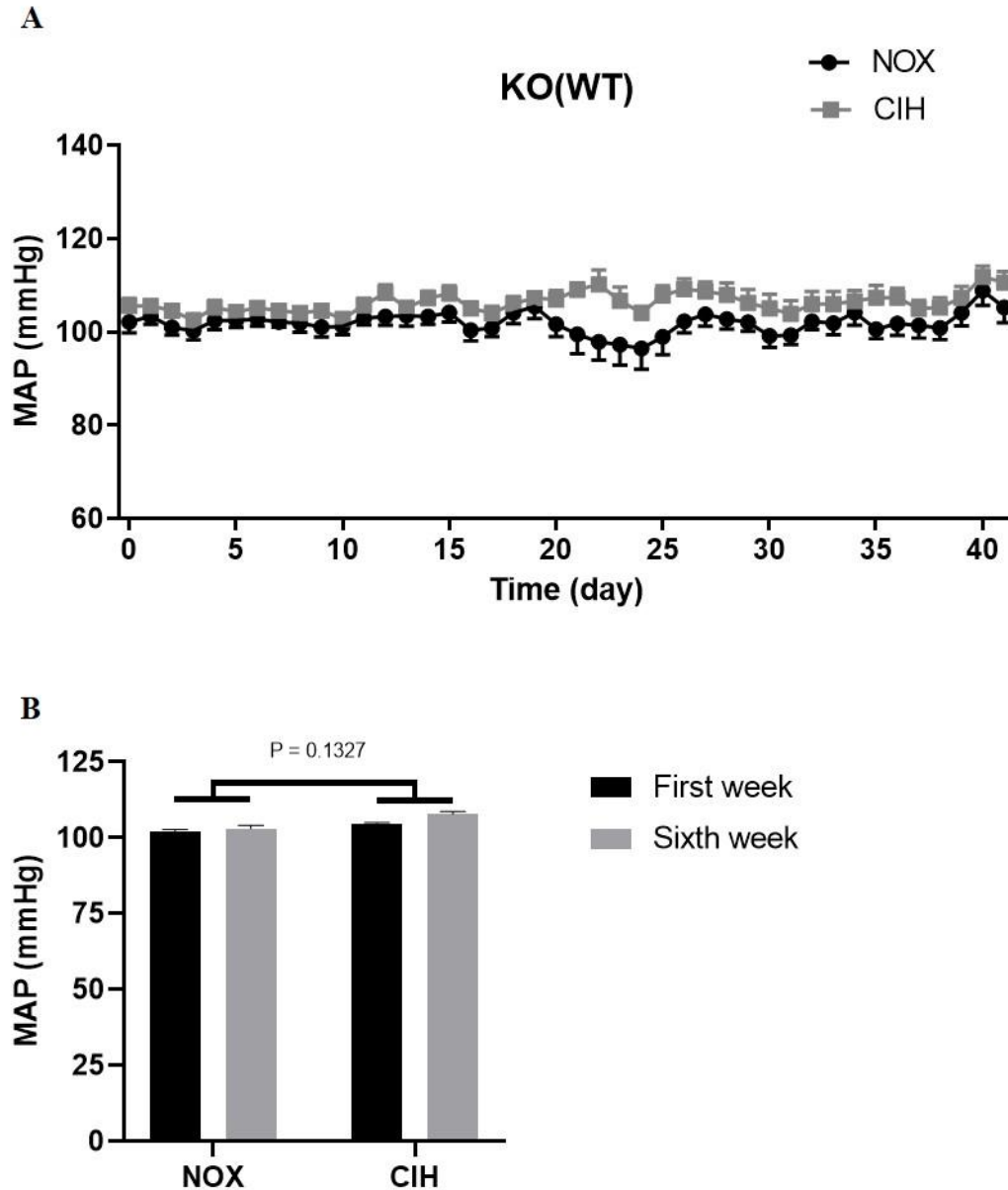


Figure 11: Mean arterial pressure (MAP) of KO(WT) mice in the CIH

KO(WT) = KO mice transplanted with WT bone marrow, NOX = normoxia, CIH = chronic intermittent hypoxia, WT = C57BL/6J, KO = *iNOS*^{-/-}, mmHg = millimeter of mercury, values are depicted as mean \pm SEM, (A) mean arterial pressure (daily), (B) mean arterial pressure (first week vs. sixth week), analysis by two-way ANOVA, (NOX n = 10, CIH n = 13)

3.5.1.4. Knock out mice with knock out bone marrow

The mean arterial pressure of the KO(KO) mice was measured by the telemetric system. Two-way interaction was not significant for the changes of MAP between first and sixth week of exposure for NOX- vs. CIH-exposed mice (Fig. 12).

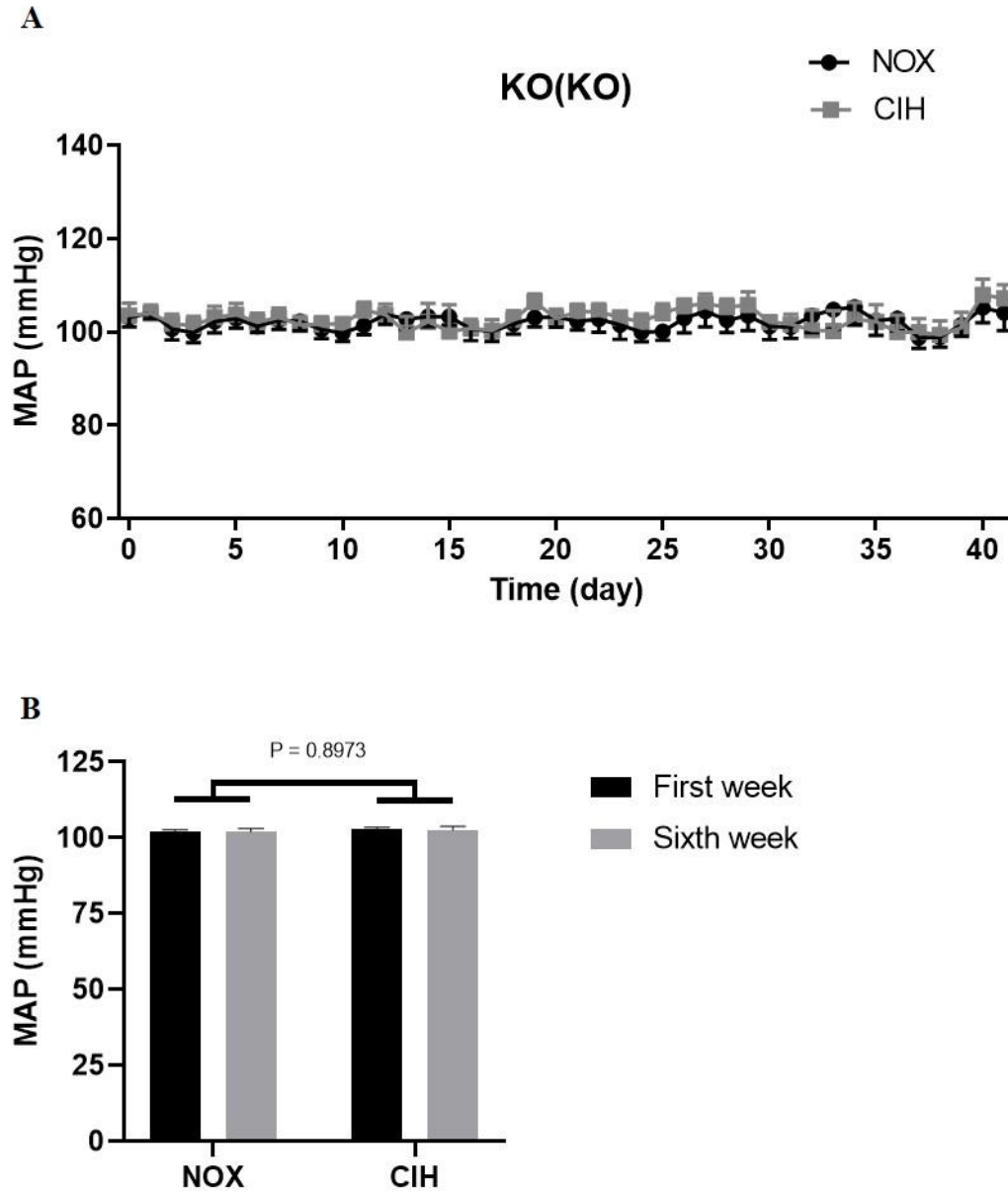


Figure 12: Mean arterial pressure (MAP) of KO(KO) mice in the CIH

KO(KO) = KO mice transplanted with KO bone marrow, NOX = normoxia, CIH = chronic intermittent hypoxia, KO = $iNOS^{-/-}$, mmHg = millimeter of mercury, values are depicted as mean \pm SEM, (A) mean arterial pressure (daily), (B) mean arterial pressure (first week vs. sixth week), analysis by two-way ANOVA, (NOX n = 9, CIH n = 12)

3.5.2. Systolic blood pressure measurements

3.5.2.1. Wild type mice with wild type bone marrow

The systolic blood pressure of the WT(WT) mice was measured by the telemetric system. Two-way interaction was not significant for the changes of SBP between first and sixth week of exposure for NOX- vs. CIH-exposed mice (Fig. 13).

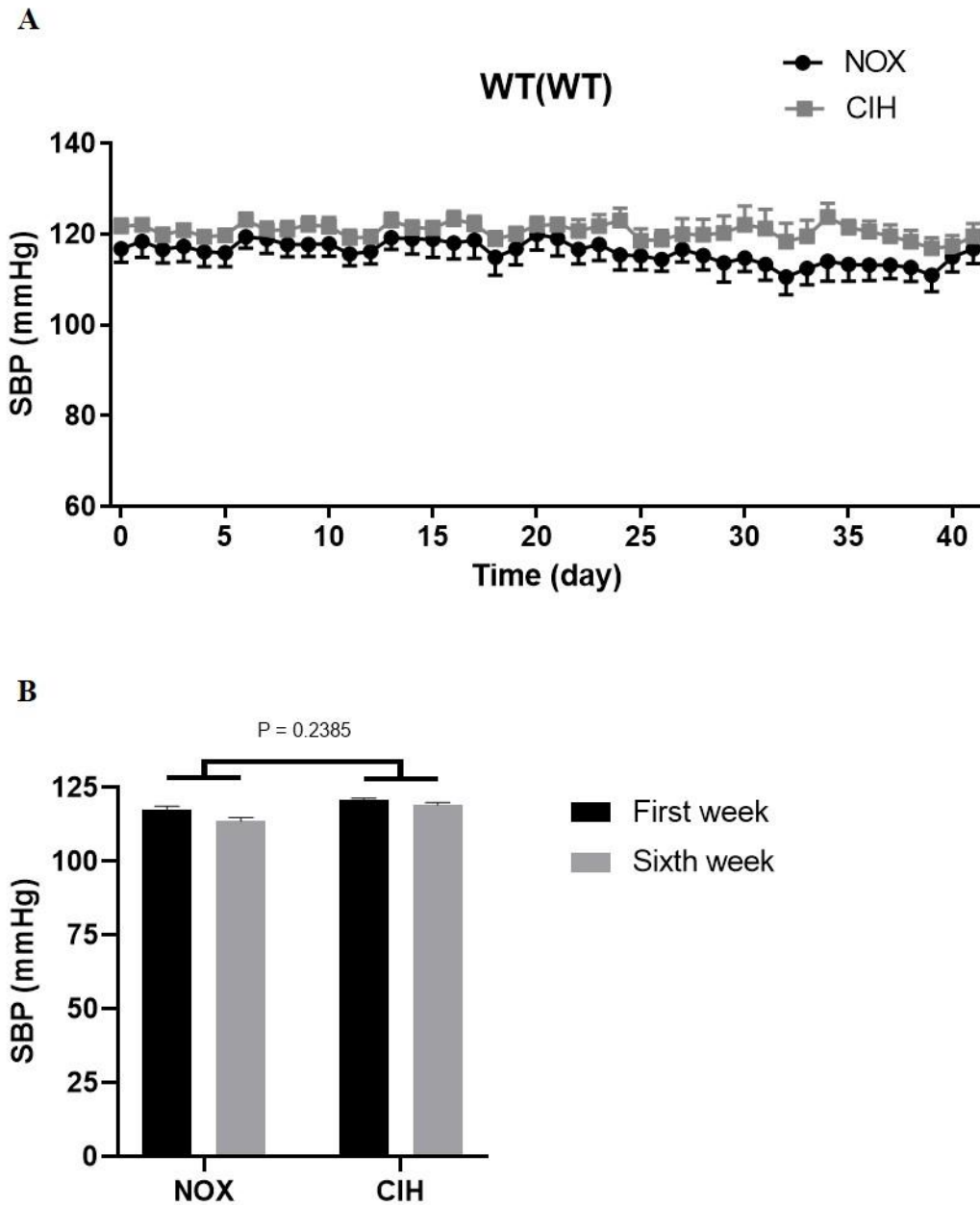


Figure 13: Systolic blood pressure (SBP) of WT(WT) mice in the CIH

WT(WT) = WT mice transplanted with WT bone marrow, NOX = normoxia, CIH = chronic intermittent hypoxia, WT = C57BL/6J, mmHg = millimeter of mercury, values are depicted as mean \pm SEM, (A) systolic blood pressure (daily), (B) systolic blood pressure (first week vs. sixth week), analysis by two-way ANOVA, (NOX n = 9, CIH n = 12)

3.5.2.2. Wild type mice with knock out bone marrow

The systolic blood pressure of the WT(KO) mice was measured by the telemetric system. Two-way interaction was not significant for the changes of SBP between first and sixth week of exposure for NOX- vs. CIH-exposed mice (Fig. 14).

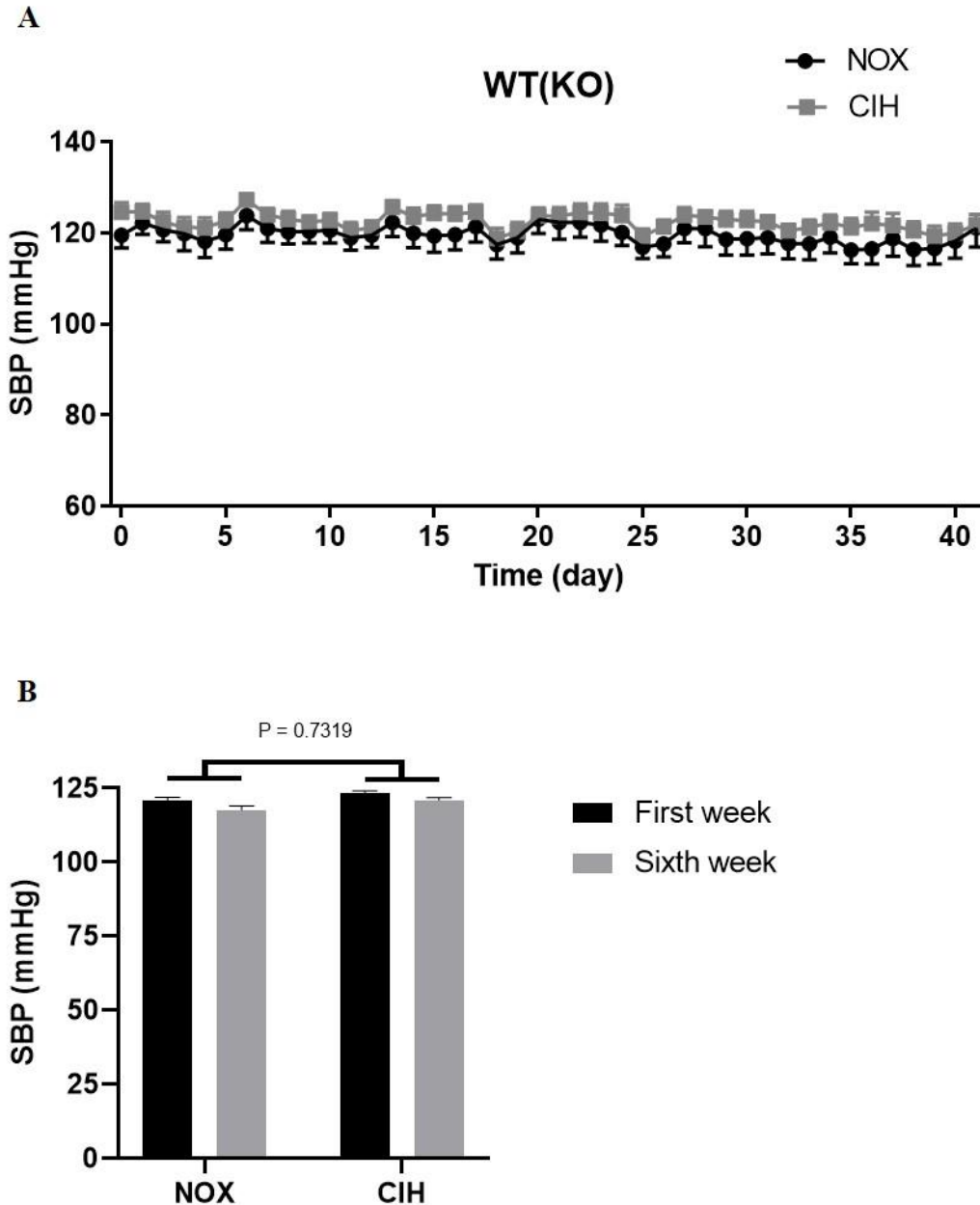


Figure 14: Systolic blood pressure (SBP) of WT(KO) mice in the CIH

WT(KO) = WT mice transplanted with KO bone marrow, NOX = normoxia, CIH = chronic intermittent hypoxia, WT = C57BL/6J, KO = *iNOS*^{-/-}, mmHg = millimeter of mercury, values are depicted as mean \pm SEM, (A) systolic blood pressure (daily), (B) systolic blood pressure (first week vs. sixth week), analysis by two-way ANOVA, (NOX n = 8, CIH n = 10)

3.5.2.3. Knock out mice with wild type bone marrow

The systolic blood pressure of the KO(WT) mice was measured by the telemetric system. Two-way interaction was not significant for the changes of SBP between first and sixth week of exposure for NOX- vs. CIH-exposed mice (Fig. 15).

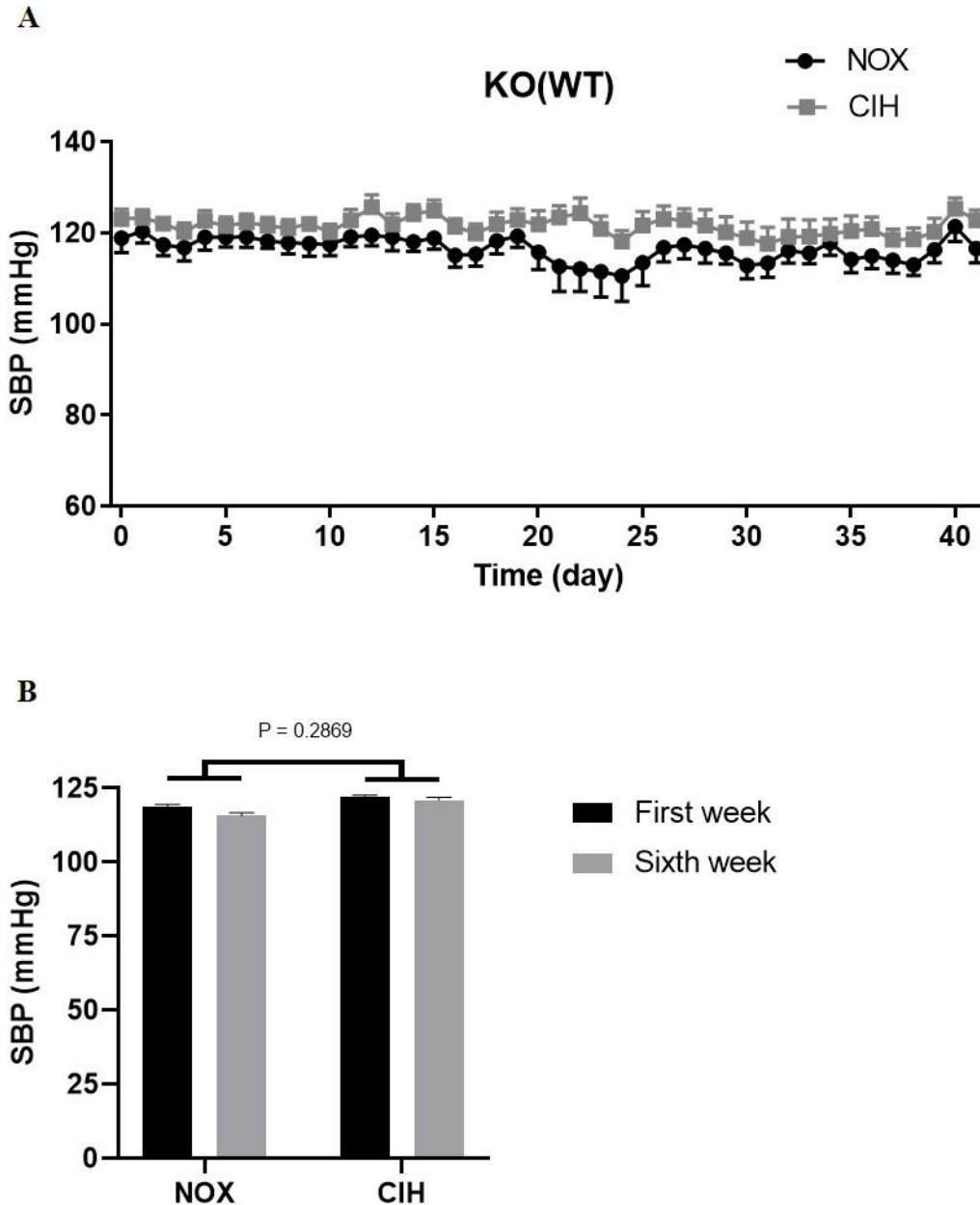


Figure 15: Systolic blood pressure (SBP) of KO(WT) mice in the CIH

KO(WT) = KO mice transplanted with WT bone marrow, NOX = normoxia, CIH = chronic intermittent hypoxia, WT = C57BL/6J, KO = *iNOS*^{-/-}, mmHg = millimeter of mercury, values are depicted as mean \pm SEM, (A) systolic blood pressure (daily), (B) systolic blood pressure (first week vs. sixth week), analysis by two-way ANOVA, (NOX n = 10, CIH n = 13)

3.5.2.4. Knock out mice with knock out bone marrow

The systolic blood pressure of the KO(KO) mice was measured by the telemetric system. Two-way interaction was not significant for the changes of SBP between first and sixth week of exposure for NOX- vs. CIH-exposed mice (Fig. 16).

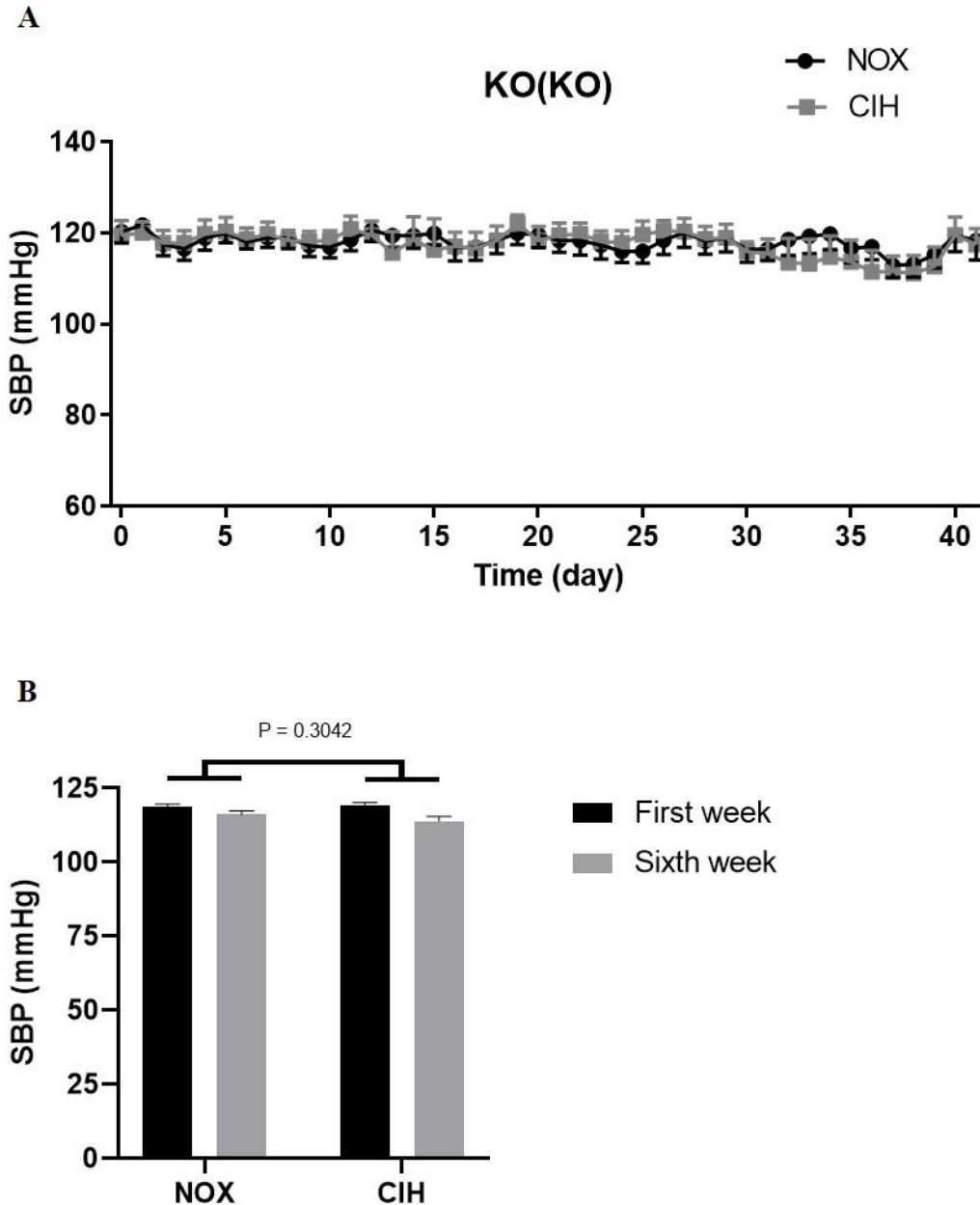


Figure 16: Systolic blood pressure (SBP) of KO(KO) mice in the CIH

KO(KO) = KO mice transplanted with KO bone marrow, NOX = normoxia, CIH = chronic intermittent hypoxia, KO = $iNOS^{-/-}$, mmHg = millimeter of mercury, values are depicted as mean \pm SEM, (A) systolic blood pressure (daily), (B) systolic blood pressure (first week vs. sixth week), analysis by two-way ANOVA, (NOX n = 9, CIH n = 12)

3.5.3. Diastolic blood pressure measurements

3.5.3.1. Wild type mice with wild type bone marrow

The diastolic blood pressure of the WT(WT) mice was measured by the telemetric system. Two-way interaction was not significant for the changes of DBP between first and sixth week of exposure for NOX- vs. CIH-exposed mice (Fig. 17).

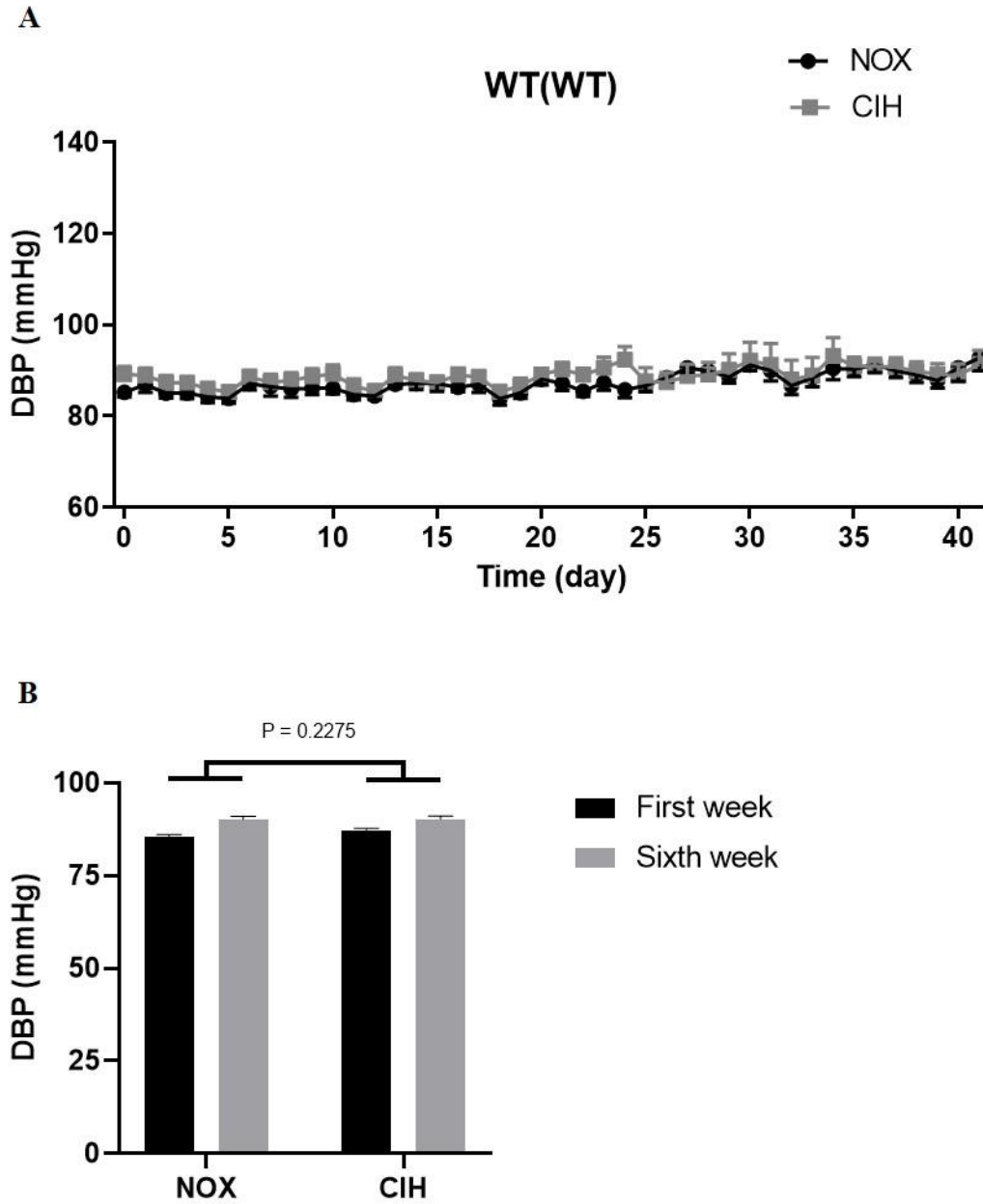


Figure 17: Diastolic blood pressure (DBP) of WT(WT) mice in the CIH

WT(WT) = WT mice transplanted with WT bone marrow, NOX = normoxia, CIH = chronic intermittent hypoxia, WT = C57BL/6J, mmHg = millimeter of mercury, values are depicted as mean \pm SEM, (A) diastolic blood pressure (daily), (B) diastolic blood pressure (first week vs. sixth week), analysis by two-way ANOVA, (NOX n = 9, CIH n = 12)

3.5.3.2. Wild type mice with knock out bone marrow

The diastolic blood pressure of the WT(KO) mice was measured by the telemetric system. Two-way interaction was significant for the changes of DBP between first and sixth week of exposure for NOX- vs. CIH-exposed mice. With a closer review of the individual values of DBP in the WT(KO) mice, it became evident that the observed change was related to one individual NOX-exposed mouse which had developed a relatively high DBP in the course of NOX exposure (Fig. 18).

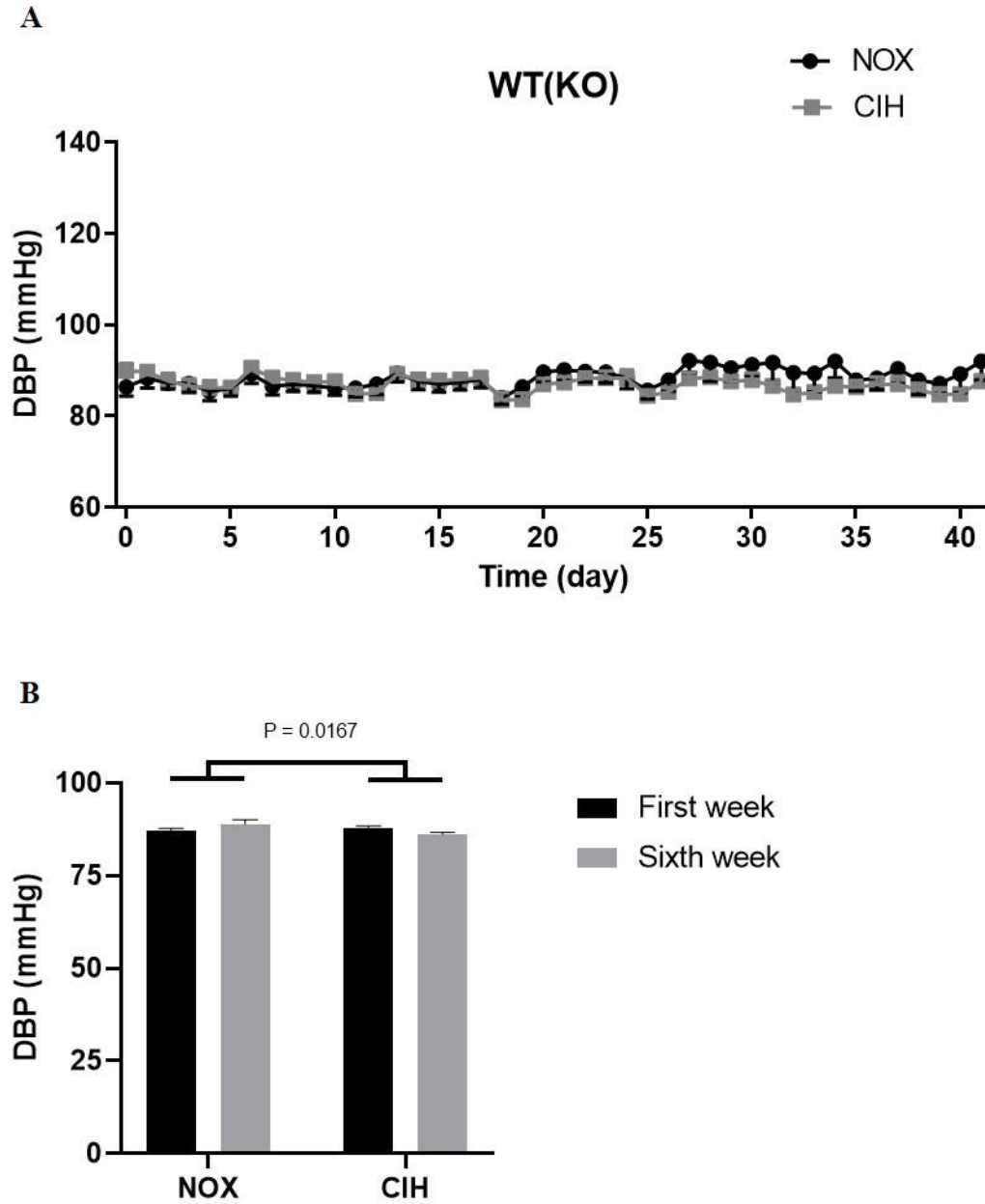


Figure 18: Diastolic blood pressure (DBP) of WT(KO) mice in the CIH

WT(KO) = WT mice transplanted with KO bone marrow, NOX = normoxia, CIH = chronic intermittent hypoxia, WT = C57BL/6J, KO = *iNOS*^{-/-}, mmHg = millimeter of mercury, values are depicted as mean \pm SEM, (A) diastolic blood pressure (daily), (B) diastolic blood pressure (first week vs. sixth week), analysis by two-way ANOVA, (NOX n = 8, CIH n = 10)

3.5.3.3. Knock out mice with wild type bone marrow

The diastolic blood pressure of the KO(WT) mice was measured by the telemetric system. Two-way interaction was not significant for the changes of DBP between first and sixth week of exposure for NOX- vs. CIH-exposed mice (Fig. 19).

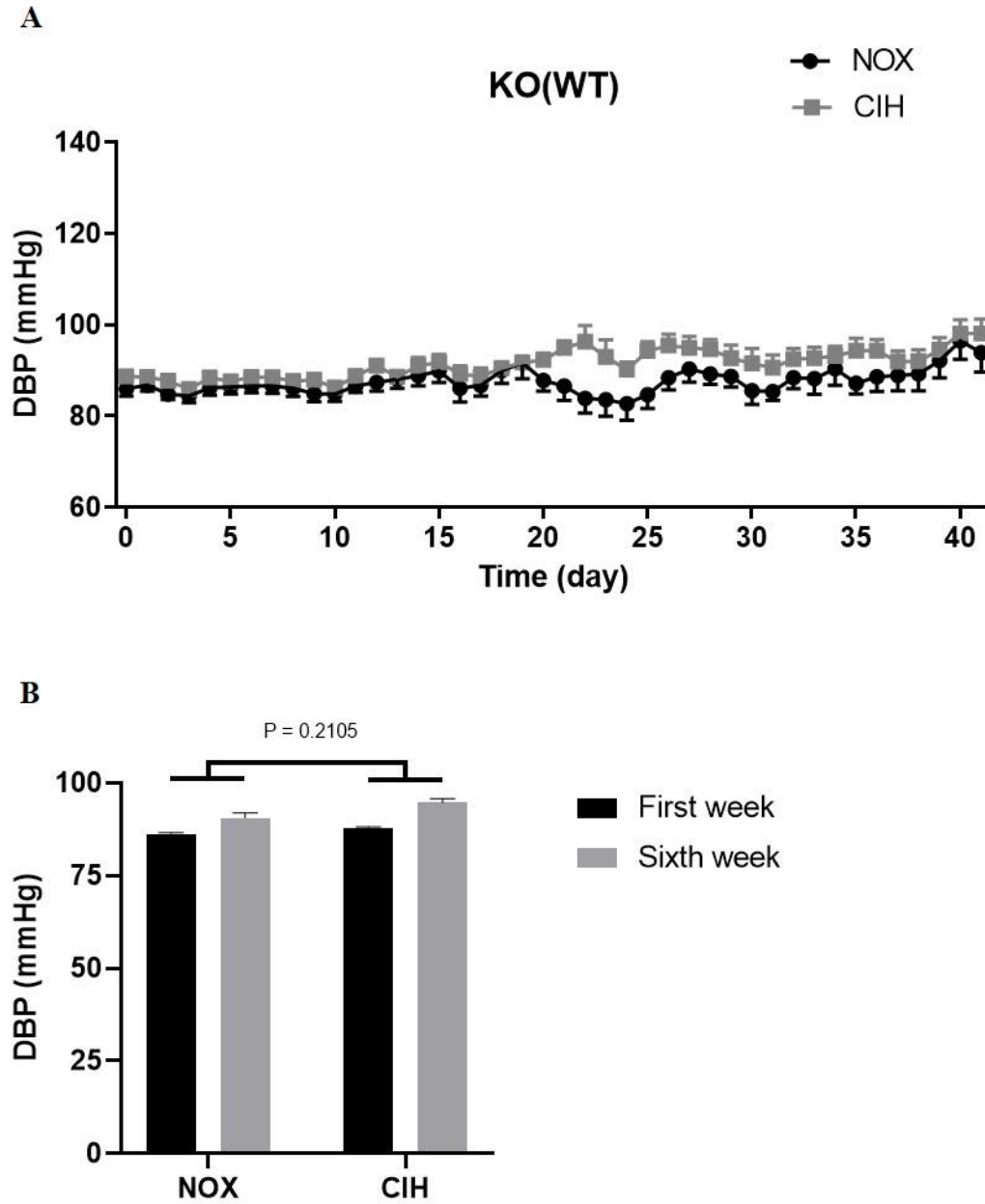


Figure 19: Diastolic blood pressure (DBP) of KO(WT) mice in the CIH

KO(WT) = KO mice transplanted with WT bone marrow, NOX = normoxia, CIH = chronic intermittent hypoxia, WT = C57BL/6J, KO = *iNOS*^{-/-}, mmHg = millimeter of mercury, values are depicted as mean \pm SEM, (A) diastolic blood pressure (daily), (B) diastolic blood pressure (first week vs. sixth week), analysis by two-way ANOVA, (NOX n = 10, CIH n = 13)

3.5.3.4. Knock out mice with knock out bone marrow

The diastolic blood pressure of the KO(KO) mice was measured by the telemetric system. Two-way interaction was not significant for the changes of DBP between first and sixth week of exposure for NOX- vs. CIH-exposed mice (Fig. 20).

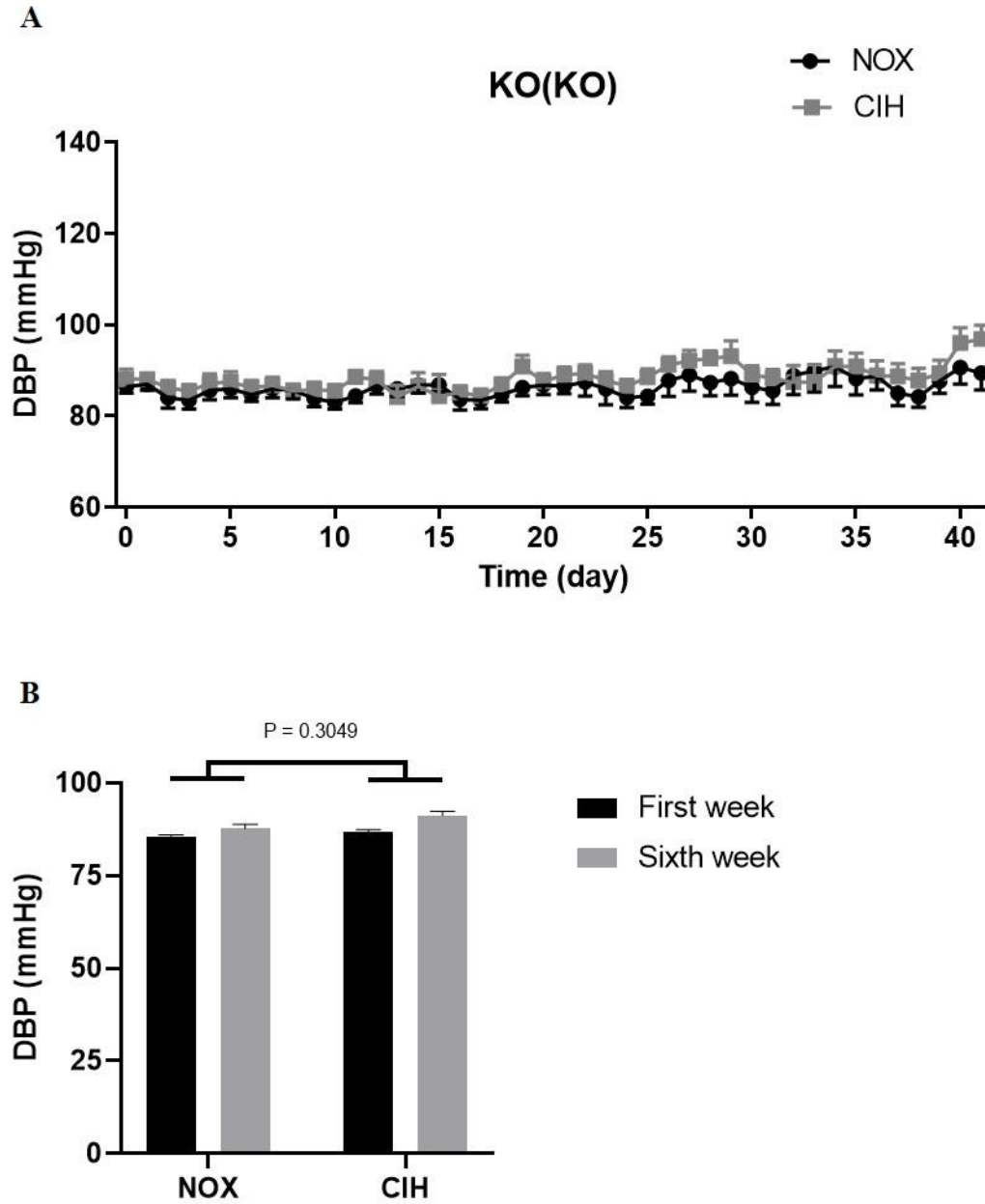


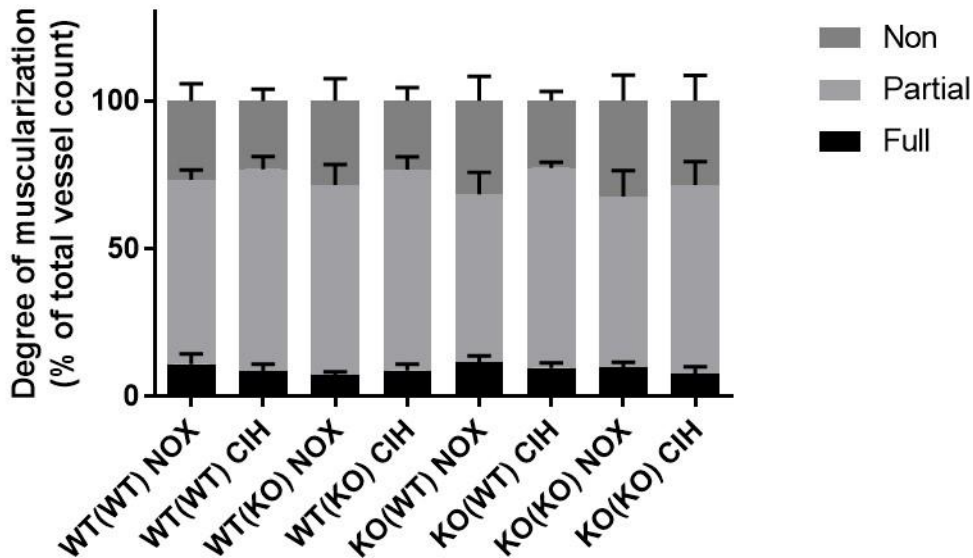
Figure 20: Diastolic blood pressure (DBP) of KO(KO) mice in the CIH

KO(KO) = KO mice transplanted with KO bone marrow, NOX = normoxia, CIH = chronic intermittent hypoxia, KO = $iNOS^{-/-}$, mmHg = millimeter of mercury, values are depicted as mean \pm SEM, (A) diastolic blood pressure (daily), (B) diastolic blood pressure (first week vs. sixth week), analysis by two-way ANOVA, (NOX n = 9, CIH n = 12)

3.6. Histological assessment of the degree of muscularization in pulmonary vessels

In order to determine the effects of CIH on the vascular remodeling and muscularization of pulmonary vessels in the chimeric mice, the smooth muscle cells of pulmonary vessels were stained and then the degree of muscularization was evaluated quantitatively. CIH resulted in no significant remodeling of the small and medium pulmonary vessels. The pulmonary vessels of CIH-exposed chimeric mice showed no significant difference in proportion of non-, partial-, and full-muscularized vessels compared to the respective chimeric normoxic group (Fig. 21 and 22).

A



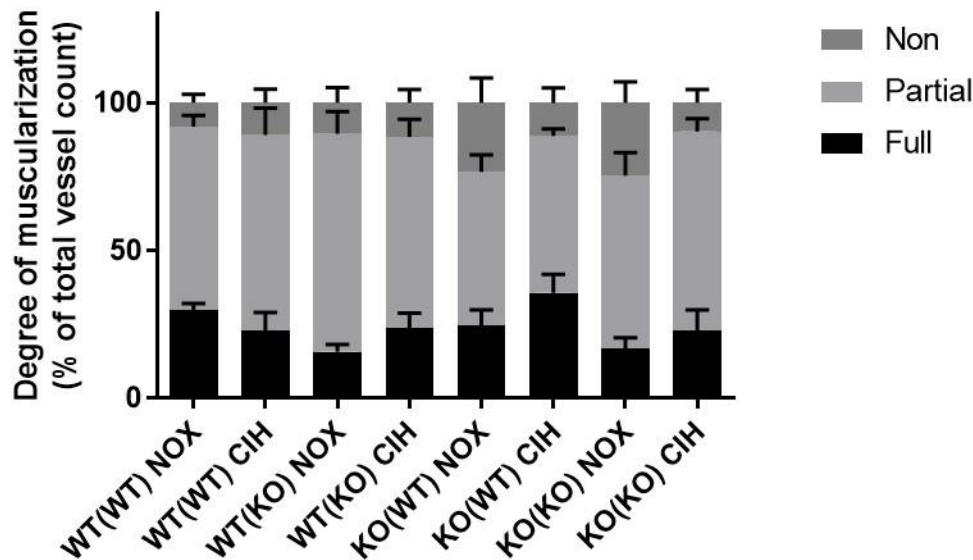
B

Small pulmonary vessels	P value		
	Full-muscularized	Partial-muscularized	Non-muscularized
WT(WT) NOX vs. WT(WT) CIH	> 0.9999	0.9911	0.9996
WT(KO) NOX vs. WT(KO) CIH	> 0.9999	0.9997	0.9963
KO(WT) NOX vs. KO(WT) CIH	> 0.9999	0.8525	0.9390
KO(KO) NOX vs. KO(KO) CIH	> 0.9999	0.9928	0.9996

Figure 21: Quantification of vascular remodeling as degree of muscularization in small pulmonary arterial vessels (20-70 μm of diameter) of different chimeric mice in the CIH

Muscularization of vessels classified as non-, partial-, and full-muscularized after immunostaining against alpha smooth muscle actin as marker for muscularized parts of the vessel wall and von Willebrand factor as marker for endothelium. WT(WT) = WT mice transplanted with WT bone marrow, WT(KO) = WT mice transplanted with KO bone marrow, KO(WT) = KO mice transplanted with WT bone marrow, KO(KO) = KO mice transplanted with KO bone marrow, NOX = normoxia, CIH = chronic intermittent hypoxia, WT = C57BL/6J, KO = $i\text{NOS}^{-/-}$, (A) degree of muscularization in small pulmonary arterial vessels, values are depicted as mean \pm SEM, (B) analysis by two-way ANOVA and Tukey's multiple comparisons test, (n = 6-7 each group)

A



B

Medium pulmonary vessels	P value		
	Full-muscularized	Partial-muscularized	Non-muscularized
WT(WT) NOX vs. WT(WT) CIH	0.9830	0.9994	> 0.9999
WT(KO) NOX vs. WT(KO) CIH	0.9693	0.9380	> 0.9999
KO(WT) NOX vs. KO(WT) CIH	0.8713	> 0.9999	0.8091
KO(KO) NOX vs. KO(KO) CIH	0.9951	0.9571	0.5903

Figure 22: Quantification of vascular remodeling as degree of muscularization in medium pulmonary arterial vessels (70-150 μ m of diameter) of different chimeric mice in the CIH

Muscularization of vessels classified as non-, partial-, and full-muscularized after immunostaining against alpha smooth muscle actin as marker for muscularized parts of the vessel wall and von Willebrand factor as marker for endothelium. WT(WT) = WT mice transplanted with WT bone marrow, WT(KO) = WT mice transplanted with KO bone marrow, KO(WT) = KO mice transplanted with WT bone marrow, KO(KO) = KO mice transplanted with KO bone marrow, NOX = normoxia, CIH = chronic intermittent hypoxia, WT = C57BL/6J, KO = *iNOS*^{-/-}, (A) degree of muscularization in medium pulmonary arterial vessels, values are depicted as mean \pm SEM, (B) analysis by two-way ANOVA and Tukey's multiple comparisons test, (n = 6-7 each group)

3.7. Echocardiographic assessments

The function and contractility of the heart were assessed with several echocardiographic parameters. The parameters measured in chimeric mice after 6 weeks of CIH or NOX exposure are presented in this part.

3.7.1. Left ventricular internal diameter at end-diastole (LVIDd)

The three-way interaction was not significant ($P = 0.2797$). None of the two-way interactions were significant. In none of the chimeric groups any significant change was observed in the LVIDd as a result of CIH (Fig. 23).

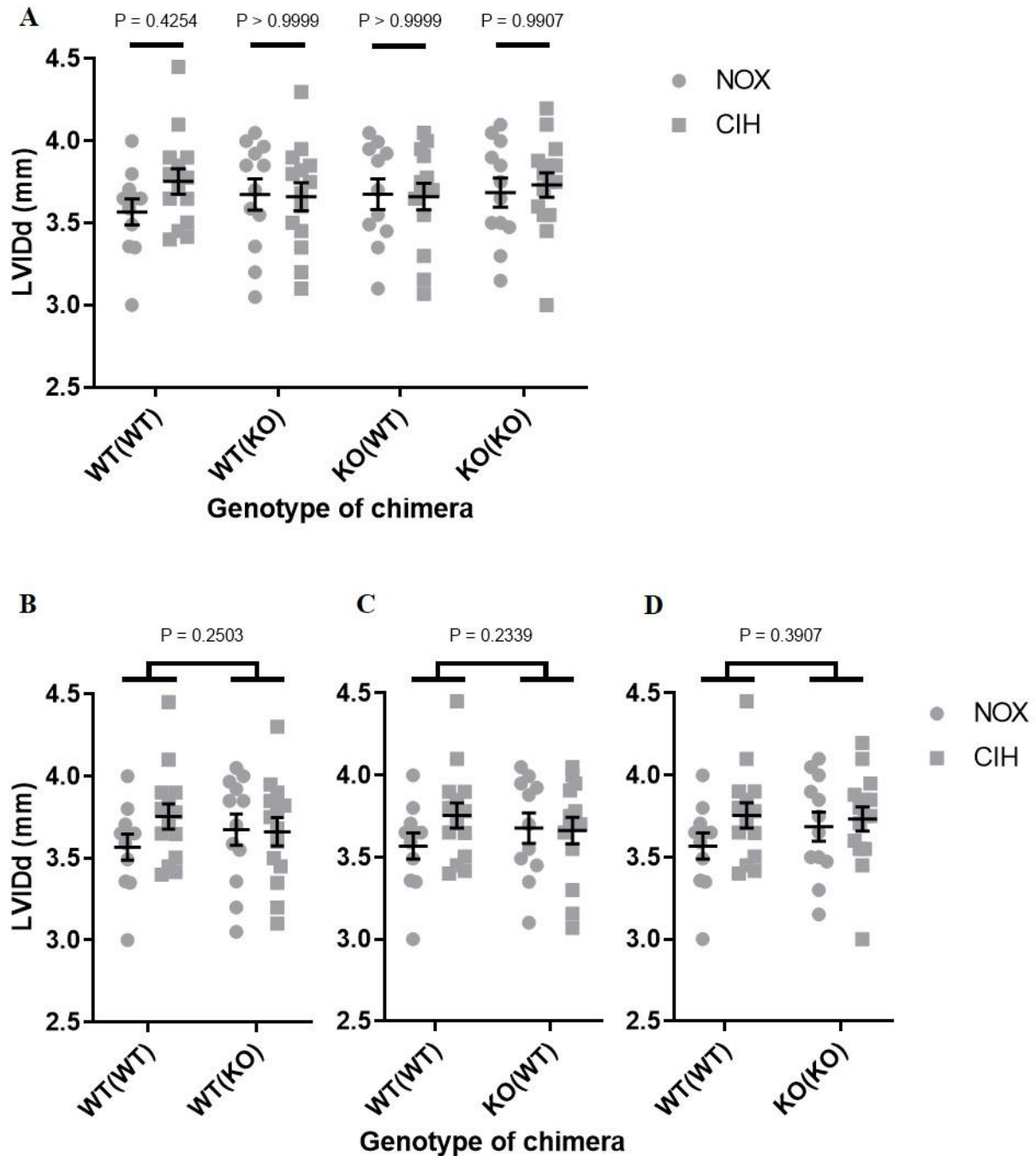


Figure 23: Endpoint left ventricular internal diameter at end-diastole (LVIDd) of different chimeric mice in the CIH

WT(WT) = WT mice transplanted with WT bone marrow, WT(KO) = WT mice transplanted with KO bone marrow, KO(WT) = KO mice transplanted with WT bone marrow, KO(KO) = KO mice transplanted with KO bone marrow, NOX = normoxia, CIH = chronic intermittent hypoxia, WT = C57BL/6J, KO = iNOS^{-/-},

mm = millimeter, values are depicted as mean \pm SEM, **(A)** analysis by three-way ANOVA and Sidak's multiple comparisons test, **(B-D)** analyses by two-way ANOVA, (n = 11-15 each group)

3.7.2. Left ventricular wall thickness at end-diastole (LVWTd)

The three-way interaction was not significant ($P = 0.8345$). None of the two-way interactions were significant. In none of the chimeric groups any significant change was observed in the LVWTd as a result of CIH (Fig. 24).

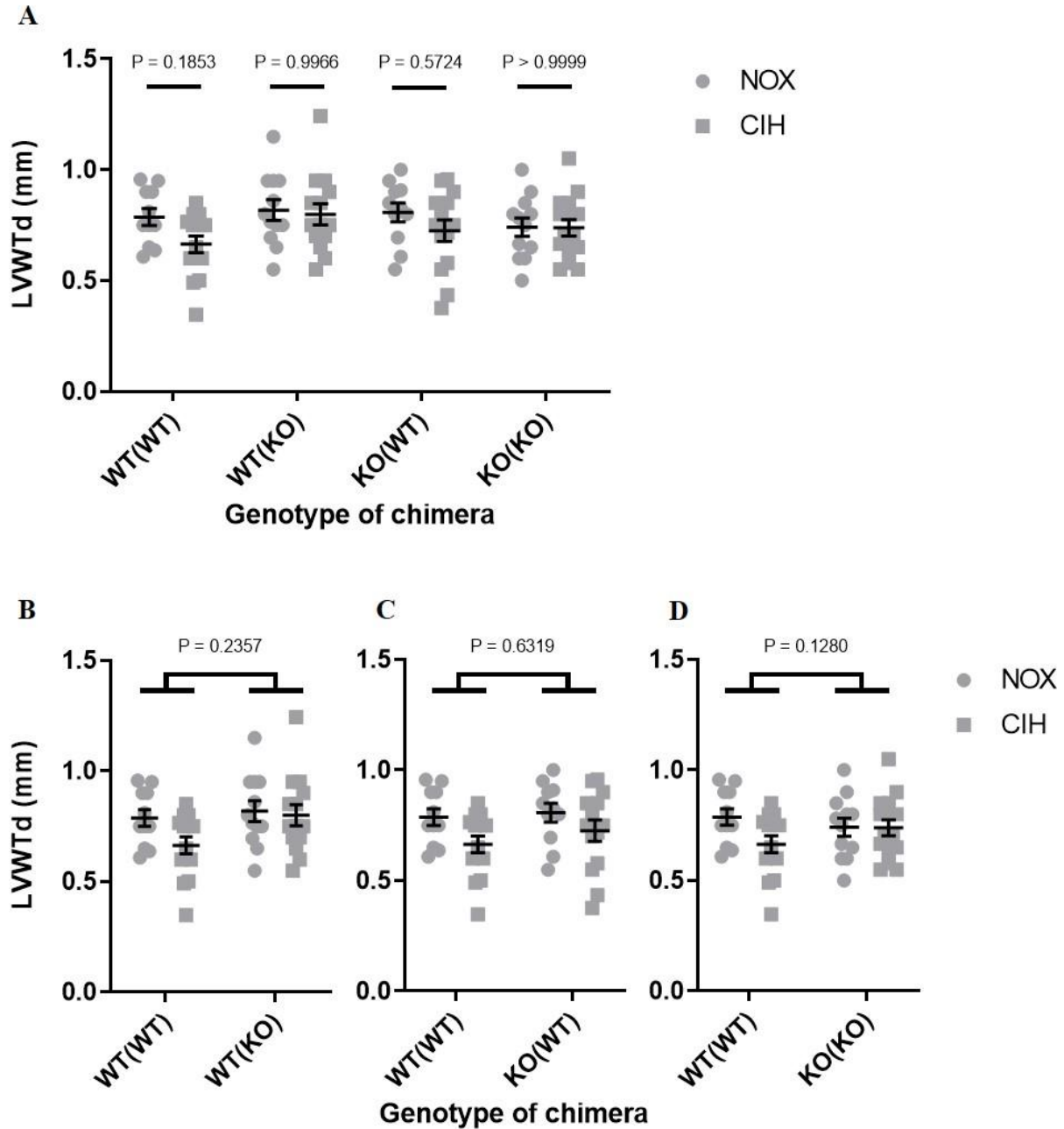


Figure 24: Endpoint left ventricular wall thickness at end-diastole (LVWTd) of different chimeric mice in the CIH

WT(WT) = WT mice transplanted with WT bone marrow, WT(KO) = WT mice transplanted with KO bone marrow, KO(WT) = KO mice transplanted with WT bone marrow, KO(KO) = KO mice transplanted with KO bone marrow, NOX = normoxia, CIH = chronic intermittent hypoxia, WT = C57BL/6J, KO = *iNOS*^{-/-}, mm = millimeter, values are depicted as mean \pm SEM, (A) analysis by three-way ANOVA and Sidak's multiple comparisons test, (B-D) analyses by two-way ANOVA, (n = 11-15 each group)

3.7.3. Cardiac output and index

The cardiac output (CO) was determined to indicate the pumping function of the heart. The cardiac index (CI) was calculated to exclude possible bias of CO due to the different body weights of mice. Regarding CO, the three-way interaction was not significant ($P = 0.9821$). The two-way interactions of “WT(WT) NOX and CIH vs. KO(WT) NOX and CIH” and “WT(WT) NOX and CIH vs. KO(KO) NOX and CIH” were significant. The other two-way interaction was not significant. The WT(WT) mice exposed to CIH showed significant lower CO compared to NOX-exposed WT(WT) mice. However, no statistically significant difference was observed in CO after 6 weeks of CIH or NOX exposure in the other chimeric groups (Fig. 25).

Regarding CI, the three-way interaction was not significant ($P = 0.9630$). The two-way interaction of “WT(WT) NOX and CIH vs. KO(KO) NOX and CIH” was significant (the decrease of CI in WT(WT) mice in response to CIH was significantly different from the change of CI in KO(KO) mice in response to CIH). The other two-way interactions were not significant. The CIH-exposed mice showed no statistically significant change in CI compared to NOX-exposed mice in any of the chimeric groups (Fig. 26).

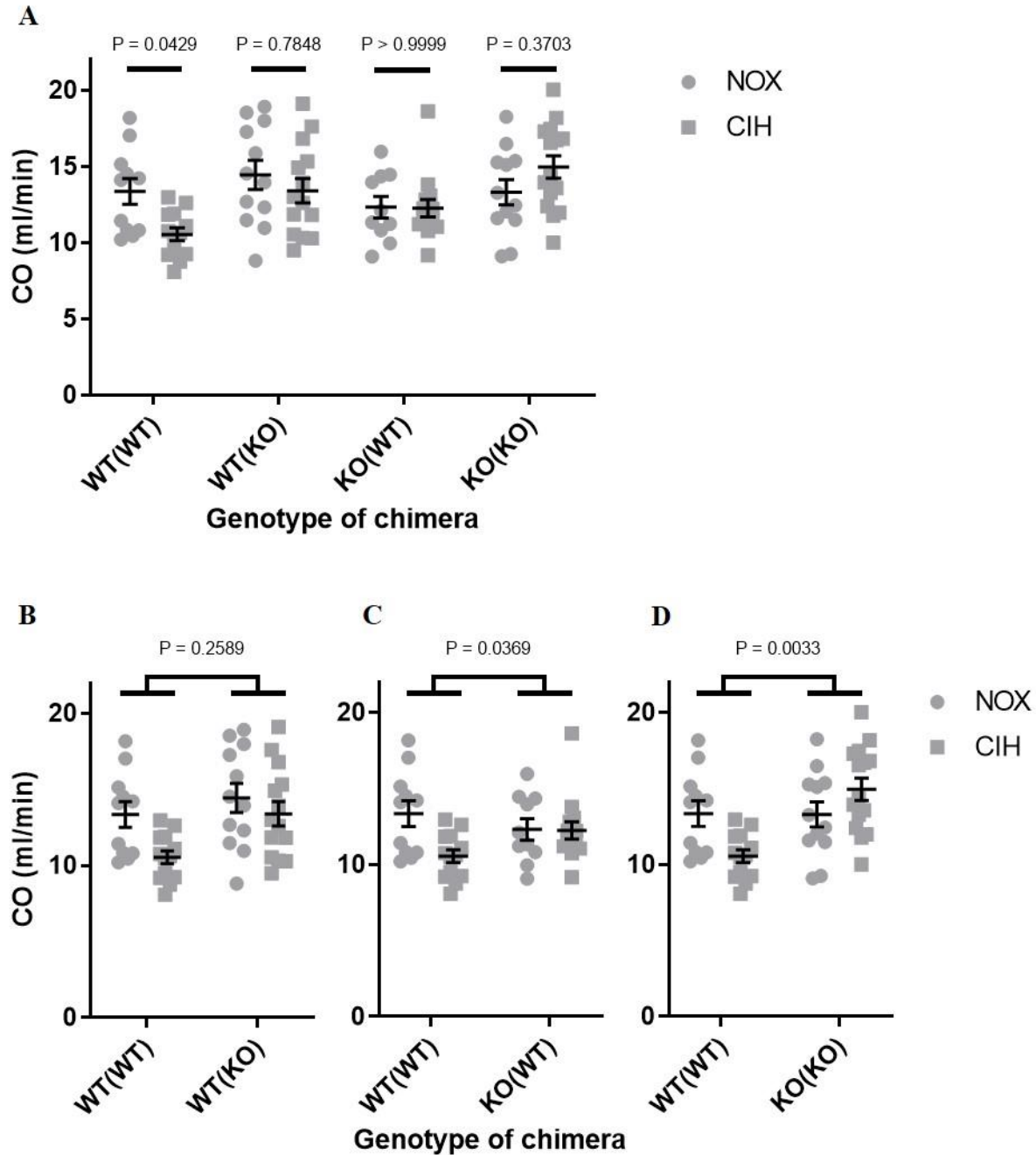


Figure 25: Endpoint cardiac output (CO) of different chimeric mice in the CIH

WT(WT) = WT mice transplanted with WT bone marrow, WT(KO) = WT mice transplanted with KO bone marrow, KO(WT) = KO mice transplanted with WT bone marrow, KO(KO) = KO mice transplanted with KO bone marrow, NOX = normoxia, CIH = chronic intermittent hypoxia, WT = C57BL/6J, KO = *iNOS*^{-/-}, ml = milliliter, min = minute, values are depicted as mean ± SEM, (A) analysis by three-way ANOVA and Sidak's multiple comparisons test, (B-D) analyses by two-way ANOVA, (n = 10-15 each group)

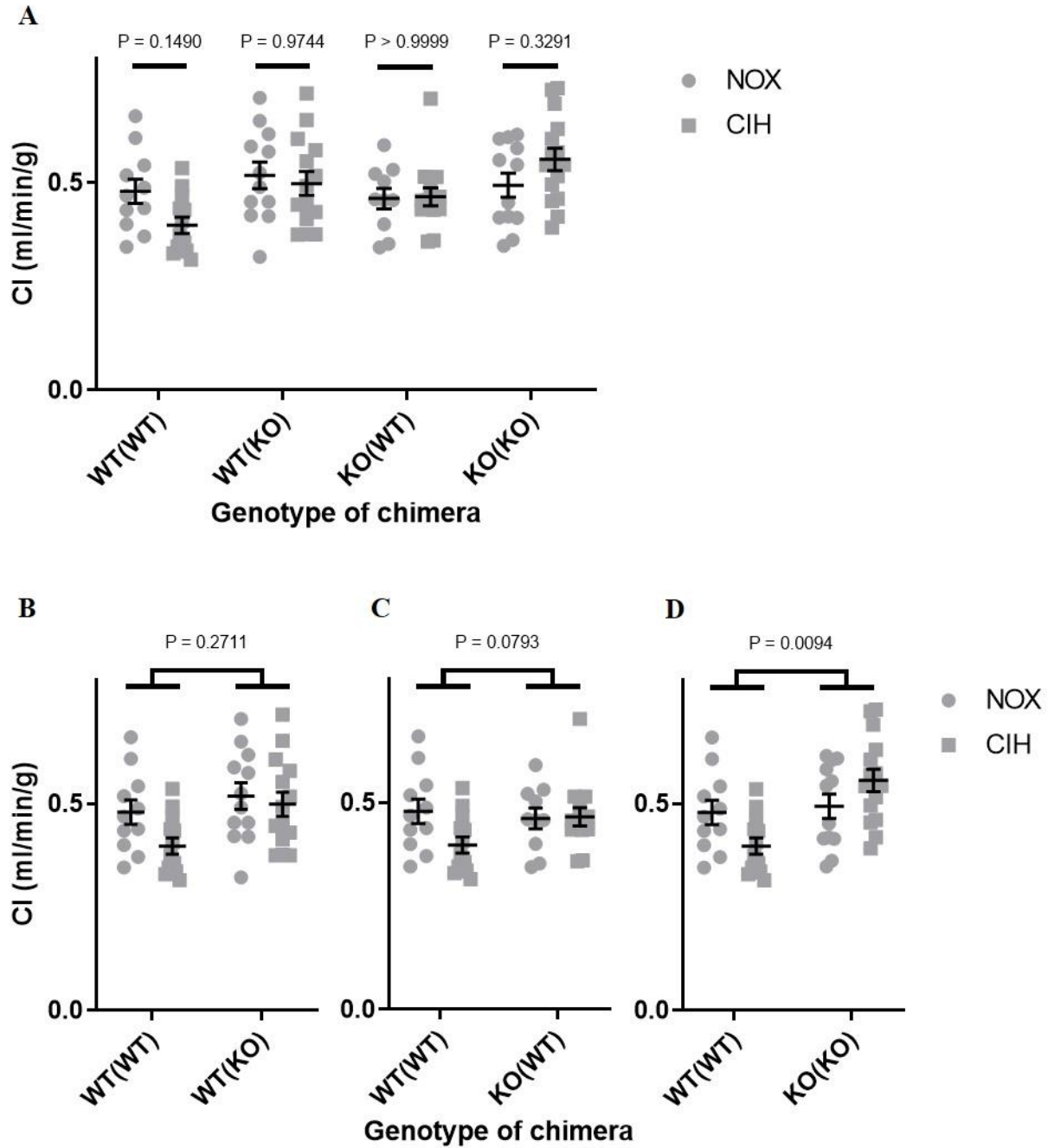


Figure 26: Endpoint cardiac index (CI) of different chimeric mice in the CIH

WT(WT) = WT mice transplanted with WT bone marrow, WT(KO) = WT mice transplanted with KO bone marrow, KO(WT) = KO mice transplanted with WT bone marrow, KO(KO) = KO mice transplanted with KO bone marrow, NOX = normoxia, CIH = chronic intermittent hypoxia, WT = C57BL/6J, KO = iNOS^{-/-}, ml = milliliter, min = minute, g = gram body weight, values are depicted as mean ± SEM, (A) analysis by

three-way ANOVA and Sidak's multiple comparisons test, **(B-D)** analyses by two-way ANOVA, (n = 10-15 each group)

3.7.4. Left ventricular ejection fraction (LVEF)

The LVEF was used to analyze the systolic function of the left ventricle. The three-way interaction was not significant (P = 0.7856). None of the two-way interactions were significant. No significant change was observed in the LVEF as a result of CIH in any of the chimeric groups (Fig. 27).

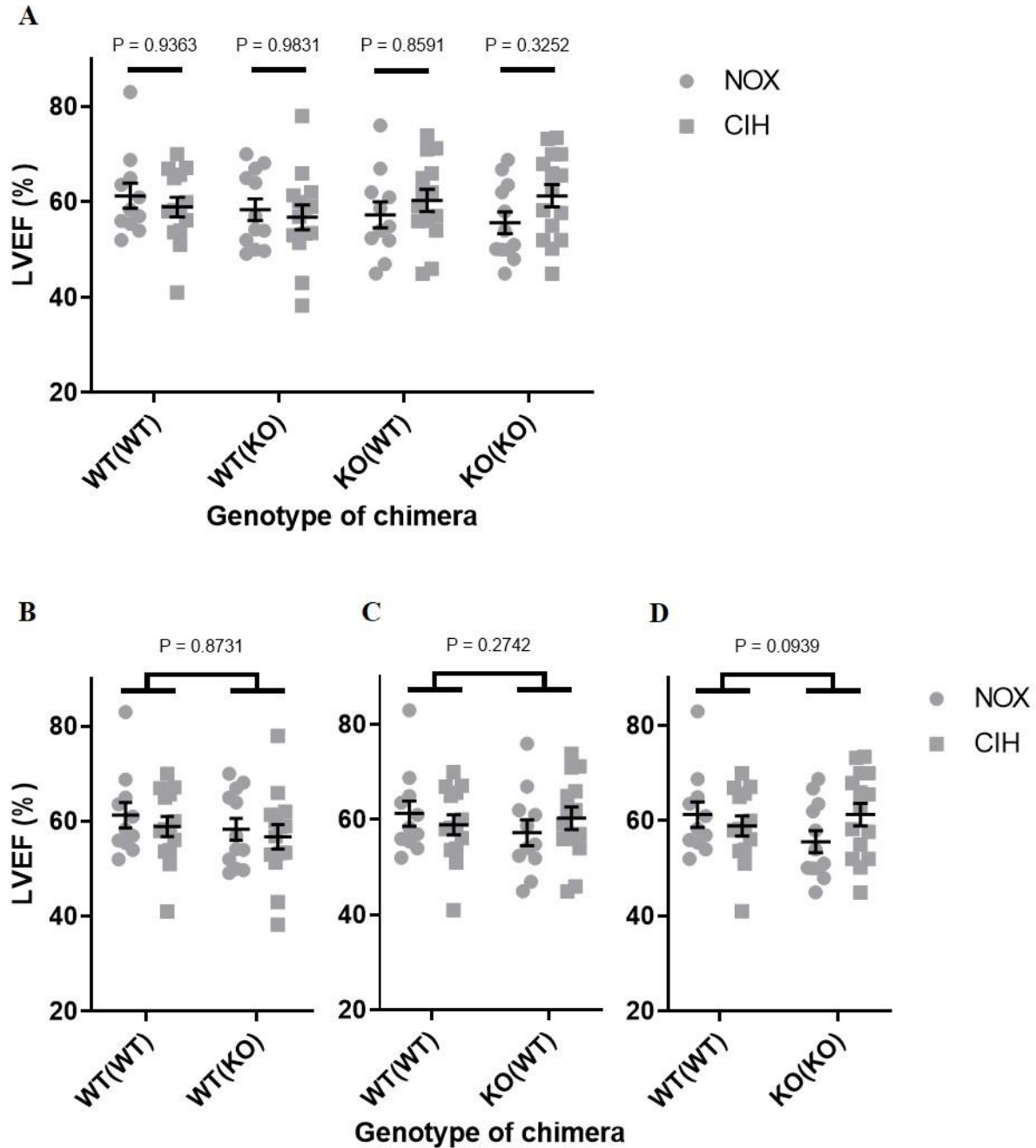


Figure 27: Endpoint left ventricular ejection fraction (LVEF) of different chimeric mice in the CIH
 WT(WT) = WT mice transplanted with WT bone marrow, WT(KO) = WT mice transplanted with KO bone marrow, KO(WT) = KO mice transplanted with WT bone marrow, KO(KO) = KO mice transplanted with KO bone marrow, NOX = normoxia, CIH = chronic intermittent hypoxia, WT = C57BL/6J, KO = iNOS^{-/-}, values are depicted as mean ± SEM, (A) analysis by three-way ANOVA and Sidak's multiple comparisons test, (B-D) analyses by two-way ANOVA, (n = 11-15 each group)

3.7.5. Right ventricular internal diameter at end-diastole (RVIDd)

The three-way interaction was not significant ($P = 0.7802$). None of the two-way interactions were significant. In the chimeric groups, no significant change was observed in the RVIDd as a result of CIH (Fig. 28).

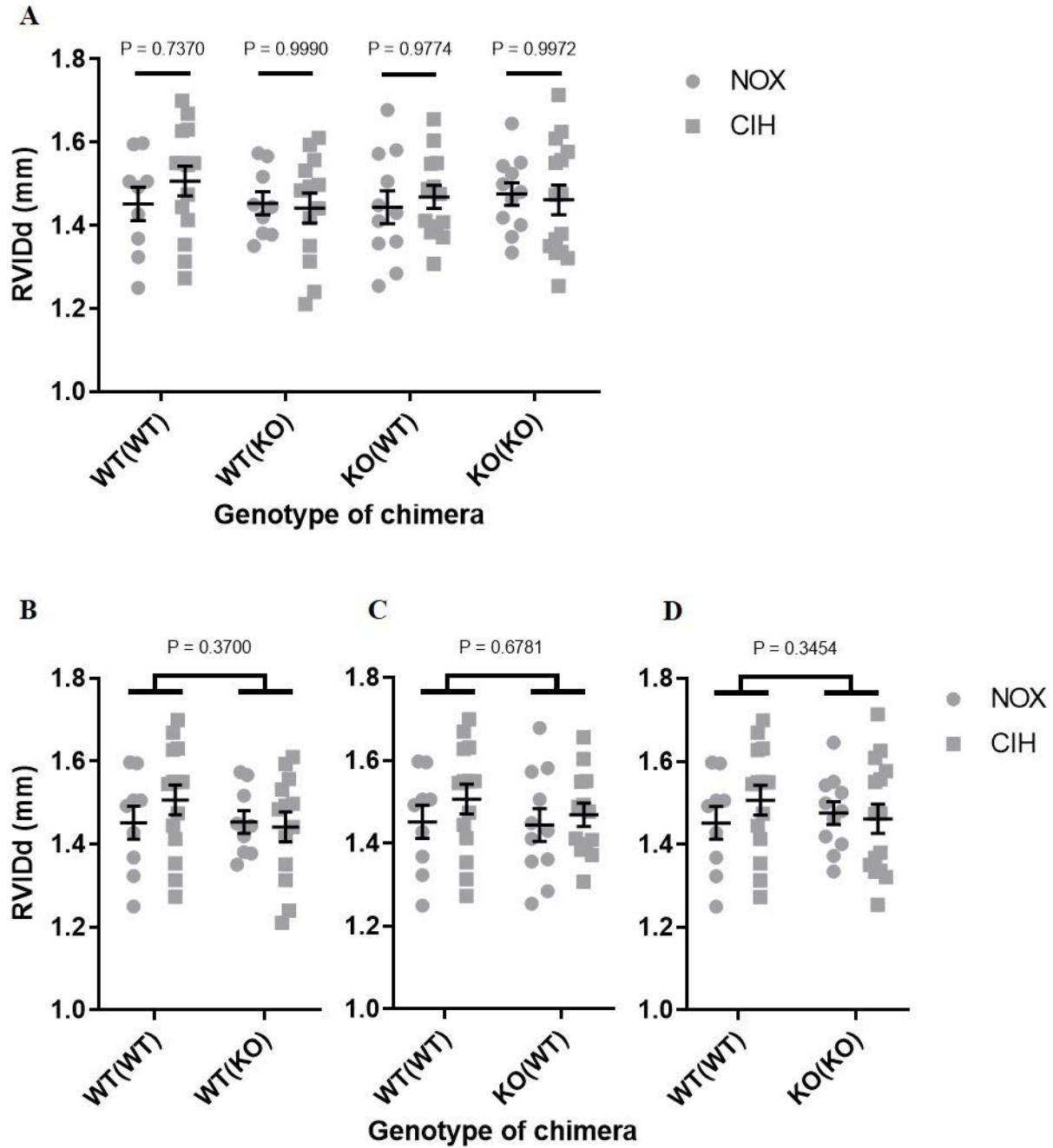


Figure 28: Endpoint right ventricular internal diameter at end-diastole (RVIDd) of different chimeric mice in the CIH

WT(WT) = WT mice transplanted with WT bone marrow, WT(KO) = WT mice transplanted with KO bone marrow, KO(WT) = KO mice transplanted with WT bone marrow, KO(KO) = KO mice transplanted with KO bone marrow, NOX = normoxia, CIH = chronic intermittent hypoxia, WT = C57BL/6J, KO = *iNOS*^{-/-},

mm = millimeter, values are depicted as mean \pm SEM, **(A)** analysis by three-way ANOVA and Sidak's multiple comparisons test, **(B-D)** analyses by two-way ANOVA, (n = 9-15 each group)

3.7.6. Right ventricular wall thickness at end-diastole (RVWTd)

The three-way interaction was not significant ($P = 0.2200$). The two-way interaction of "WT(WT) NOX and CIH vs. KO(WT) NOX and CIH" was significant. The other two-way interactions were not significant. The WT(WT) mice exposed to CIH showed significant higher RVWTd compared to NOX-exposed WT(WT) mice. In the other chimeric groups, no significant change was observed in the RVWTd as a result of CIH (Fig. 29).

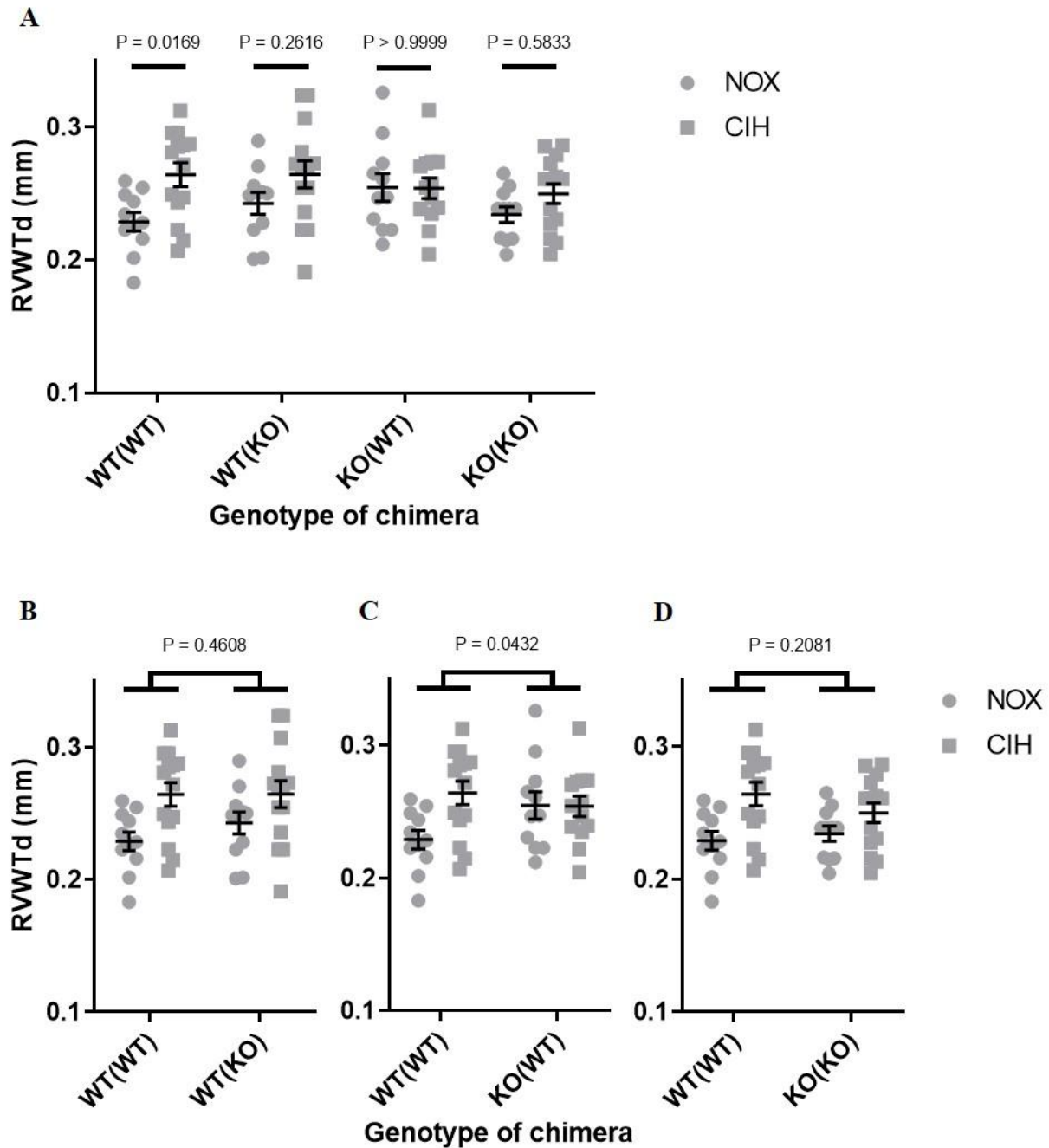


Figure 29: Endpoint right ventricular wall thickness at end-diastole (RVWTd) of different chimeric mice in the CIH

WT(WT) = WT mice transplanted with WT bone marrow, WT(KO) = WT mice transplanted with KO bone marrow, KO(WT) = KO mice transplanted with WT bone marrow, KO(KO) = KO mice transplanted with KO bone marrow, NOX = normoxia, CIH = chronic intermittent hypoxia, WT = C57BL/6J, KO = iNOS^{-/-},

mm = millimeter, values are depicted as mean \pm SEM, **(A)** analysis by three-way ANOVA and Sidak's multiple comparisons test, **(B-D)** analyses by two-way ANOVA, (n = 11-15 each group)

3.7.7. Tricuspid annular plane systolic excursion (TAPSE)

The TAPSE was used to analyze the systolic function of the right ventricle. The three-way interaction was not significant ($P = 0.9008$). The two-way interactions of “WT(WT) NOX and CIH vs. WT(KO) NOX and CIH” and “WT(WT) NOX and CIH vs. KO(KO) NOX and CIH” were significant. The other two-way interaction was not significant. After 6 weeks of CIH exposure WT(WT) and KO(WT) mice showed statistically significant lower TAPSE compared to their NOX controls, whereas neither WT(KO) nor KO(KO) mice showed significant changes as a result of CIH (Fig. 30).

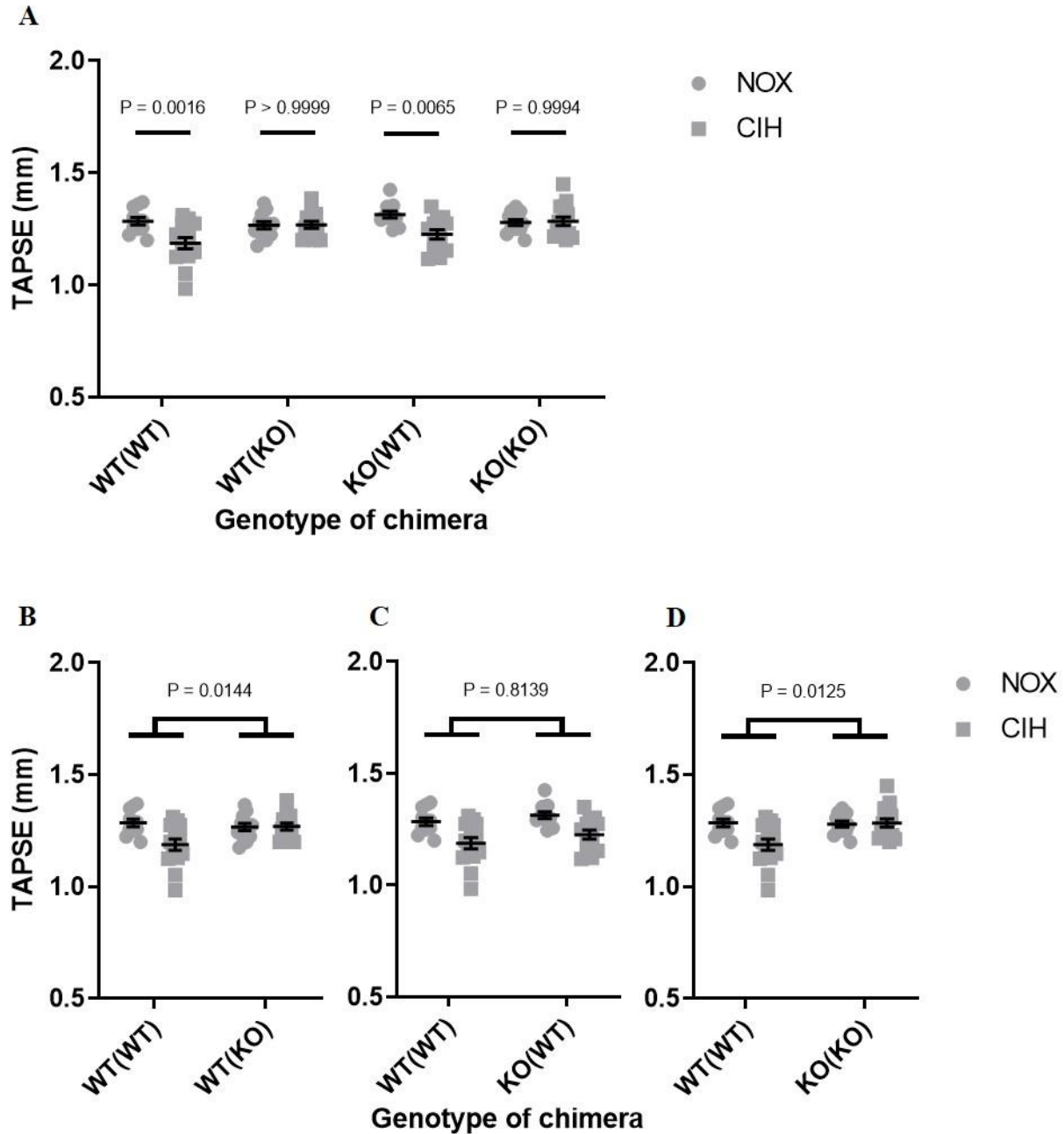


Figure 30: Endpoint tricuspid annular plane systolic excursion (TAPSE) of different chimeric mice in the CIH

WT(WT) = WT mice transplanted with WT bone marrow, WT(KO) = WT mice transplanted with KO bone marrow, KO(WT) = KO mice transplanted with WT bone marrow, KO(KO) = KO mice transplanted with KO bone marrow, NOX = normoxia, CIH = chronic intermittent hypoxia, WT = C57BL/6J, KO = $iNOS^{-/-}$, mm = millimeter, values are depicted as mean \pm SEM, (A) analysis by three-way ANOVA and Sidak's multiple comparisons test, (B-D) analyses by two-way ANOVA, (n = 11-15 each group)

3.7.8. Pulmonary acceleration time/pulmonary ejection time (PAT/PET)

The three-way interaction was not significant ($P = 0.6033$). None of the two-way interactions were significant. No statistically significant change was observed in PAT/PET after 6 weeks of CIH or NOX exposure in any of the chimeric groups (Fig. 31).

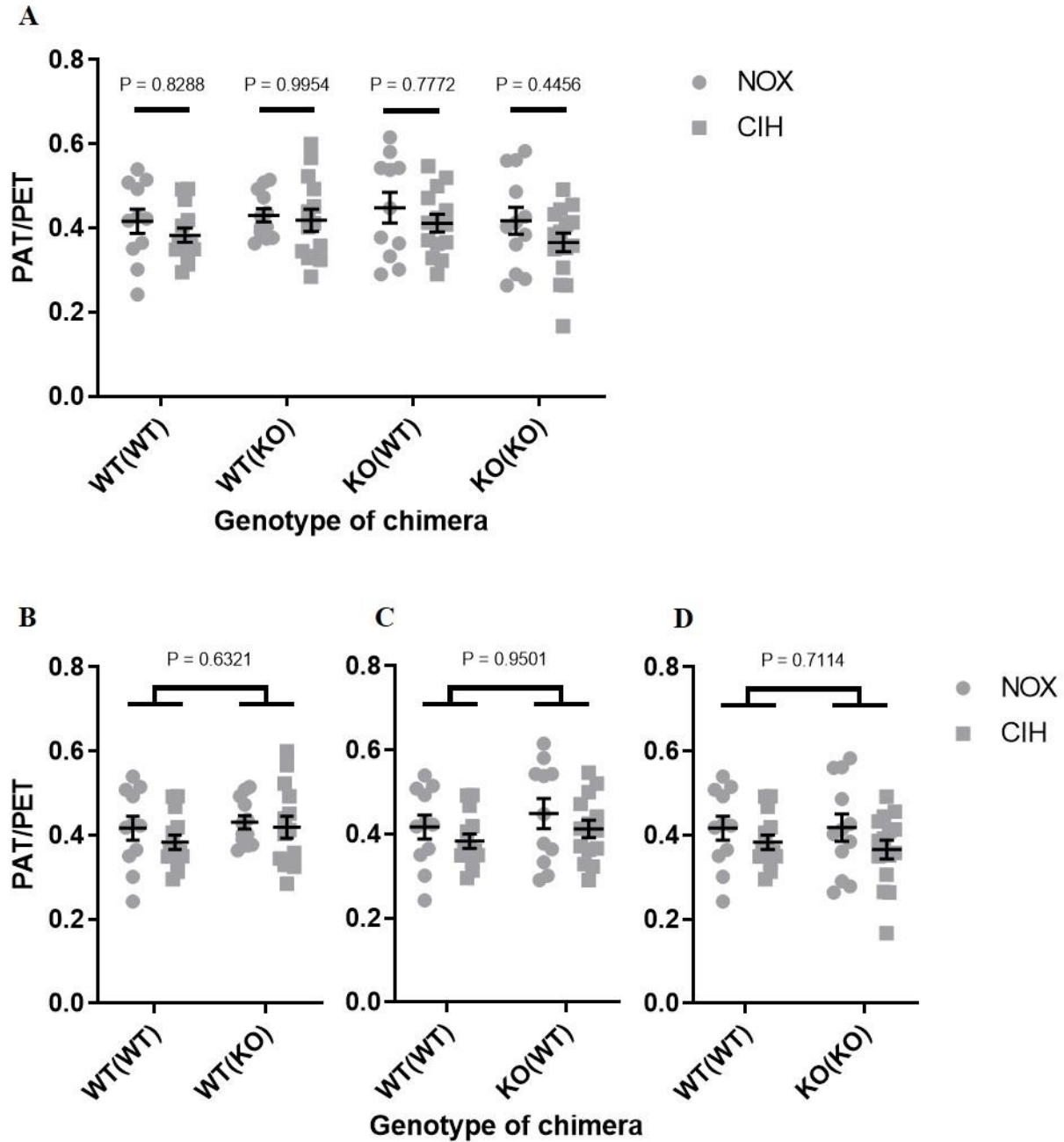


Figure 31: Endpoint pulmonary acceleration time/pulmonary ejection time (PAT/PET) of different chimeric mice in the CIH

WT(WT) = WT mice transplanted with WT bone marrow, WT(KO) = WT mice transplanted with KO bone marrow, KO(WT) = KO mice transplanted with WT bone marrow, KO(KO) = KO mice transplanted with KO bone marrow, NOX = normoxia, CIH = chronic intermittent hypoxia, WT = C57BL/6J, KO = *iNOS*^{-/-}, values are depicted as mean \pm SEM, (A) analysis by three-way ANOVA and Sidak's multiple comparisons test, (B-D) analyses by two-way ANOVA, (n = 11-15 each group)

3.8. Superoxide anion measurement by electron spin resonance spectroscopy

Superoxide anion was measured in lung homogenate and blood samples after hemodynamic measurements.

3.8.1. Blood samples

The three-way interaction was not significant ($P = 0.2705$). None of the two-way interactions were significant. In blood samples of the different chimeric groups, no significant change was observed in the superoxide anion concentration as a result of CIH (Fig. 32).

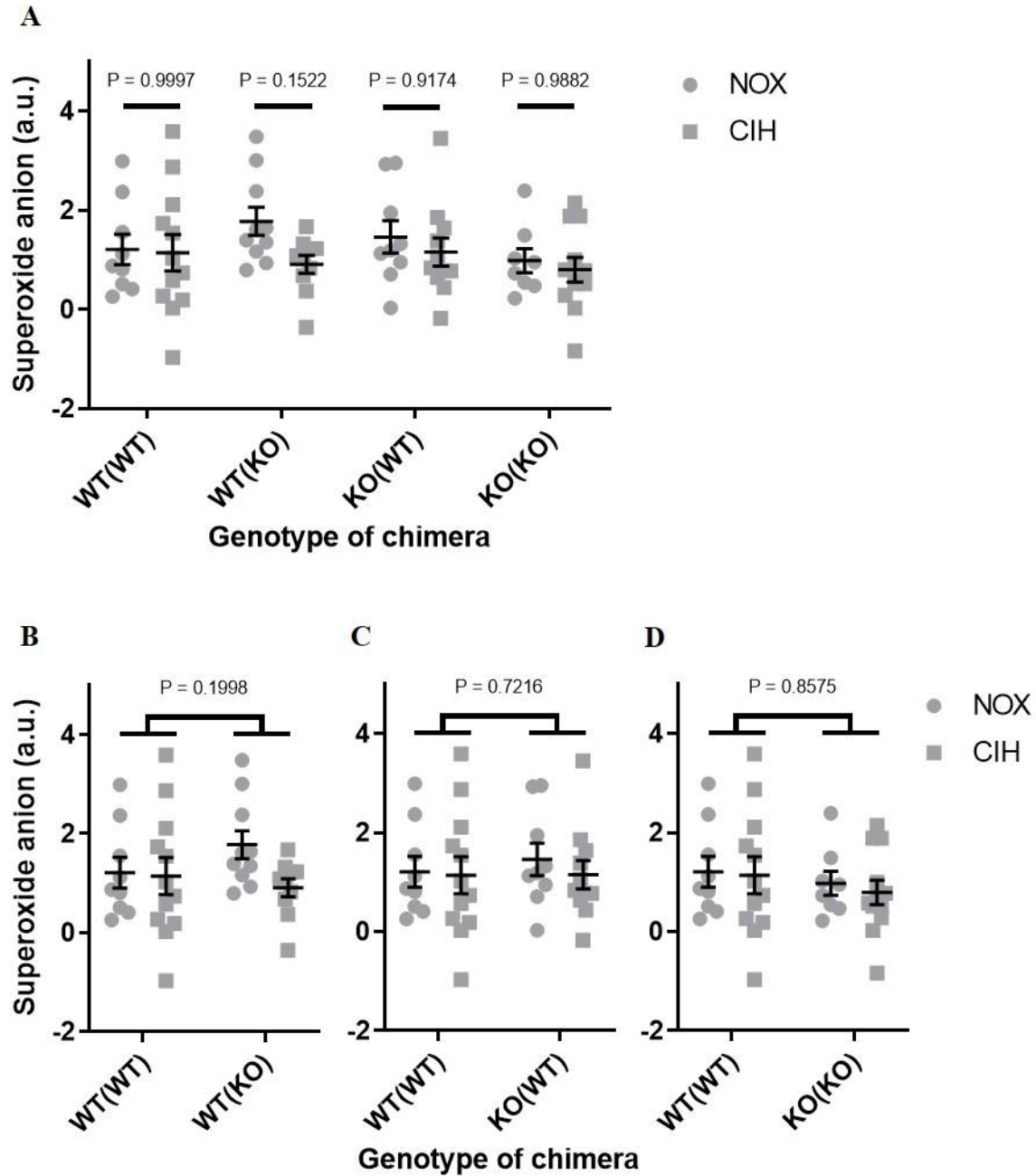


Figure 32: Superoxide anion in blood samples of different chimeric mice in the CIH

WT(WT) = WT mice transplanted with WT bone marrow, WT(KO) = WT mice transplanted with KO bone marrow, KO(WT) = KO mice transplanted with WT bone marrow, KO(KO) = KO mice transplanted with KO bone marrow, NOX = normoxia, CIH = chronic intermittent hypoxia, WT = C57BL/6J, KO = *iNOS*^{-/-}, a.u. = arbitrary unit, values are depicted as mean \pm SEM, (A) analysis by three-way ANOVA and Sidak's multiple comparisons test, (B-D) analyses by two-way ANOVA, (n = 8-12 each group)

3.8.2. Lung samples

The three-way interaction was not significant ($P = 0.2048$). The two-way interaction of “WT(WT) NOX and CIH vs. KO(KO) NOX and CIH” was significant (the decrease of superoxide anion concentration in WT(WT) mice in response to CIH was significantly different from the change of superoxide anion concentration in KO(KO) mice in response to CIH). The other two-way interactions were not significant. In lung homogenate of the different chimeric groups, no significant change was observed in the superoxide anion concentration as a result of CIH (Fig. 33).

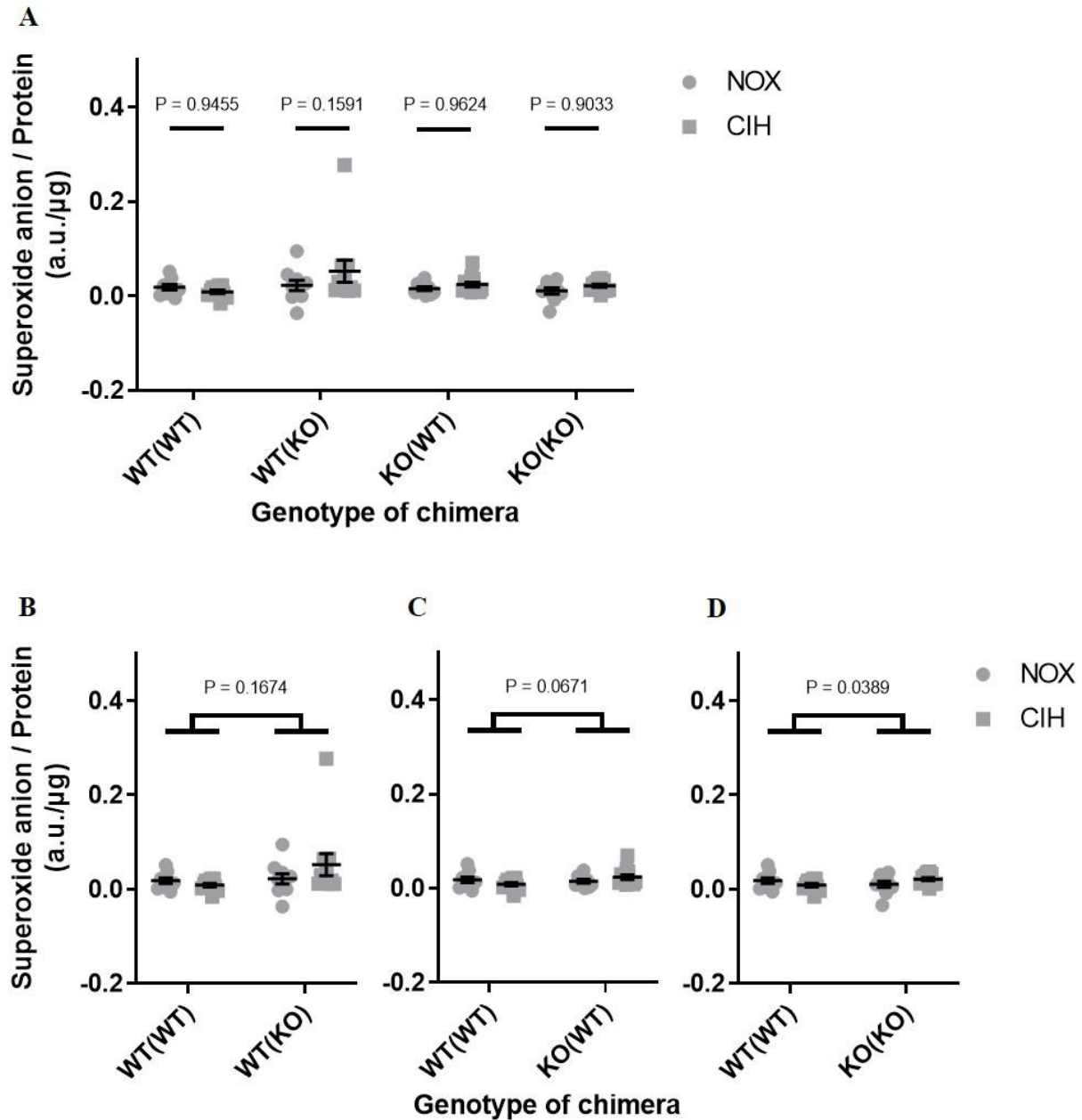


Figure 33: Superoxide anion in lung homogenate samples of different chimeric mice in the CIH

WT(WT) = WT mice transplanted with WT bone marrow, WT(KO) = WT mice transplanted with KO bone marrow, KO(WT) = KO mice transplanted with WT bone marrow, KO(KO) = KO mice transplanted with KO bone marrow, NOX = normoxia, CIH = chronic intermittent hypoxia, WT = C57BL/6J, KO = *iNOS*^{-/-}, a.u. = arbitrary unit, μg = microgram, values are depicted as mean \pm SEM, (A) analysis by three-way ANOVA and Sidak's multiple comparisons test, (B-D) analyses by two-way ANOVA, (n = 9-13 each group)

4. Discussion

4.1. Mouse model

This project was designed according to the previous investigations in our research group (Kraut, 2014), therefore in all steps of the experiments, the designs and conditions in performing of the experiments were kept similar to the previous plans and conditions. These similarities include the animal model of CIH, WT and iNOS KO mice strains, CIH protocol, and cardiopulmonary functional readouts.

The mouse model of CIH has been used to simulate OSAS. OSAS is associated with different changes in the cardiovascular and pulmonary systems including the induction of systemic and pulmonary hypertension. One of the key questions in this project was the study of influence of CIH on systemic hypertension of mice. The pathogenesis of increased systemic blood pressure in OSAS is a complex interplay of different factors and different body systems and functions (Konecny et al., 2014). This indicates the necessity of performing investigations on the animal models. In this project a mouse model has been used for investigation of these interplays as cell culture experiments are not appropriate to simulate the complexity of the OSAS. However, an innovative system has been introduced to study IH in cell culture (Baumgardner and Otto, 2003), and the significance of cell culture experiments in increasing the knowledge about OSAS should not be denied.

The advantages of using the mice are, the availability of variety of genetically modified variants, their small size and small space requirement, and the low cost of purchase and maintenance. Moreover, in this project a mouse model was chosen because of the availability of iNOS^{-/-} mice, the possibility of irradiation and BMT and creating chimeric mice, and the relative low-cost and low-effort exposure of the mice to CIH.

4.2. Bone marrow transplantation

In this project, BMT was used in order to investigate the role of bone marrow derived cells in CIH. BMT consists of two major steps, myeloablation of the recipient mice and reconstitution of the bone marrow in these mice with the bone marrow cells isolated from donor mice. A frequently used method for myeloablation of mice is irradiation of the entire body of the animals (Duran-Struuck and Dysko, 2009). Fast proliferating hematopoietic stem cells are eradicated by irradiation of the animal. Fractionated total body irradiation (FTBI) has some advantages compared to single high-

dose irradiation. Irradiation influences other fast proliferating cells as well, however FTBI causes less side effects (e.g. gastrointestinal damage) than single high-dose irradiation (Cui et al., 2002). Reconstitution of bone marrow with hematopoietic cells can be accomplished by injection of donor bone marrow cells in the peripheral blood of recipient animals. Injection can be performed through tail vein which can be challenging. As alternative retroorbital injections can be performed under anesthesia which is more invasive but easier compared to tail vein injections. If the transplantation is not successful and donor hematopoietic stem cells cannot reconstitute the bone marrow, recipient mice die because of severe deficiency of erythrocytes or thrombocytes, or secondary infection due to bone marrow aplasia (Duran-Struuck and Dysko, 2009).

4.2.1. Effect of irradiation, BMT, and bone marrow-derived stem cells on OSA

It has been shown that irradiation and BMT can change the recruitment of inflammatory cells in an experimental ApoE^{-/-} mouse models of aortic aneurysm and atherosclerosis. Therefore, it has been suggested that irradiation and BMT can display more complicated consequences on inflammatory processes of the vessels which requires more investigations (Patel et al., 2018). However, the effect of irradiation and BMT on CIH mouse model requires further investigations. Besides, it has been suggested that in OSA, stem cells originated from bone marrow can migrate to peripheral blood and play a protective, immunomodulatory, and anti-inflammatory role to reduce the damages caused by OSA (Almendros et al., 2012) (Carreras et al., 2011). In this project, through irradiation and BMT, different bone marrow-derived stem cells have been injected to the recipient mice which could have played a protective role in the following CIH exposures. Nevertheless, this idea needs to be confirmed by further experiments.

4.3. Simulation of OSAS with CIH exposure of chimeric mice

The mouse model of CIH has been used as previously described (Kraut, 2014) to simulate the OSAS, aiming to elucidate some aspects of its pathogenesis. Chimeric mice were exposed to CIH for 8 hours a day, 5 days per week, for 6 weeks. In the CIH chamber O₂ concentration was reduced from 21% to 7% and then returned to 21% in 2 minutes (each complete cycle took 2 minutes). The mice were exposed to CIH for 8 hours during the day (pCO₂ was not controlled during the cycles). The mice were kept in normoxic conditions during the night. As mice are nocturnal animals, the CIH exposure can be considered in their night phase. In this work CIH was performed independent from the mice sleep status and no EEG or EMG was used. Several different animal models are

available for simulation of OSAS, among which CIH (with different protocols) is non-invasive and commonly used (Dematteis et al., 2009) (Davis and O'Donnell, 2013).

In most of CIH protocols used for rodent models, each cycle of normoxia-hypoxia is completed in 30 seconds to 5 minutes. In most of accomplished CIH studies, the oxygen concentration during the hypoxic phase varies from 3% to 10% which reaches 21% during the normoxic phase and pCO₂ is uncontrolled (Foster et al., 2007).

4.3.1. Limitations and criticisms of the CIH animal model

The animal model of CIH is a described and commonly used model for simulation of OSAS, and is a helpful tool to study the pathophysiological mechanisms of OSAS. However, it has some limitations and criticisms. A limiting factor in rodent models of IH is that different research groups perform experiments with their specific IH protocol and setting. This point has made comparability of the results of different researches very hard. Moreover, an ideal animal model of OSAS should simulate all the characteristics of OSAS. The common criticism of IH model is that this model is not associated with hypercapnia, intrathoracic pressure fluctuations, sleep fragmentation, and arousals which are characteristics of OSAS (Lee et al., 2009).

4.4. Final weight of chimeric mice following CIH exposure

Weight loss and decreased food intake in IH-exposed mice have been reported (Jun et al., 2008). Another study showed that severity of weight loss of mice as a result of CIH, depends on severity of CIH (Li et al., 2007). Similarly, IH in humans leads to a decrease in body weight through suppression of appetite and facilitating decrease of fat tissue (Urdampilleta et al., 2012).

In this project, regarding the final weight, the three-way interaction was not significant, indicating the data did not demonstrate that the CIH-related changes in weight are influenced by the iNOS genotype combination of non-bone marrow-derived cells and bone marrow-derived cells. Furthermore, no significant difference was observed between the weights of the NOX-exposed mice and the CIH-exposed mice in any of the chimeric groups. This finding that the irradiated and bone marrow transplanted mice showed less susceptibility to CIH-related changes in weight, should be investigated further.

4.5. Hematocrit level in chimeric mice after CIH exposure

Chronic hypoxia leads to increased hematocrit level in mice (Schreier et al., 2014). However, it has been shown that CIH leads to less increase in hematocrit than chronic continuous hypoxia (Kang et al., 2016).

In the current project after 6 weeks of CIH exposure and assessment of final hematocrit level the three-way interaction was not significant, indicating the data did not demonstrate that the CIH-related changes in hematocrit depend on the iNOS genotype combination of non-bone marrow-derived cells and bone marrow-derived cells. No statistically significant different hematocrit level was seen in any of the CIH-exposed chimeric groups compared to their corresponding normoxic groups. In this project, the O₂ concentration was monitored via an oxygen sensor inside the chamber during all CIH exposures and all the recordings were saved on the server of Justus Liebig University, Giessen. Moreover, the O₂ concentration inside the chamber was confirmed by another portable oxygen sensor (Dräger X-am 2000). Here, it can be speculated that the unexpected observations of final hematocrit level can be associated with the lower susceptibility of irradiated and bone marrow transplanted mice to CIH-related changes of hematocrit level and further experiments should be considered to confirm this finding.

4.6. Assessments of pulmonary hypertension and right ventricular hypertrophy in chimeric mice

Human OSAS and also animal models of OSAS are associated with PH and right heart hypertrophy (Wong et al., 2017) (Sajkov and McEvoy, 2009) (Fagan, 2001). In this regard, CIH-induced PH has been reported in different studies in mice (Nisbet et al., 2009) (Campen et al., 2005). In the chimeric mice of the present study, the Fulton index (the ratio of right ventricle weight to left ventricle plus septum weight) and also the ratio of the right ventricle weight to tibia length were measured as parameters indicating right ventricular hypertrophy. With regard to both of these ratios, the three-way interactions were not significant, showing the data did not demonstrate that the CIH-related changes in right ventricular weight depend on the iNOS genotype combination of non-bone marrow-derived cells and bone marrow-derived cells. Both ratios showed no statistically significant differences in any of the CIH-exposed chimeric groups in comparison to their corresponding normoxic control groups.

Besides, RVID and RVWT of all chimeric groups were echocardiographically evaluated. In the same way, the three-way interactions were not significant, however, CIH-exposed WT(WT) mice showed significantly higher RVWT compared to their control normoxic mice (which can indicate

the sensitivity of this readout for detection of right ventricular hypertrophy in the absence of significant increase in right ventricular mass or right ventricular dilatation).

Regarding the terminal RVSP of the chimeric mice, the three-way interaction was not significant, indicating the data did not demonstrate that the CIH-related changes in RVSP depend on the iNOS genotype combination of non-bone marrow-derived cells and bone marrow-derived cells. The CIH-exposed WT(WT) and WT(KO) mice showed significant higher RVSP compared to NOX-exposed mice in these chimeric groups. The RVSP of CIH-exposed KO(WT) and KO(KO) chimeric groups did not show significant change compared to NOX-exposed mice. However, none of the two-way interactions were significant, indicating the data did not demonstrate that the CIH-related changes in RVSP in WT(KO), KO(WT), and KO(KO) groups have been significantly different from CIH-related RVSP increase in WT(WT) group.

In a mouse model of cigarette smoke-induced PH, it has been observed that the increase in RVSP occurs before the increase of Fulton index (Seimetz et al., 2011). Similarly, in the current study CIH-exposed WT(WT) mice showed a higher RVSP compared to NOX-exposed control mice, however Fulton index was not significantly higher in these mice after 6 weeks of CIH exposure.

4.7. Assessments of systemic hypertension and left ventricular hypertrophy in chimeric mice

Human OSAS and animal models of OSAS are associated with systemic hypertension and left heart hypertrophy (Marin et al., 2012) (Pedrosa et al., 2011) (Campen et al., 2005). In this regard, CIH-induced systemic hypertension has been reported in several studies in rats (Li et al., 2018) (Diogo et al., 2015) (Knight et al., 2011) and mice (Elliot-Portal et al., 2018) (Schulz et al., 2014). In the chimeric mice of the present study, the ratio of the left ventricle weight to tibia length was measured as a parameter showing left ventricular hypertrophy. The three-way interaction was not significant, showing the data did not demonstrate that the CIH-related changes of this ratio depend on the iNOS genotype combination of non-bone marrow-derived cells and bone marrow-derived cells. This ratio did not show any differences in any of the CIH-exposed chimeric mice groups in comparison to their corresponding normoxic control groups.

Moreover, LVID and LVWT of chimeric groups were echocardiographically evaluated. Similarly, the three-way interactions were not significant, indicating the data did not demonstrate that the CIH-related changes of these readouts depend on the iNOS genotype combination of non-bone marrow-derived cells and bone marrow-derived cells. No significant differences were observed in

LVID and LVWT of CIH-exposed chimeric mice compared to their control normoxic mice. These findings indicate that CIH exposure has not induced significant anatomical changes and hypertrophy in the left ventricle of the chimeric mice.

These results accompany the terminal hemodynamic measurements of LVSP and MAP of the chimeric mice in which the three-way interactions were not significant, and the CIH-exposed chimeric mice showed no difference compared to the respective normoxic groups. Similarly, the telemetry blood pressure measurement of systolic and diastolic blood pressure as well as MAP during 6 weeks of CIH exposure showed no significant change in blood pressure in any of the chimeric groups compared to their corresponding normoxic control.

There is the probability that these unexpected observations are caused by the altered vascular inflammation, which in turn is caused by irradiation and/or BMT. To address the effect of irradiation and BMT on the systemic hypertension and left ventricular hypertrophy in CIH model additional experiments should be performed.

4.8. Histological assessment of the degree of muscularization in pulmonary vessels of chimeric mice

In order to be able to quantify the effect of CIH on the vascular remodeling in different chimeric mice, assessment of the degree of muscularization was performed for pulmonary vessels as described previously (Kraut, 2014) (Dahal et al., 2011) (Dahal et al., 2010). It has been reported that CIH exposure of mice is associated with increased pulmonary vessels muscularization (Kraut, 2014) (Fagan, 2001) (Nisbet et al., 2009).

In the own project, no significant difference was observed in the degree of muscularization of small and medium pulmonary vessels in the chimeric groups exposed to CIH compared to their respective normoxic control groups. It can be speculated that these findings are associated to the effects of irradiation and/or BMT on the mice which require additional experiments.

4.9. Echocardiographic readouts in chimeric mice

Transthoracic echocardiography can be used as a noninvasive technique to assess cardiac function and cardiac phenotype in mice (Respress and Wehrens, 2010).

In order to determine function of the heart, CO and CI were assessed. Regarding both of these readouts, the three-way interactions were not significant, indicating the data did not demonstrate that the CIH-related changes of these readouts depend on the iNOS genotype combination of non-bone marrow-derived cells and bone marrow-derived cells.

However, for both CO and CI significant two-way interaction of “WT(WT) NOX and CIH vs. KO(KO) NOX and CIH” has been observed which can show the cardioprotective effect of iNOS deletion in CIH model. Higher levels of iNOS has previously been reported in OSA patients and also different CIH models compared to the control subjects (Jelic et al., 2008) (Liu et al., 2018) (Greenberg et al., 2006) (Lee et al., 2016).

To determine systolic function of the right heart, TAPSE was evaluated. The three-way interaction was not significant regarding TAPSE, indicating the data did not demonstrate that the CIH-related changes of TAPSE are influenced by the iNOS genotype combination of non-bone marrow-derived cells and bone marrow-derived cells. The two-way interactions of “WT(WT) NOX and CIH vs. WT(KO) NOX and CIH” and “WT(WT) NOX and CIH vs. KO(KO) NOX and CIH” were significant, demonstrating that the CIH-related TAPSE change in WT(KO) and KO(KO) groups has been significantly different from CIH-related TAPSE reduction in WT(WT) group. In other words, CIH did not lead to significant change of TAPSE in WT(KO) and KO(KO) mice (which lacked iNOS in bone marrow-derived cells) compared to WT(WT) mice, which can indicate protection of these mice against the deterioration of TAPSE in this CIH mouse model.

Regarding TAPSE, the mentioned significant two-way interaction of “WT(WT) NOX and CIH vs. KO(KO) NOX and CIH” can also indicate the cardioprotective effect of iNOS deletion in CIH model.

The two-way interactions of “WT(WT) NOX and CIH vs. KO(WT) NOX and CIH” was not significant, showing the data did not demonstrate that the CIH-related TAPSE reduction in KO(WT) group has been significantly different from CIH-related TAPSE reduction in WT(WT) group. It can be speculated that iNOS deletion only in non-bone marrow-derived cells cannot be protective against the deterioration of TAPSE in this CIH model.

TAPSE was significantly lower in CIH-exposed WT(WT) and KO(WT) groups compared to their respective normoxic control groups, whereas in the WT(KO) and KO(KO) groups no significant difference was observed between the NOX- and CIH-exposed mice. Here the sensitivity of echocardiography in CIH mouse model can be observed. In the same way, new echocardiographic methods can be used in OSA patients as a valuable sensitive tool to detect the subclinical RV dysfunctions which are not even accompanied by RV failure and PH (Altekin et al., 2012).

To determine systolic function of the left heart, LVEF was used. The three-way interaction was not significant, indicating the data did not demonstrate that the CIH-related changes of LVEF depend

on the iNOS genotype combination of non-bone marrow-derived cells and bone marrow-derived cells. No significant differences were observed in CIH-exposed chimeric mice, compared to their respective normoxic controls. Similarly, in another study no significant changes of LVEF have been reported in WT or iNOS knockout mice due to CIH (Kraut, 2014).

4.10. Superoxide anion measurement by electron spin resonance spectroscopy

Oxidative stress has been suggested to be involved in the pathogenesis of OSAS (Passali et al., 2015) (Zhang and Veasey, 2012). It has been reported that although myocardial superoxide anion is increased in both wild type and iNOS^{-/-} mice in transverse aortic constriction mouse model, the iNOS^{-/-} mice showed significantly less increase in superoxide anion compared to wild type mice in this model (Zhang et al., 2007). In the own project, superoxide anion measurement was performed by ESR spectroscopy for both blood and lung homogenate samples. The three-way interactions were not significant, indicating the data did not demonstrate that the CIH-related changes of superoxide anion in blood and lung samples depend on the iNOS genotype combination of non-bone marrow-derived cells and bone marrow-derived cells. However, regarding the superoxide anion of the lung homogenate samples, significant two-way interaction of “WT(WT) NOX and CIH vs. KO(KO) NOX and CIH” was observed. This slight but significant difference in response to CIH exposure can show the influence of iNOS deletion on superoxide anion in CIH model.

No statistically significant change was observed in the concentration of superoxide anion in the blood samples as a result of CIH in any of the chimeric groups. To address the effect of irradiation and BMT on the ROS level in CIH model additional experiments should be performed. Furthermore, as superoxide anion can react very fast with NO and form peroxynitrite (Schiffrin, 2008) (Hill et al., 2010), it can be suggested to carry out experiments on bone marrow transplanted mice to investigate CIH effects on other ROS (e.g. peroxynitrite) which were not measured in this project.

While on the subject, it should be mentioned that the samples for ESR spectroscopy were prepared as fresh as possible from blood and lung homogenates. However, organ and blood harvesting were performed after invasive hemodynamic measurements in which the mice were for approximately 30 minutes under inhalation anesthesia. Thus, the obtained results might be influenced by the mentioned considerable time under anesthesia.

4.11. Conclusion

In the current study, regarding all the assessed readouts, the three-way interactions were not significant, indicating the data did not demonstrate that the CIH-related responses depend on the iNOS genotype combination of non-bone marrow-derived cells and bone marrow-derived cells. However, regarding the echocardiographically measured CO and CI (indicators of pumping function of the heart), the two-way interactions of “WT(WT) NOX and CIH vs. KO(KO) NOX and CIH” were significant, indicating the cardioprotective effects of iNOS deletion in CIH model.

Concerning the right ventricular hypertrophy, no significant change was observed in Fulton index and the ratio of right ventricle to tibia length in the chimeric mice. However, echocardiographically measured RVWT was significantly higher in CIH-exposed WT(WT) mice compared to respective control normoxic mice. CIH-exposed WT(WT) and WT(KO) mice showed significantly higher RVSP, compared to respective NOX-exposed chimeric mice. TAPSE, as an indicator of systolic function of the right ventricle, was significantly lower in CIH-exposed WT(WT) and KO(WT) mice compared to control mice, whereas in CIH- and NOX-exposed WT(KO) and KO(KO) mice no significant difference was observed. Regarding TAPSE, the two-way interactions of “WT(WT) NOX and CIH vs. KO(KO) NOX and CIH” was significant which indicates the cardioprotective effect of iNOS deletion in CIH model.

Unexpectedly, no significant change was observed in the degree of muscularization of pulmonary vessels in chimeric mice as a result of CIH.

With regard to left ventricular hypertrophy in the chimeric mice, no significant change was observed in the different readouts as a result of CIH. LVEF (an indicator of systolic function of the left ventricle) displayed no significant difference between CIH- and NOX-exposed mice. Furthermore, no significant change was observed in the systemic blood pressure of the chimeric mice due to CIH.

Measurement of concentration of superoxide anion in the lung homogenate samples revealed slight but significant difference in response to CIH exposure in two-way interaction of “WT(WT) NOX and CIH vs. KO(KO) NOX and CIH” which can show the influence of iNOS deletion on superoxide anion in CIH model. Superoxide anion in the blood samples of chimeric mice indicated no significant change caused by CIH.

It was unexpected that the CIH had no significant effect in elevation of systemic blood pressure in WT(WT) mice as it has been previously shown that CIH, as applied here, leads to systemic

hypertension in WT mice (Kraut, 2014). Therefore, it can be speculated that irradiation and/or BMT prevented the development of CIH-related systemic hypertension. Although there is already a report from protective effects of irradiation and BMT on large arteries of a mouse model of aortic aneurysm and atherosclerosis (Patel et al., 2018), cardiovascular protective effects of irradiation and BMT on CIH mouse model should be studied further.

The unexpected observations regarding some of the readouts (e.g. degree of muscularization of pulmonary vessels, systemic blood pressure, and etc.) can be due to irradiation and/or BMT, and requires further investigation to confirm or contradict this idea.

5. Summary

Obstructive sleep apnea syndrome (OSAS) is a prevalent breathing disorder during sleep. It is considered a serious disease and has a high impact on quality of life of the affected people. OSAS can lead to cardiovascular and pulmonary complications including pulmonary and systemic hypertension. So far, the mechanisms involved in pathogenesis of OSAS are not quite clarified. The available treatment methods, such as continuous positive airway pressure, surgical intervention and oral appliances which keep the upper airways open during sleep, improve symptoms and decrease the incidence of cardiovascular diseases resulted from OSAS. However, these treatments are not tolerated by all patients. Moreover, there is no effective pharmacological treatment for OSAS.

For simulation of OSAS several different animal models are available. In the current thesis the chronic intermittent hypoxia (CIH) mouse model was used which is appropriate to investigate the pathophysiological mechanisms of OSAS.

The results of previous studies and also investigations performed in the CIH mouse model, from the laboratory where the current work was performed, have shown that the inducible nitric oxide synthase (iNOS) plays an important role in the pathogenesis of OSAS and its associated cardiovascular and pulmonary consequences. Wild type (WT) mice and iNOS knockout (KO) mice were investigated in a mouse model of CIH. The mice lacking iNOS showed less systemic hypertension, pulmonary hypertension (PH), and pulmonary vascular remodeling compared to WT mice in the CIH model.

The main aim of this study was to further investigate the role of iNOS and reactive oxygen species (ROS) in the pathogenesis of systemic and pulmonary hypertension in the CIH model of OSAS. The objective was to clarify whether iNOS is originated from the cells that are derived from bone marrow or from other cell types (non-bone marrow-derived cells). For this purpose, iNOS KO and WT mice were irradiated at the beginning of the experiment until complete bone marrow suppression, and were transplanted with either iNOS KO or WT bone marrow cells. By using bone marrow transplantation (BMT), four different groups of chimeric mice were created namely, WT(WT), irradiated WT mice that received bone marrow cells from WT mice; KO(KO), irradiated iNOS^{-/-} mice that received bone marrow cells from iNOS^{-/-} mice; WT(KO), irradiated WT mice that received bone marrow cells from iNOS^{-/-} mice; and KO(WT), irradiated iNOS^{-/-} mice that

received bone marrow cells from WT mice. The chimeric mice were exposed to either CIH or normoxia-normoxia cycles (NOX).

Daily blood pressure measurements, final invasive hemodynamic measurements, determination of different heart ratios, echocardiographic studies and histological determination of degree of muscularization of pulmonary vessels were used to assess the development of systemic and pulmonary hypertension. Superoxide anion production was measured in lung homogenate and blood samples of chimeric mice by electron spin resonance spectroscopy.

Regarding all the readouts, the three-way interactions were not significant, indicating the data did not demonstrate that the CIH-related responses depend on the iNOS genotype combination of non-bone marrow-derived cells and bone marrow-derived cells.

The two-way interactions of “WT(WT) NOX and CIH vs. KO(KO) NOX and CIH” for the echocardiographically measured cardiac output, cardiac index, and tricuspid annular plane systolic excursion (indicators of pumping function of the heart) were significant, indicating the cardioprotective effects of iNOS deletion in CIH model.

CIH-exposed WT(WT) and WT(KO) chimeric mice showed significant higher right ventricular systolic pressure (RVSP) compared to respective NOX-exposed control mice. However, the degree of muscularization of the pulmonary vessels did not show significant change in any of the chimeric mice compared to their corresponding NOX groups.

No statistically significant changes were observed in systemic blood pressure as a result of CIH in chimeric mice.

Measurement of concentration of superoxide anion in the lung homogenate samples revealed slight but significant difference in response to CIH exposure in two-way interaction of “WT(WT) NOX and CIH vs. KO(KO) NOX and CIH”. No significant difference was observed in the concentration of superoxide anion of the blood samples as a result of CIH in any of the chimeric groups.

As it has been already shown that CIH leads to systemic hypertension and higher degree of muscularization of the pulmonary vessels in WT mice, it was unexpected that CIH had no effect on these readouts in WT(WT) mice. The unexpected observations of the current study regarding some of the readouts (e.g. systemic blood pressure, degree of muscularization of pulmonary vessels, and etc.) can be associated to the effects of irradiation and/or BMT on CIH mouse model which should be investigated further.

6. Zusammenfassung

Das obstruktive Schlafapnoesyndrom (OSAS) ist eine weitverbreitete schlafbezogene Atemstörung, die die Lebensqualität der Betroffenen negativ beeinflusst. OSAS kann zu kardiovaskulären und pulmonalen Erkrankungen, wie z.B. pulmonaler und arterieller Hypertonie führen. Obwohl Behandlungsmethoden wie z.B. *continuous positive airway pressure*, chirurgische Eingriffe, und orale Apparaturen zur Verfügung stehen, werden die Symptome dadurch lediglich verbessert und eine Heilung der Grunderkrankung ist zum momentanen Zeitpunkt nicht möglich. Bisher sind die Mechanismen der Pathogenese von OSAS jedoch nicht vollständig geklärt, was eine pharmakologische Therapie verhindert. Ziel dieser Arbeit war es, mittels eines Mausmodells der chronisch intermittierenden Hypoxie (CIH) diese Pathomechanismen weiter zu entschlüsseln. Die Ergebnisse früherer Studien und laborinterne Untersuchungen haben gezeigt, dass die induzierbare NO-Synthase (iNOS) eine wichtige Rolle bei der Pathogenese von OSAS und den damit verbundenen kardiovaskulären und pulmonalen Erkrankungen spielt. Die iNOS Knockout (KO) Mäuse zeigten im Vergleich zu Wildtyp (WT) Mäusen im CIH-Modell keine arterielle und pulmonale Hypertonie und weniger stark ausgeprägte pulmonale Gefäßveränderungen.

Das Ziel dieser Arbeit bestand darin den/die iNOS produzierende Zelltypen zu identifizieren, die bei der Entstehung des OSAS von Bedeutung sind. Es sollte spezifisch die Frage beantwortet werden, ob iNOS aus Knochenmarks-stämmigen oder aus Nichtknochenmarks-stämmigen Zellen für die Pathogenese des OSAS verantwortlich ist. Zu diesem Zweck wurden iNOS^{-/-} und WT Mäuse vor Beginn der CIH-Exposition bis zur vollständigen Knochenmarkssuppression bestrahlt und durch Knochenmarktransplantation (KMT) entweder mit Knochenmarkszellen von WT oder iNOS^{-/-} Mäusen rekonstituiert. So wurden insgesamt vier verschiedene Gruppen von chimären Mäusen erzeugt: WT(WT), bestrahlte WT Mäuse, die Knochenmarkszellen von WT Mäusen erhielten; KO(KO), bestrahlte iNOS^{-/-} Mäuse, die Knochenmarkszellen von iNOS^{-/-} Mäusen erhielten; WT(KO), bestrahlte WT Mäuse, die Knochenmarkszellen von iNOS^{-/-} Mäusen erhielten und KO(WT), bestrahlte iNOS^{-/-} Mäuse, die Knochenmarkszellen von WT Mäusen erhielten. Diese chimären Mäuse wurden entweder CIH oder Kontroll-Bedingungen (Normoxie (NOX)) ausgesetzt. Tägliche Blutdruckmessungen, endgültige invasive hämodynamische Messungen, Bestimmung verschiedener Herzratios, echokardiographische Studien, und histologische Bestimmung des Muskularisierungsgrades von pulmonalen Gefäßen wurden verwendet, um die Entwicklung von

systemischer und pulmonaler Hypertonie zu bewerten. Weiterhin wurde die Produktion von Superoxidanionen in Lungenhomogenat und Blutproben mittels Elektronenspinresonanz-Spektroskopie gemessen.

In Bezug auf alle gemessenen Parameter, waren die Drei-Wege-Interaktionen nicht signifikant, was darauf hinweist, dass die Daten nicht zeigen, dass die CIH-bezogenen Reaktionen von der iNOS-Genotypkombination von Nichtknochenmarks-stämmigen Zellen und Knochenmarks-stämmigen Zellen abhängen.

Die Zwei-Wege-Interaktionen von „WT(WT) NOX und CIH vs. KO(KO) NOX und CIH“ für das echokardiographisch gemessene *cardiac output*, *cardiac index*, und *tricuspid annular plane systolic excursion* (Indikatoren für die Pumpfunktion des Herzens) waren signifikant, was auf die kardioprotektiven Effekte der iNOS-Deletion im CIH Modell hinweist.

CIH-exponierte chimäre WT(WT) und WT(KO) Mäuse zeigten im Vergleich zu den jeweiligen NOX-exponierten Kontrollmäusen einen signifikant höheren rechtsventrikulären systolischen Druck (RVSP). Der Muskularisierungsgrad der Lungengefäße zeigte jedoch bei keiner der chimären Mäuse eine signifikante Veränderung im Vergleich zu ihren entsprechenden NOX Gruppen. Außerdem wurden keine statistisch signifikanten Veränderungen des systemischen Blutdrucks als Folge von CIH bei chimären Mäusen beobachtet.

Die Messung der Konzentration des Superoxidanions in den Lungenhomogenatproben ergab einen geringfügigen, aber signifikanten Unterschied in der Reaktion auf die CIH-Exposition in der Zwei-Wege-Interaktion von „WT(WT) NOX und CIH vs. KO(KO) NOX und CIH“. Es wurde kein signifikanter Unterschied in der Konzentration des Superoxidanions der Blutproben als Folge von CIH in einer der chimären Gruppen beobachtet.

Da bereits gezeigt wurde, dass CIH bei WT Mäusen zu arterieller Hypertonie und einem höheren Muskularisierungsgrad der Lungengefäße führt, war es unerwartet, dass diese Veränderungen bei den CIH-exponierten bei WT(WT) Mäusen nicht zu sehen waren. Die unerwarteten Beobachtungen der aktuellen Studie in Bezug auf einige der gemessenen Parameter (z. B. systemischer Blutdruck, Muskularisierungsgrad der pulmonalen Gefäße usw.) können mit den Auswirkungen von Bestrahlung und/oder KMT auf das CIH Mausmodell in Verbindung gebracht werden, die weiter erforscht werden sollten.

7. References

AASM (1999). Sleep-related breathing disorders in adults: recommendations for syndrome definition and measurement techniques in clinical research. The Report of an American Academy of Sleep Medicine Task Force. *Sleep* 22, 667-689.

Agita, A., and Alsagaff, M.T. (2017). Inflammation, Immunity, and Hypertension. *Acta Medica Indonesiana* 49, 158-165.

Alchanatis, M., Tourkhoriti, G., Kakouros, S., Kosmas, E., Podaras, S., and Jordanoglou, J.B. (2001). Daytime pulmonary hypertension in patients with obstructive sleep apnea: the effect of continuous positive airway pressure on pulmonary hemodynamics. *Respiration; International Review of Thoracic Diseases* 68, 566-572.

Alderton, W.K., Cooper, C.E., and Knowles, R.G. (2001). Nitric oxide synthases: structure, function and inhibition. *The Biochemical Journal* 357, 593-615.

Almendros, I., Carreras, A., Montserrat, J.M., Gozal, D., Navajas, D., and Farre, R. (2012). Potential role of adult stem cells in obstructive sleep apnea. *Frontiers in Neurology* 3, 112.

Altekin, R.E., Karakas, M.S., Yanikoglu, A., Ozel, D., Ozbudak, O., Demir, I., and Deger, N. (2012). Determination of right ventricular dysfunction using the speckle tracking echocardiography method in patients with obstructive sleep apnea. *Cardiology Journal* 19, 130-139.

Banno, K., and Kryger, M.H. (2007). Sleep apnea: clinical investigations in humans. *Sleep Medicine* 8, 400-426.

Bartolome, S., Hooper, M.M., and Klepetko, W. (2017). Advanced pulmonary arterial hypertension: mechanical support and lung transplantation. *European Respiratory Review : an Official Journal of the European Respiratory Society* 26.

Baumgardner, J.E., and Otto, C.M. (2003). In vitro intermittent hypoxia: challenges for creating hypoxia in cell culture. *Respiratory Physiology & Neurobiology* 136, 131-139.

Bazzano, L.A., Khan, Z., Reynolds, K., and He, J. (2007). Effect of nocturnal nasal continuous positive airway pressure on blood pressure in obstructive sleep apnea. *Hypertension (Dallas, Tex : 1979)* 50, 417-423.

Bergmann, B.M., Kushida, C.A., Everson, C.A., Gilliland, M.A., Obermeyer, W., and Rechtschaffen, A. (1989). Sleep deprivation in the rat: II. Methodology. *Sleep* 12, 5-12.

Berry, R.B., Budhiraja, R., Gottlieb, D.J., Gozal, D., Iber, C., Kapur, V.K., Marcus, C.L., Mehra, R., Parthasarathy, S., Quan, S.F., *et al.* (2012). Rules for scoring respiratory events in sleep: update of the 2007 AASM Manual for the Scoring of Sleep and Associated Events. Deliberations of the Sleep Apnea Definitions Task Force of the American Academy of Sleep Medicine. *Journal of*

Clinical Sleep Medicine : JCSM : official publication of the American Academy of Sleep Medicine 8, 597-619.

Bonderman, D., Jakowitsch, J., Adlbrecht, C., Schemper, M., Kyrle, P.A., Schonauer, V., Exner, M., Klepetko, W., Kneussl, M.P., Maurer, G., *et al.* (2005). Medical conditions increasing the risk of chronic thromboembolic pulmonary hypertension. *Thrombosis and Haemostasis* 93, 512-516.

Bonderman, D., Turecek, P.L., Jakowitsch, J., Weltermann, A., Adlbrecht, C., Schneider, B., Kneussl, M., Rubin, L.J., Kyrle, P.A., Klepetko, W., *et al.* (2003). High prevalence of elevated clotting factor VIII in chronic thromboembolic pulmonary hypertension. *Thrombosis and Haemostasis* 90, 372-376.

Bonsignore, M.R., Marrone, O., Insalaco, G., and Bonsignore, G. (1994). The cardiovascular effects of obstructive sleep apnoeas: analysis of pathogenic mechanisms. *European Respiratory Journal* 7, 786-805.

Boudewyns, A., Marklund, M., and Hochban, W. (2007). Alternatives for OSAHS treatment: selection of patients for upper airway surgery and oral appliances. *European Respiratory Review* 16, 132-145.

Brennick, M.J., Pickup, S., Cater, J.R., and Kuna, S.T. (2006). Phasic respiratory pharyngeal mechanics by magnetic resonance imaging in lean and obese Zucker rats. *American Journal of Respiratory and Critical Care Medicine* 173, 1031-1037.

Brooks, D., Horner, R.L., Kozar, L.F., Render-Teixeira, C.L., and Phillipson, E.A. (1997). Obstructive sleep apnea as a cause of systemic hypertension. Evidence from a canine model. *The Journal of Clinical Investigation* 99, 106-109.

Buchwald, H., Avidor, Y., Braunwald, E., Jensen, M.D., Pories, W., Fahrbach, K., and Schoelles, K. (2004). Bariatric surgery: a systematic review and meta-analysis. *Journal of the American Medical Association* 292, 1724-1737.

Calhoun, D.A., Jones, D., Textor, S., Goff, D.C., Murphy, T.P., Toto, R.D., White, A., Cushman, W.C., White, W., Sica, D., *et al.* (2008). Resistant hypertension: diagnosis, evaluation, and treatment. A scientific statement from the American Heart Association Professional Education Committee of the Council for High Blood Pressure Research. *Hypertension (Dallas, Tex : 1979)* 51, 1403-1419.

Campbell, M.G., Smith, B.C., Potter, C.S., Carragher, B., and Marletta, M.A. (2014). Molecular architecture of mammalian nitric oxide synthases. *Proceedings of the National Academy of Sciences of the United States of America* 111, E3614-3623.

Campen, M.J., Shimoda, L.A., and O'Donnell, C.P. (2005). Acute and chronic cardiovascular effects of intermittent hypoxia in C57BL/6J mice. *Journal of Applied Physiology (Bethesda, Md : 1985)* 99, 2028-2035.

- Carlson, J.T., Hedner, J.A., Ejjnell, H., and Peterson, L.E. (1994). High prevalence of hypertension in sleep apnea patients independent of obesity. *American Journal of Respiratory and Critical Care Medicine* 150, 72-77.
- Carreras, A., Almendros, I., and Farre, R. (2011). Potential role of bone marrow mesenchymal stem cells in obstructive sleep apnea. *International Journal of Stem Cells* 4, 43-49.
- Ceccato, F., Bernkopf, E., and Scaroni, C. (2015). Sleep apnea syndrome in endocrine clinics. *Journal of Endocrinological Investigation* 38, 827-834.
- Chan, A.S., Lee, R.W., and Cistulli, P.A. (2008). Non-positive airway pressure modalities: mandibular advancement devices/positional therapy. *Proceedings of the American Thoracic Society* 5, 179-184.
- Charles, L., Triscott, J., and Dobbs, B. (2017). Secondary Hypertension: Discovering the Underlying Cause. *American Family Physician* 96, 453-461.
- Chaumais, M.C., Macari, E.A., and Sitbon, O. (2013). Calcium-channel blockers in pulmonary arterial hypertension. *Handbook of Experimental Pharmacology* 218, 161-175.
- Chen, L., Shi, Q., and Scharf, S.M. (2000). Hemodynamic effects of periodic obstructive apneas in sedated pigs with congestive heart failure. *Journal of Applied Physiology (Bethesda, Md : 1985)* 88, 1051-1060.
- Cho, J.H., Suh, J.D., Han, K.D., and Lee, H.M. (2019). Uvulopalatopharyngoplasty reduces the incidence of depression caused by obstructive sleep apnea. *The Laryngoscope* 129, 1005-1009.
- Chopra, S., Polotsky, V.Y., and Jun, J.C. (2016). Sleep Apnea Research in Animals. Past, Present, and Future. *American Journal of Respiratory Cell and Molecular Biology* 54, 299-305.
- Chung, F., Liao, P., Elsaid, H., Islam, S., Shapiro, C.M., and Sun, Y. (2012). Oxygen desaturation index from nocturnal oximetry: a sensitive and specific tool to detect sleep-disordered breathing in surgical patients. *Anesthesia and Analgesia* 114, 993-1000.
- Courand, P.Y., and Lantelme, P. (2014). Significance, prognostic value and management of heart rate in hypertension. *Archives of Cardiovascular Diseases* 107, 48-57.
- Cui, Y.Z., Hisha, H., Yang, G.X., Fan, T.X., Jin, T., Li, Q., Lian, Z., and Ikehara, S. (2002). Optimal protocol for total body irradiation for allogeneic bone marrow transplantation in mice. *Bone Marrow Transplantation* 30, 843-849.
- Dahal, B.K., Cornitescu, T., Tretyn, A., Pullamsetti, S.S., Kosanovic, D., Dumitrascu, R., Ghofrani, H.A., Weissmann, N., Voswinkel, R., Banat, G.A., *et al.* (2010). Role of epidermal growth factor inhibition in experimental pulmonary hypertension. *American Journal of Respiratory and Critical Care Medicine* 181, 158-167.

Dahal, B.K., Heuchel, R., Pullamsetti, S.S., Wilhelm, J., Ghofrani, H.A., Weissmann, N., Seeger, W., Grimminger, F., and Schermuly, R.T. (2011). Hypoxic pulmonary hypertension in mice with constitutively active platelet-derived growth factor receptor-beta. *Pulmonary Circulation* 1, 259-268.

Dancey, D.R., Hanly, P.J., Soong, C., Lee, B., and Hoffstein, V. (2001). Impact of menopause on the prevalence and severity of sleep apnea. *Chest* 120, 151-155.

Davie, N.J., Crossno, J.T., Jr., Frid, M.G., Hofmeister, S.E., Reeves, J.T., Hyde, D.M., Carpenter, T.C., Brunetti, J.A., McNiece, I.K., and Stenmark, K.R. (2004). Hypoxia-induced pulmonary artery adventitial remodeling and neovascularization: contribution of progenitor cells. *American Journal of Physiology - Lung Cellular and Molecular Physiology* 286, L668-678.

Davies, R.J., Ali, N.J., and Stradling, J.R. (1992). Neck circumference and other clinical features in the diagnosis of the obstructive sleep apnoea syndrome. *Thorax* 47, 101-105.

Davis, E.M., and O'Donnell, C.P. (2013). Rodent models of sleep apnea. *Respiratory Physiology & Neurobiology* 188, 355-361.

de Lima, F.F., Mazzotti, D.R., Tufik, S., and Bittencourt, L. (2016). The role inflammatory response genes in obstructive sleep apnea syndrome: a review. *Sleep & Breathing = Schlaf & Atmung* 20, 331-338.

Dematteis, M., Godin-Ribuot, D., Arnaud, C., Ribuot, C., Stanke-Labesque, F., Pepin, J.L., and Levy, P. (2009). Cardiovascular consequences of sleep-disordered breathing: contribution of animal models to understanding the human disease. *ILAR journal* 50, 262-281.

Dias-Junior, C.A., Cau, S.B., and Tanus-Santos, J.E. (2008). Role of nitric oxide in the control of the pulmonary circulation: physiological, pathophysiological, and therapeutic implications. *Jornal Brasileiro de Pneumologia : publicacao oficial da Sociedade Brasileira de Pneumologia e Tisiologia* 34, 412-419.

Diogo, L.N., Pereira, S.A., Nunes, A.R., Afonso, R.A., Santos, A.I., and Monteiro, E.C. (2015). Efficacy of carvedilol in reversing hypertension induced by chronic intermittent hypoxia in rats. *European Journal of Pharmacology* 765, 58-67.

Duchna, H.W., Stoohs, R., Guilleminault, C., Christine Anspach, M., Schultze-Werninghaus, G., and Orth, M. (2006). Vascular endothelial dysfunction in patients with mild obstructive sleep apnea syndrome. *Wiener Medizinische Wochenschrift (1946)* 156, 596-604.

Dunlap, B., and Weyer, G. (2016). Pulmonary Hypertension: Diagnosis and Treatment. *American Family Physician* 94, 463-469.

Duran-Struuck, R., and Dysko, R.C. (2009). Principles of bone marrow transplantation (BMT): providing optimal veterinary and husbandry care to irradiated mice in BMT studies. *Journal of the American Association for Laboratory Animal Science : JAALAS* 48, 11-22.

Elliot-Portal, E., Laouafa, S., Arias-Reyes, C., Janes, T.A., Joseph, V., and Soliz, J. (2018). Brain-derived erythropoietin protects from intermittent hypoxia-induced cardiorespiratory dysfunction and oxidative stress in mice. *Sleep* 41.

Epstein, L.J., Kristo, D., Strollo, P.J., Jr., Friedman, N., Malhotra, A., Patil, S.P., Ramar, K., Rogers, R., Schwab, R.J., Weaver, E.M., *et al.* (2009). Clinical guideline for the evaluation, management and long-term care of obstructive sleep apnea in adults. *Journal of Clinical Sleep Medicine : JCSM : official publication of the American Academy of Sleep Medicine* 5, 263-276.

Escobar, E. (2002). Hypertension and coronary heart disease. *Journal of Human Hypertension* 16 *Suppl 1*, S61-63.

Esler, M., Lambert, E., and Schlaich, M. (2010). Point: Chronic activation of the sympathetic nervous system is the dominant contributor to systemic hypertension. *Journal of Applied Physiology (Bethesda, Md : 1985)* 109, 1996-1998; discussion 2016.

Fagan, K.A. (2001). Selected Contribution: Pulmonary hypertension in mice following intermittent hypoxia. *Journal of Applied Physiology (Bethesda, Md : 1985)* 90, 2502-2507.

Farre, R., Rotger, M., Montserrat, J.M., Calero, G., and Navajas, D. (2003). Collapsible upper airway segment to study the obstructive sleep apnea/hypopnea syndrome in rats. *Respiratory Physiology & Neurobiology* 136, 199-209.

Ferguson, K.A., Cartwright, R., Rogers, R., and Schmidt-Nowara, W. (2006). Oral appliances for snoring and obstructive sleep apnea: a review. *Sleep* 29, 244-262.

Fewell, J.E., Williams, B.J., Szabo, J.S., and Taylor, B.J. (1988). Influence of repeated upper airway obstruction on the arousal and cardiopulmonary response to upper airway obstruction in lambs. *Pediatric Research* 23, 191-195.

Foster, G.E., Poulin, M.J., and Hanly, P.J. (2007). Intermittent hypoxia and vascular function: implications for obstructive sleep apnoea. *Experimental Physiology* 92, 51-65.

Garg, S., de Lemos, J.A., Ayers, C., Khouri, M.G., Pandey, A., Berry, J.D., Peshock, R.M., and Drazner, M.H. (2015). Association of a 4-Tiered Classification of LV Hypertrophy With Adverse CV Outcomes in the General Population. *JACC Cardiovascular Imaging* 8, 1034-1041.

George, C.F. (2001). Reduction in motor vehicle collisions following treatment of sleep apnoea with nasal CPAP. *Thorax* 56, 508-512.

Gibson, G.J. (2004). Obstructive sleep apnoea syndrome: underestimated and undertreated. *British Medical Bulletin* 72, 49-65.

Go, A.S., Bauman, M.A., Coleman King, S.M., Fonarow, G.C., Lawrence, W., Williams, K.A., and Sanchez, E. (2014). An effective approach to high blood pressure control: a science advisory from the American Heart Association, the American College of Cardiology, and the Centers for Disease Control and Prevention. *Hypertension (Dallas, Tex : 1979)* 63, 878-885.

Greenberg, H., Ye, X., Wilson, D., Htoo, A.K., Hendersen, T., and Liu, S.F. (2006). Chronic intermittent hypoxia activates nuclear factor-kappaB in cardiovascular tissues in vivo. *Biochemical and Biophysical Research Communications* 343, 591-596.

Guazzi, M., and Galie, N. (2012). Pulmonary hypertension in left heart disease. *European Respiratory Review : an Official Journal of the European Respiratory Society* 21, 338-346.

Guilleminault, C., Partinen, M., Hollman, K., Powell, N., and Stoohs, R. (1995). Familial aggregates in obstructive sleep apnea syndrome. *Chest* 107, 1545-1551.

Hamrahi, H., Stephenson, R., Mahamed, S., Liao, K.S., and Horner, R.L. (2001). Selected Contribution: Regulation of sleep-wake states in response to intermittent hypoxic stimuli applied only in sleep. *Journal of Applied Physiology (Bethesda, Md : 1985)* 90, 2490-2501.

Hawrylkiewicz, I., Sliwinski, P., Gorecka, D., Plywaczewski, R., and Zielinski, J. (2004). Pulmonary haemodynamics in patients with OSAS or an overlap syndrome. *Monaldi Archives for Chest Disease = Archivio Monaldi Per le Malattie del Torace* 61, 148-152.

Hendricks, J.C., Kline, L.R., Kovalski, R.J., O'Brien, J.A., Morrison, A.R., and Pack, A.I. (1987). The English bulldog: a natural model of sleep-disordered breathing. *Journal of Applied Physiology (Bethesda, Md : 1985)* 63, 1344-1350.

Hill, B.G., Dranka, B.P., Bailey, S.M., Lancaster, J.R., Jr., and Darley-Usmar, V.M. (2010). What part of NO don't you understand? Some answers to the cardinal questions in nitric oxide biology. *The Journal of Biological Chemistry* 285, 19699-19704.

Hoepfer, M.M., Humbert, M., Souza, R., Idrees, M., Kawut, S.M., Sliwa-Hahnle, K., Jing, Z.C., and Gibbs, J.S. (2016). A global view of pulmonary hypertension. *The Lancet Respiratory Medicine* 4, 306-322.

Hoepfer, M.M., Mayer, E., Simonneau, G., and Rubin, L.J. (2006). Chronic thromboembolic pulmonary hypertension. *Circulation* 113, 2011-2020.

Howard, L.S. (2011). Prognostic factors in pulmonary arterial hypertension: assessing the course of the disease. *European respiratory review : an Official Journal of the European Respiratory Society* 20, 236-242.

Hudgel, D.W. (2016). Sleep Apnea Severity Classification - Revisited. *Sleep* 39, 1165-1166.

Humbert, M. (2008). Update in pulmonary arterial hypertension 2007. *American Journal of Respiratory and Critical Care Medicine* 177, 574-579.

Humbert, M., Morrell, N.W., Archer, S.L., Stenmark, K.R., MacLean, M.R., Lang, I.M., Christman, B.W., Weir, E.K., Eickelberg, O., Voelkel, N.F., *et al.* (2004). Cellular and molecular pathobiology of pulmonary arterial hypertension. *Journal of the American College of Cardiology* 43, 13s-24s.

- Ip, M.S., Lam, B., Chan, L.Y., Zheng, L., Tsang, K.W., Fung, P.C., and Lam, W.K. (2000). Circulating nitric oxide is suppressed in obstructive sleep apnea and is reversed by nasal continuous positive airway pressure. *American Journal of Respiratory and Critical Care Medicine* 162, 2166-2171.
- James, P.A., Oparil, S., Carter, B.L., Cushman, W.C., Dennison-Himmelfarb, C., Handler, J., Lackland, D.T., LeFevre, M.L., MacKenzie, T.D., Ogedegbe, O., *et al.* (2014). 2014 evidence-based guideline for the management of high blood pressure in adults: report from the panel members appointed to the Eighth Joint National Committee (JNC 8). *Journal of the American Medical Association* 311, 507-520.
- Javaheri, S., Barbe, F., Campos-Rodriguez, F., Dempsey, J.A., Khayat, R., Javaheri, S., Malhotra, A., Martinez-Garcia, M.A., Mehra, R., Pack, A.I., *et al.* (2017). Sleep Apnea: Types, Mechanisms, and Clinical Cardiovascular Consequences. *Journal of the American College of Cardiology* 69, 841-858.
- Jelic, S., Padeletti, M., Kawut, S.M., Higgins, C., Canfield, S.M., Onat, D., Colombo, P.C., Basner, R.C., Factor, P., and LeJemtel, T.H. (2008). Inflammation, oxidative stress, and repair capacity of the vascular endothelium in obstructive sleep apnea. *Circulation* 117, 2270-2278.
- Jun, J., and Polotsky, V.Y. (2007). Sleep disordered breathing and metabolic effects: evidence from animal models. *Sleep Medicine Clinics* 2, 263-277.
- Jun, J., Reinke, C., Bedja, D., Berkowitz, D., Bevans-Fonti, S., Li, J., Barouch, L.A., Gabrielson, K., and Polotsky, V.Y. (2010). Effect of intermittent hypoxia on atherosclerosis in apolipoprotein E-deficient mice. *Atherosclerosis* 209, 381-386.
- Jun, J., Savransky, V., Nanayakkara, A., Bevans, S., Li, J., Smith, P.L., and Polotsky, V.Y. (2008). Intermittent hypoxia has organ-specific effects on oxidative stress. *American Journal of Physiology Regulatory, Integrative and Comparative Physiology* 295, R1274-1281.
- Kang, J., Li, Y., Hu, K., Lu, W., Zhou, X., Yu, S., and Xu, L. (2016). Chronic intermittent hypoxia versus continuous hypoxia: Same effects on hemorheology? *Clinical Hemorheology and Microcirculation* 63, 245-255.
- Kessler, R., Chaouat, A., Weitzenblum, E., Oswald, M., Ehrhart, M., Apprill, M., and Krieger, J. (1996). Pulmonary hypertension in the obstructive sleep apnoea syndrome: prevalence, causes and therapeutic consequences. *European Respiratory Journal* 9, 787-794.
- Kim, N.H., Delcroix, M., Jenkins, D.P., Channick, R., Darteville, P., Jansa, P., Lang, I., Madani, M.M., Ogino, H., Pengo, V., *et al.* (2013). Chronic thromboembolic pulmonary hypertension. *Journal of the American College of Cardiology* 62, D92-99.
- Kimoff, R.J., Makino, H., Horner, R.L., Kozar, L.F., Lue, F., Slutsky, A.S., and Phillipson, E.A. (1994). Canine model of obstructive sleep apnea: model description and preliminary application. *Journal of Applied Physiology (Bethesda, Md : 1985)* 76, 1810-1817.

Kleinert, H., Pautz, A., Linker, K., and Schwarz, P.M. (2004). Regulation of the expression of inducible nitric oxide synthase. *European Journal of Pharmacology* 500, 255-266.

Knappe, S.W., Bakke, M., Svanholt, P., Petersson, A., and Sonnesen, L. (2017). Long-term side effects on the temporomandibular joints and oro-facial function in patients with obstructive sleep apnoea treated with a mandibular advancement device. *Journal of Oral Rehabilitation* 44, 354-362.

Knight, W.D., Little, J.T., Carreno, F.R., Toney, G.M., Mifflin, S.W., and Cunningham, J.T. (2011). Chronic intermittent hypoxia increases blood pressure and expression of FosB/DeltaFosB in central autonomic regions. *American Journal of Physiology Regulatory, Integrative and Comparative Physiology* 301, R131-139.

Knowles, R.G., and Moncada, S. (1994). Nitric oxide synthases in mammals. *The Biochemical Journal* 298 (Pt 2), 249-258.

Kohut, A., Patel, N., and Singh, H. (2016). Comprehensive Echocardiographic Assessment of the Right Ventricle in Murine Models. *Journal of Cardiovascular Ultrasound* 24, 229-238.

Kone, B.C., Kuncewicz, T., Zhang, W., and Yu, Z.Y. (2003). Protein interactions with nitric oxide synthases: controlling the right time, the right place, and the right amount of nitric oxide. *American Journal of Physiology Renal physiology* 285, F178-190.

Konecny, T., Kara, T., and Somers, V.K. (2014). Obstructive sleep apnea and hypertension: an update. *Hypertension (Dallas, Tex : 1979)* 63, 203-209.

Kostrzewa-Janicka, J., Sliwinski, P., Wojda, M., Rolski, D., and Mierzwinska-Nastalska, E. (2017). Mandibular Advancement Appliance for Obstructive Sleep Apnea Treatment. *Advances in Experimental Medicine and Biology* 944, 63-71.

Kryger, M.H. (2000). Diagnosis and management of sleep apnea syndrome. *Clinical Cornerstone* 2, 39-47.

Kushida, C.A., Littner, M.R., Hirshkowitz, M., Morgenthaler, T.I., Alessi, C.A., Bailey, D., Boehlecke, B., Brown, T.M., Coleman, J., Jr., Friedman, L., *et al.* (2006). Practice parameters for the use of continuous and bilevel positive airway pressure devices to treat adult patients with sleep-related breathing disorders. *Sleep* 29, 375-380.

Laubach, V.E., Shesely, E.G., Smithies, O., and Sherman, P.A. (1995). Mice lacking inducible nitric oxide synthase are not resistant to lipopolysaccharide-induced death. *Proceedings of the National Academy of Sciences of the United States of America* 92, 10688-10692.

Launois, S.H., Averill, N., Abraham, J.H., Kirby, D.A., and Weiss, J.W. (2001). Cardiovascular responses to nonrespiratory and respiratory arousals in a porcine model. *Journal of Applied Physiology (Bethesda, Md : 1985)* 90, 114-120.

Lee, E.J., Woodske, M.E., Zou, B., and O'Donnell, C.P. (2009). Dynamic arterial blood gas analysis in conscious, unrestrained C57BL/6J mice during exposure to intermittent hypoxia. *Journal of Applied Physiology* (Bethesda, Md : 1985) *107*, 290-294.

Lee, M.Y., Wang, Y., Mak, J.C., and Ip, M.S. (2016). Intermittent hypoxia induces NF-kappaB-dependent endothelial activation via adipocyte-derived mediators. *American Journal of Physiology Cell Physiology* *310*, C446-455.

Li, J., Savransky, V., Nanayakkara, A., Smith, P.L., O'Donnell, C.P., and Polotsky, V.Y. (2007). Hyperlipidemia and lipid peroxidation are dependent on the severity of chronic intermittent hypoxia. *Journal of Applied Physiology* (Bethesda, Md : 1985) *102*, 557-563.

Li, T., Chen, Y., Gua, C., and Wu, B. (2018). Elevated Oxidative Stress and Inflammation in Hypothalamic Paraventricular Nucleus Are Associated With Sympathetic Excitation and Hypertension in Rats Exposed to Chronic Intermittent Hypoxia. *Frontiers in Physiology* *9*, 840.

Liu, F., Liu, T.W., and Kang, J. (2018). The role of NF-kappaB-mediated JNK pathway in cognitive impairment in a rat model of sleep apnea. *Journal of Thoracic Disease* *10*, 6921-6931.

Logan, A.G., Perlikowski, S.M., Mente, A., Tisler, A., Tkacova, R., Niroumand, M., Leung, R.S., and Bradley, T.D. (2001). High prevalence of unrecognized sleep apnoea in drug-resistant hypertension. *Journal of Hypertension* *19*, 2271-2277.

Lonergan, R.P., 3rd, Ware, J.C., Atkinson, R.L., Winter, W.C., and Suratt, P.M. (1998). Sleep apnea in obese miniature pigs. *Journal of Applied Physiology* (Bethesda, Md : 1985) *84*, 531-536.

Lovic, D., Narayan, P., Pittaras, A., Faselis, C., Doumas, M., and Kokkinos, P. (2017). Left ventricular hypertrophy in athletes and hypertensive patients. *Journal of Clinical Hypertension* (Greenwich, Conn) *19*, 413-417.

Luo, S., Lei, H., Qin, H., and Xia, Y. (2014). Molecular mechanisms of endothelial NO synthase uncoupling. *Current Pharmaceutical Design* *20*, 3548-3553.

Maekawa, M., Shiomi, T., Usui, K., Sasanabe, R., and Kobayashi, T. (1998). Prevalence of ischemic heart disease among patients with sleep apnea syndrome. *Psychiatry and Clinical Neurosciences* *52*, 219-220.

Mandegar, M., Fung, Y.C., Huang, W., Remillard, C.V., Rubin, L.J., and Yuan, J.X. (2004). Cellular and molecular mechanisms of pulmonary vascular remodeling: role in the development of pulmonary hypertension. *Microvascular Research* *68*, 75-103.

Marin, J.M., Agusti, A., Villar, I., Forner, M., Nieto, D., Carrizo, S.J., Barbe, F., Vicente, E., Wei, Y., Nieto, F.J., *et al.* (2012). Association between treated and untreated obstructive sleep apnea and risk of hypertension. *Journal of the American Medical Association* *307*, 2169-2176.

Mason, M., Welsh, E.J., and Smith, I. (2013). Drug therapy for obstructive sleep apnoea in adults. *The Cochrane Database of Systematic Reviews*, Cd003002.

Maspero, C., Giannini, L., Galbiati, G., Rosso, G., and Farronato, G. (2015). Obstructive sleep apnea syndrome: a literature review. *Minerva Stomatologica* 64, 97-109.

McCoy, J.G., Tartar, J.L., Bebis, A.C., Ward, C.P., McKenna, J.T., Baxter, M.G., McGaughy, J., McCarley, R.W., and Strecker, R.E. (2007). Experimental sleep fragmentation impairs attentional set-shifting in rats. *Sleep* 30, 52-60.

McMurray, J.J., Adamopoulos, S., Anker, S.D., Auricchio, A., Bohm, M., Dickstein, K., Falk, V., Filippatos, G., Fonseca, C., Gomez-Sanchez, M.A., *et al.* (2012). ESC Guidelines for the diagnosis and treatment of acute and chronic heart failure 2012: The Task Force for the Diagnosis and Treatment of Acute and Chronic Heart Failure 2012 of the European Society of Cardiology. Developed in collaboration with the Heart Failure Association (HFA) of the ESC. *European Heart Journal* 33, 1787-1847.

McNeil, K., and Dunning, J. (2007). Chronic thromboembolic pulmonary hypertension (CTEPH). *Heart (British Cardiac Society)* 93, 1152-1158.

McNicholas, W.T. (2007). Cardiovascular outcomes of CPAP therapy in obstructive sleep apnea syndrome. *American Journal of Physiology Regulatory, Integrative and Comparative Physiology* 293, R1666-1670.

McNicholas, W.T. (2008). Diagnosis of obstructive sleep apnea in adults. *Proceedings of the American Thoracic Society* 5, 154-160.

Mesarwi, O.A., Sharma, E.V., Jun, J.C., and Polotsky, V.Y. (2015). Metabolic dysfunction in obstructive sleep apnea: A critical examination of underlying mechanisms. *Sleep and Biological Rhythms* 13, 2-17.

Montani, D., Lau, E.M., Dorfmuller, P., Girerd, B., Jais, X., Savale, L., Perros, F., Nossent, E., Garcia, G., Parent, F., *et al.* (2016). Pulmonary veno-occlusive disease. *European Respiratory Journal* 47, 1518-1534.

Morris, L.G., Kleinberger, A., Lee, K.C., Liberatore, L.A., and Burschtin, O. (2008). Rapid risk stratification for obstructive sleep apnea, based on snoring severity and body mass index. *Otolaryngology-Head and Neck surgery : Official Journal of American Academy of Otolaryngology-Head and Neck Surgery* 139, 615-618.

Mukherjee, S., Saxena, R., and Palmer, L.J. (2018). The genetics of obstructive sleep apnoea. *Respirology (Carlton, Vic)* 23, 18-27.

Nacher, M., Serrano-Mollar, A., Farre, R., Panes, J., Segui, J., and Montserrat, J.M. (2007). Recurrent obstructive apneas trigger early systemic inflammation in a rat model of sleep apnea. *Respiratory Physiology & Neurobiology* 155, 93-96.

Navar, L.G. (2010). Counterpoint: Activation of the intrarenal renin-angiotensin system is the dominant contributor to systemic hypertension. *Journal of Applied Physiology* (Bethesda, Md : 1985) *109*, 1998-2000; discussion 2015.

Ng, J.H., and Yow, M. (2019). Oral Appliances in the Management of Obstructive Sleep Apnea. *Sleep Medicine Clinics* *14*, 109-118.

Nieto, F.J., Young, T.B., Lind, B.K., Shahar, E., Samet, J.M., Redline, S., D'Agostino, R.B., Newman, A.B., Lebowitz, M.D., and Pickering, T.G. (2000). Association of sleep-disordered breathing, sleep apnea, and hypertension in a large community-based study. Sleep Heart Health Study. *Journal of the American Medical Association* *283*, 1829-1836.

Nisbet, R.E., Graves, A.S., Kleinhenz, D.J., Rupnow, H.L., Reed, A.L., Fan, T.H., Mitchell, P.O., Sutliff, R.L., and Hart, C.M. (2009). The role of NADPH oxidase in chronic intermittent hypoxia-induced pulmonary hypertension in mice. *American Journal of Respiratory Cell and Molecular Biology* *40*, 601-609.

Ohayon, M.M., Guilleminault, C., Priest, R.G., Zulley, J., and Smirne, S. (2000). Is sleep-disordered breathing an independent risk factor for hypertension in the general population (13,057 subjects)? *Journal of Psychosomatic Research* *48*, 593-601.

Orr, W.C., Heading, R., Johnson, L.F., and Kryger, M. (2004). Review article: sleep and its relationship to gastro-oesophageal reflux. *Alimentary Pharmacology & Therapeutics* *20 Suppl 9*, 39-46.

Pack, A.I., and Gislason, T. (2009). Obstructive sleep apnea and cardiovascular disease: a perspective and future directions. *Progress in Cardiovascular Diseases* *51*, 434-451.

Paravicini, T.M., and Touyz, R.M. (2008). NADPH oxidases, reactive oxygen species, and hypertension: clinical implications and therapeutic possibilities. *Diabetes Care* *31 Suppl 2*, S170-180.

Passali, D., Corallo, G., Yaremchuk, S., Longini, M., Proietti, F., Passali, G.C., and Bellussi, L. (2015). Oxidative stress in patients with obstructive sleep apnoea syndrome. *Acta Otorhinolaryngologica Italica : Organo Ufficiale Della Societa Italiana di Otorinolaringologia E Chirurgia Cervico-Facciale* *35*, 420-425.

Patel, J., Douglas, G., Kerr, A.G., Hale, A.B., and Channon, K.M. (2018). Effect of irradiation and bone marrow transplantation on angiotensin II-induced aortic inflammation in ApoE knockout mice. *Atherosclerosis* *276*, 74-82.

Patel, S.R., White, D.P., Malhotra, A., Stanchina, M.L., and Ayas, N.T. (2003). Continuous positive airway pressure therapy for treating sleepiness in a diverse population with obstructive sleep apnea: results of a meta-analysis. *Archives of Internal Medicine* *163*, 565-571.

Pedrosa, R.P., Drager, L.F., Gonzaga, C.C., Sousa, M.G., de Paula, L.K., Amaro, A.C., Amodeo, C., Bortolotto, L.A., Krieger, E.M., Bradley, T.D., *et al.* (2011). Obstructive sleep apnea: the most

common secondary cause of hypertension associated with resistant hypertension. *Hypertension* (Dallas, Tex : 1979) 58, 811-817.

Peppard, P.E., Young, T., Barnet, J.H., Palta, M., Hagen, E.W., and Hla, K.M. (2013). Increased prevalence of sleep-disordered breathing in adults. *American Journal of Epidemiology* 177, 1006-1014.

Peppard, P.E., Young, T., Palta, M., and Skatrud, J. (2000). Prospective study of the association between sleep-disordered breathing and hypertension. *The New England Journal of Medicine* 342, 1378-1384.

Philip, P., Gross, C.E., Taillard, J., Bioulac, B., and Guilleminault, C. (2005). An animal model of a spontaneously reversible obstructive sleep apnea syndrome in the monkey. *Neurobiology of Disease* 20, 428-431.

Pinto, J.M., Garpestad, E., Weiss, J.W., Bergau, D.M., and Kirby, D.A. (1993). Hemodynamic changes associated with obstructive sleep apnea followed by arousal in a porcine model. *Journal of Applied Physiology* (Bethesda, Md : 1985) 75, 1439-1443.

Polotsky, V.Y., Rubin, A.E., Balbir, A., Dean, T., Smith, P.L., Schwartz, A.R., and O'Donnell, C.P. (2006). Intermittent hypoxia causes REM sleep deficits and decreases EEG delta power in NREM sleep in the C57BL/6J mouse. *Sleep Medicine* 7, 7-16.

Prabhat, K.C., Goyal, L., Bey, A., and Maheshwari, S. (2012). Recent advances in the management of obstructive sleep apnea: The dental perspective. *Journal of Natural Science, Biology, and Medicine* 3, 113-117.

Prinsell, J.R. (2002). Maxillomandibular advancement surgery for obstructive sleep apnea syndrome. *Journal of the American Dental Association* (1939) 133, 1489-1497; quiz 1539-1440.

Prisant, L.M. (2005). Hypertensive heart disease. *Journal of Clinical Hypertension* (Greenwich, Conn) 7, 231-238.

Punjabi, N.M. (2008). The epidemiology of adult obstructive sleep apnea. *Proceedings of the American Thoracic Society* 5, 136-143.

Rabinovitch, M. (2012). Molecular pathogenesis of pulmonary arterial hypertension. *The Journal of Clinical Investigation* 122, 4306-4313.

Rabkin, S.W., and Chan, S.H. (2012). Correlation of pulse wave velocity with left ventricular mass in patients with hypertension once blood pressure has been normalized. *Heart International* 7, e5.

Respress, J.L., and Wehrens, X.H. (2010). Transthoracic echocardiography in mice. *Journal of Visualized Experiments : JoVE*.

Rosenkranz, S. (2007). Pulmonary hypertension: current diagnosis and treatment. *Clinical Research in Cardiology : Official Journal of the German Cardiac Society* 96, 527-541.

Rosenkranz, S., and Preston, I.R. (2015). Right heart catheterisation: best practice and pitfalls in pulmonary hypertension. *European Respiratory Review : an Official Journal of the European Respiratory Society* 24, 642-652.

Saareanta, T., Hedner, J., Bonsignore, M.R., Riha, R.L., McNicholas, W.T., Penzel, T., Anttalainen, U., Kivimäki, J.A., Pretl, M., Sliwinski, P., *et al.* (2016). Clinical Phenotypes and Comorbidity in European Sleep Apnoea Patients. *PloS one* 11, e0163439.

Sajkov, D., and McEvoy, R.D. (2009). Obstructive sleep apnea and pulmonary hypertension. *Progress in Cardiovascular Diseases* 51, 363-370.

Sajkov, D., Wang, T., Saunders, N.A., Bune, A.J., and McEvoy, R.D. (2002). Continuous positive airway pressure treatment improves pulmonary hemodynamics in patients with obstructive sleep apnea. *American Journal of Respiratory and Critical Care Medicine* 165, 152-158.

Sajkov, D., Wang, T., Saunders, N.A., Bune, A.J., Neill, A.M., and Douglas McEvoy, R. (1999). Daytime pulmonary hemodynamics in patients with obstructive sleep apnea without lung disease. *American Journal of Respiratory and Critical Care Medicine* 159, 1518-1526.

Sankri-Tarbichi, A.G. (2012). Obstructive sleep apnea-hypopnea syndrome: Etiology and diagnosis. *Avicenna Journal of Medicine* 2, 3-8.

Sarkar, P., Mukherjee, S., Chai-Coetzer, C.L., and McEvoy, R.D. (2018). The epidemiology of obstructive sleep apnoea and cardiovascular disease. *Journal of Thoracic Disease* 10, S4189-s4200.

Saugel, B., Mair, S., Götz, S.Q., Tschirdewahn, J., Frank, J., Höllthaler, J., Schmid, R.M., and Huber, W. (2015). Indexation of cardiac output to biometric parameters in critically ill patients: A systematic analysis of a transpulmonary thermodilution-derived database. *Journal of Critical Care* 30, 957-962.

Savransky, V., Nanayakkara, A., Li, J., Bevans, S., Smith, P.L., Rodriguez, A., and Polotsky, V.Y. (2007). Chronic intermittent hypoxia induces atherosclerosis. *American Journal of Respiratory and Critical Care Medicine* 175, 1290-1297.

Schermyly, R.T., Ghofrani, H.A., Wilkins, M.R., and Grimminger, F. (2011). Mechanisms of disease: pulmonary arterial hypertension. *Nature Reviews Cardiology* 8, 443-455.

Schifffrin, E.L. (2008). Oxidative stress, nitric oxide synthase, and superoxide dismutase: a matter of imbalance underlies endothelial dysfunction in the human coronary circulation. *Hypertension (Dallas, Tex : 1979)* 51, 31-32.

Schlosshan, D., and Elliott, M.W. (2004). Sleep . 3: Clinical presentation and diagnosis of the obstructive sleep apnoea hypopnoea syndrome. *Thorax* 59, 347-352.

Schmieder, R.E. (2010). End organ damage in hypertension. *Deutsches Arzteblatt International* 107, 866-873.

Schreier, D.A., Hacker, T.A., Hunter, K., Eickoff, J., Liu, A., Song, G., and Chesler, N. (2014). Impact of increased hematocrit on right ventricular afterload in response to chronic hypoxia. *Journal of Applied Physiology* (Bethesda, Md : 1985) *117*, 833-839.

Schulz, R., Murzabekova, G., Egemnazarov, B., Kraut, S., Eisele, H.J., Dumitrascu, R., Heitmann, J., Seimetz, M., Witzenrath, M., Ghofrani, H.A., *et al.* (2014). Arterial hypertension in a murine model of sleep apnea: role of NADPH oxidase 2. *Journal of Hypertension* *32*, 300-305.

Schulz, R., Schmidt, D., Blum, A., Lopes-Ribeiro, X., Lucke, C., Mayer, K., Olschewski, H., Seeger, W., and Grimminger, F. (2000). Decreased plasma levels of nitric oxide derivatives in obstructive sleep apnoea: response to CPAP therapy. *Thorax* *55*, 1046-1051.

Schwartz, A.R., Patil, S.P., Laffan, A.M., Polotsky, V., Schneider, H., and Smith, P.L. (2008). Obesity and obstructive sleep apnea: pathogenic mechanisms and therapeutic approaches. *Proceedings of the American Thoracic Society* *5*, 185-192.

Seeger, W., Adir, Y., Barbera, J.A., Champion, H., Coghlan, J.G., Cottin, V., De Marco, T., Galie, N., Ghio, S., Gibbs, S., *et al.* (2013). Pulmonary hypertension in chronic lung diseases. *Journal of the American College of Cardiology* *62*, D109-116.

Seimetz, M., Parajuli, N., Pichl, A., Veit, F., Kwapiszewska, G., Weisel, F.C., Milger, K., Egemnazarov, B., Turowska, A., Fuchs, B., *et al.* (2011). Inducible NOS inhibition reverses tobacco-smoke-induced emphysema and pulmonary hypertension in mice. *Cell* *147*, 293-305.

Serra-Torres, S., Bellot-Arcis, C., Montiel-Company, J.M., Marco-Algarra, J., and Almerich-Silla, J.M. (2016). Effectiveness of mandibular advancement appliances in treating obstructive sleep apnea syndrome: A systematic review. *The Laryngoscope* *126*, 507-514.

Simonneau, G., Montani, D., Celermajer, D.S., Denton, C.P., Gatzoulis, M.A., Krowka, M., Williams, P.G., and Souza, R. (2019). Haemodynamic definitions and updated clinical classification of pulmonary hypertension. *European Respiratory Journal* *53*.

Somers, V.K., White, D.P., Amin, R., Abraham, W.T., Costa, F., Culebras, A., Daniels, S., Floras, J.S., Hunt, C.E., Olson, L.J., *et al.* (2008). Sleep apnea and cardiovascular disease: an American Heart Association/American College Of Cardiology Foundation Scientific Statement from the American Heart Association Council for High Blood Pressure Research Professional Education Committee, Council on Clinical Cardiology, Stroke Council, and Council On Cardiovascular Nursing. In collaboration with the National Heart, Lung, and Blood Institute National Center on Sleep Disorders Research (National Institutes of Health). *Circulation* *118*, 1080-1111.

Sommer, N., Dietrich, A., Schermuly, R.T., Ghofrani, H.A., Gudermann, T., Schulz, R., Seeger, W., Grimminger, F., and Weissmann, N. (2008). Regulation of hypoxic pulmonary vasoconstriction: basic mechanisms. *European Respiratory Journal* *32*, 1639-1651.

- Sommer, N., Huttemann, M., Pak, O., Scheibe, S., Knoepp, F., Sinkler, C., Malczyk, M., Gierhardt, M., Esfandiary, A., Kraut, S., *et al.* (2017). Mitochondrial Complex IV Subunit 4 Isoform 2 Is Essential for Acute Pulmonary Oxygen Sensing. *Circulation Research* *121*, 424-438.
- Spicuzza, L., Caruso, D., and Di Maria, G. (2015). Obstructive sleep apnoea syndrome and its management. *Therapeutic Advances in Chronic Disease* *6*, 273-285.
- Staessen, J.A., Wang, J., Bianchi, G., and Birkenhager, W.H. (2003). Essential hypertension. *Lancet (London, England)* *361*, 1629-1641.
- Stenmark, K.R., Davie, N., Frid, M., Gerasimovskaya, E., and Das, M. (2006a). Role of the adventitia in pulmonary vascular remodeling. *Physiology (Bethesda, Md)* *21*, 134-145.
- Stenmark, K.R., Fagan, K.A., and Frid, M.G. (2006b). Hypoxia-induced pulmonary vascular remodeling: cellular and molecular mechanisms. *Circulation Research* *99*, 675-691.
- Stoberl, A.S., Schwarz, E.I., Haile, S.R., Turnbull, C.D., Rossi, V.A., Stradling, J.R., and Kohler, M. (2017). Night-to-night variability of obstructive sleep apnea. *Journal of Sleep Research* *26*, 782-788.
- Sultan, S., Tseng, S., Stanziola, A.A., Hodges, T., Saggar, R., and Saggar, R. (2018). Pulmonary Hypertension: The Role of Lung Transplantation. *Heart Failure Clinics* *14*, 327-331.
- Tagaito, Y., Polotsky, V.Y., Campen, M.J., Wilson, J.A., Balbir, A., Smith, P.L., Schwartz, A.R., and O'Donnell, C.P. (2001). A model of sleep-disordered breathing in the C57BL/6J mouse. *Journal of Applied Physiology (Bethesda, Md : 1985)* *91*, 2758-2766.
- Taichman, D.B., Ornelas, J., Chung, L., Klinger, J.R., Lewis, S., Mandel, J., Palevsky, H.I., Rich, S., Sood, N., Rosenzweig, E.B., *et al.* (2014). Pharmacologic therapy for pulmonary arterial hypertension in adults: CHEST Guideline and Expert Panel Report. *Chest* *146*, 449-475.
- Tan, H.L., Kheirandish-Gozal, L., Abel, F., and Gozal, D. (2016). Craniofacial syndromes and sleep-related breathing disorders. *Sleep Medicine Reviews* *27*, 74-88.
- Taveira, K.V.M., Kuntze, M.M., Berretta, F., de Souza, B.D.M., Godolfim, L.R., Demathe, T., De Luca Canto, G., and Porporatti, A.L. (2018). Association between obstructive sleep apnea and alcohol, caffeine and tobacco: A meta-analysis. *Journal of Oral Rehabilitation* *45*, 890-902.
- Temirbekov, D., Gunes, S., Yazici, Z.M., and Sayin, I. (2018). The Ignored Parameter in the Diagnosis of Obstructive Sleep Apnea Syndrome: The Oxygen Desaturation Index. *Turkish Archives of Otorhinolaryngology* *56*, 1-6.
- Testelmans, D., Tamisier, R., Barone-Rochette, G., Baguet, J.P., Roux-Lombard, P., Pepin, J.L., and Levy, P. (2013). Profile of circulating cytokines: impact of OSA, obesity and acute cardiovascular events. *Cytokine* *62*, 210-216.

Thorpy, M.J. (2012). Classification of sleep disorders. *Neurotherapeutics : the Journal of the American Society for Experimental Neurotherapeutics* 9, 687-701.

Trammell, R.A., Verhulst, S., and Toth, L.A. (2014). Effects of sleep fragmentation on sleep and markers of inflammation in mice. *Comparative Medicine* 64, 13-24.

Tuder, R.M. (2017). Pulmonary vascular remodeling in pulmonary hypertension. *Cell and Tissue Research* 367, 643-649.

Tuomilehto, H., Seppa, J., and Uusitupa, M. (2013). Obesity and obstructive sleep apnea-clinical significance of weight loss. *Sleep Medicine Reviews* 17, 321-329.

Urdampilleta, A., Gonzalez-Muniesa, P., Portillo, M.P., and Martinez, J.A. (2012). Usefulness of combining intermittent hypoxia and physical exercise in the treatment of obesity. *Journal of Physiology and Biochemistry* 68, 289-304.

Vachiery, J.L., Adir, Y., Barbera, J.A., Champion, H., Coghlan, J.G., Cottin, V., De Marco, T., Galie, N., Ghio, S., Gibbs, J.S., *et al.* (2013). Pulmonary hypertension due to left heart diseases. *Journal of the American College of Cardiology* 62, D100-108.

Vaessen, T.J., Overeem, S., and Sitskoorn, M.M. (2015). Cognitive complaints in obstructive sleep apnea. *Sleep Medicine Reviews* 19, 51-58.

Veasey, S.C., Guilleminault, C., Strohl, K.P., Sanders, M.H., Ballard, R.D., and Magalang, U.J. (2006). Medical therapy for obstructive sleep apnea: a review by the Medical Therapy for Obstructive Sleep Apnea Task Force of the Standards of Practice Committee of the American Academy of Sleep Medicine. *Sleep* 29, 1036-1044.

Verbraecken, J., Hedner, J., and Penzel, T. (2017). Pre-operative screening for obstructive sleep apnoea. *European Respiratory Review : an Official Journal of the European Respiratory Society* 26.

Verdecchia, P., Reboldi, G., Angeli, F., Avanzini, F., de Simone, G., Pede, S., Perticone, F., Schillaci, G., Vanuzzo, D., and Maggioni, A.P. (2007). Prognostic value of serial electrocardiographic voltage and repolarization changes in essential hypertension: the HEART Survey study. *American Journal of Hypertension* 20, 997-1004.

Verdecchia, P., Schillaci, G., Borgioni, C., Ciucci, A., Gattobigio, R., Zampi, I., and Porcellati, C. (1998). Prognostic value of a new electrocardiographic method for diagnosis of left ventricular hypertrophy in essential hypertension. *Journal of the American College of Cardiology* 31, 383-390.

Versari, D., Daghini, E., Viridis, A., Ghiadoni, L., and Taddei, S. (2009). Endothelium-dependent contractions and endothelial dysfunction in human hypertension. *British Journal of Pharmacology* 157, 527-536.

Vonk-Noordegraaf, A., Haddad, F., Chin, K.M., Forfia, P.R., Kawut, S.M., Lumens, J., Naeije, R., Newman, J., Oudiz, R.J., Provencher, S., *et al.* (2013). Right heart adaptation to pulmonary arterial

hypertension: physiology and pathobiology. *Journal of the American College of Cardiology* 62, D22-33.

Vonk Noordegraaf, A., and Galie, N. (2011). The role of the right ventricle in pulmonary arterial hypertension. *European Respiratory Review : an Official Journal of the European Respiratory Society* 20, 243-253.

Voswinckel, R., Ziegelhoeffer, T., Heil, M., Kostin, S., Breier, G., Mehling, T., Haberberger, R., Clauss, M., Gaumann, A., Schaper, W., *et al.* (2003). Circulating vascular progenitor cells do not contribute to compensatory lung growth. *Circulation Research* 93, 372-379.

Vouzouneraki, K., Franklin, K.A., Forsgren, M., Warn, M., Persson, J.T., Wik, H., Dahlgren, C., Nilsson, A.S., Alkebro, C., Burman, P., *et al.* (2018). Temporal relationship of sleep apnea and acromegaly: a nationwide study. *Endocrine* 62, 456-463.

Walker-Engstrom, M.L., Tegelberg, A., Wilhelmsson, B., and Ringqvist, I. (2002). 4-year follow-up of treatment with dental appliance or uvulopalatopharyngoplasty in patients with obstructive sleep apnea: a randomized study. *Chest* 121, 739-746.

Weatherspoon, D., Sullivan, D., and Weatherspoon, C.A. (2016). Obstructive Sleep Apnea and Modifications in Sedation: An Update. *Critical Care Nursing Clinics of North America* 28, 217-226.

Weitzenblum, E., and Chaouat, A. (2009). Cor pulmonale. *Chronic Respiratory Disease* 6, 177-185.

Wetter, D.W., Young, T.B., Bidwell, T.R., Badr, M.S., and Palta, M. (1994). Smoking as a risk factor for sleep-disordered breathing. *Archives of Internal Medicine* 154, 2219-2224.

Whelton, P.K., Carey, R.M., Aronow, W.S., Casey, D.E., Jr., Collins, K.J., Dennison Himmelfarb, C., DePalma, S.M., Gidding, S., Jamerson, K.A., Jones, D.W., *et al.* (2018). 2017 ACC/AHA/AAPA/ABC/ACPM/AGS/APhA/ASH/ASPC/NMA/PCNA Guideline for the Prevention, Detection, Evaluation, and Management of High Blood Pressure in Adults: A Report of the American College of Cardiology/American Heart Association Task Force on Clinical Practice Guidelines. *Journal of the American College of Cardiology* 71, e127-e248.

White, S.G., Fletcher, E.C., and Miller, C.C., 3rd (1995). Acute systemic blood pressure elevation in obstructive and nonobstructive breath hold in primates. *Journal of Applied Physiology* (Bethesda, Md : 1985) 79, 324-330.

Wolley, M.J., Pimenta, E., Calhoun, D., Gordon, R.D., Cowley, D., and Stowasser, M. (2017). Treatment of primary aldosteronism is associated with a reduction in the severity of obstructive sleep apnoea. *Journal of Human Hypertension* 31, 561-567.

Won, C.H., Li, K.K., and Guilleminault, C. (2008). Surgical treatment of obstructive sleep apnea: upper airway and maxillomandibular surgery. *Proceedings of the American Thoracic Society* 5, 193-199.

- Wong, H.S., Williams, A.J., and Mok, Y. (2017). The relationship between pulmonary hypertension and obstructive sleep apnea. *Current Opinion in Pulmonary Medicine* 23, 517-521.
- Young, T., Palta, M., Dempsey, J., Skatrud, J., Weber, S., and Badr, S. (1993). The occurrence of sleep-disordered breathing among middle-aged adults. *The New England Journal of Medicine* 328, 1230-1235.
- Young, T., Peppard, P., Palta, M., Hla, K.M., Finn, L., Morgan, B., and Skatrud, J. (1997). Population-based study of sleep-disordered breathing as a risk factor for hypertension. *Archives of Internal Medicine* 157, 1746-1752.
- Young, T., Peppard, P.E., and Gottlieb, D.J. (2002a). Epidemiology of obstructive sleep apnea: a population health perspective. *American Journal of Respiratory and Critical Care Medicine* 165, 1217-1239.
- Young, T., Shahar, E., Nieto, F.J., Redline, S., Newman, A.B., Gottlieb, D.J., Walsleben, J.A., Finn, L., Enright, P., and Samet, J.M. (2002b). Predictors of sleep-disordered breathing in community-dwelling adults: the Sleep Heart Health Study. *Archives of Internal Medicine* 162, 893-900.
- Yu, X., Ge, L., Niu, L., Lian, X., Ma, H., and Pang, L. (2018). The Dual Role of Inducible Nitric Oxide Synthase in Myocardial Ischemia/Reperfusion Injury: Friend or Foe? *Oxidative Medicine and Cellular Longevity* 2018, 8364848.
- Zhan, G., Fenik, P., Pratico, D., and Veasey, S.C. (2005). Inducible nitric oxide synthase in long-term intermittent hypoxia: hypersomnolence and brain injury. *American Journal of Respiratory and Critical Care Medicine* 171, 1414-1420.
- Zhang, J., and Veasey, S. (2012). Making sense of oxidative stress in obstructive sleep apnea: mediator or distracter? *Frontiers in Neurology* 3, 179.
- Zhang, M., Zhang, W., Tan, J., Zhao, M., Zhang, Q., and Lei, P. (2016). Role of hypothyroidism in obstructive sleep apnea: a meta-analysis. *Current Medical Research and Opinion* 32, 1059-1064.
- Zhang, P., Xu, X., Hu, X., van Deel, E.D., Zhu, G., and Chen, Y. (2007). Inducible nitric oxide synthase deficiency protects the heart from systolic overload-induced ventricular hypertrophy and congestive heart failure. *Circulation Research* 100, 1089-1098.
- Zhang, W., and Si, L.Y. (2012). Obstructive sleep apnea syndrome (OSAS) and hypertension: pathogenic mechanisms and possible therapeutic approaches. *Upsala Journal of Medical Sciences* 117, 370-382.
- Zinchuk, A.V., Jeon, S., Koo, B.B., Yan, X., Bravata, D.M., Qin, L., Selim, B.J., Strohl, K.P., Redeker, N.S., Concato, J., *et al.* (2018). Polysomnographic phenotypes and their cardiovascular implications in obstructive sleep apnoea. *Thorax* 73, 472-480.

Kraut, S. (2014). Pathomechanismen der Schlafapnoe im Mausmodell Rolle der endothelialen und induzierbaren NO-Synthase. Inaugural Dissertation, Fachbereich Veterinärmedizin der Justus-Liebig-Universität Gießen.

8. Acknowledgments

Firstly, I would like to express my gratitude to my supervisor, Prof. Norbert Weißmann for providing me the privilege and opportunity to do my PhD work in his group, and his support and supervision during this PhD work and thesis.

I am extremely grateful to my postdoc, Dr. Simone Kraut for her great support throughout this PhD work. The completion of this PhD project would not have been possible without her help.

I would like to thank my co-supervisor, Prof. Christiane Herden from the Institute for Veterinary Pathology for all her support.

I would like to thank Dr. Akylbek Sydykov, Dr. Daniel Zahner, Dr. Martin Roderfeld, Dr. Dirk Krambrich, and Dr. Jochen Wilhelm for their assistance in different parts of this PhD work.

I appreciate the help and support of all the members Prof. Weißmann's group during this PhD work, in particular, Karin, Carmen, Ingrid, Elisabeth, Nils, Elisa, Sabine, Susan, Nasim, Katharina, Christine, Kathrin, Azadeh, Mareike, Alireza, Nicole, Inna, Bruno, Mirja, Ingrid, and Thomas.

I wish to thank Prof. Ralph Schermuly, and his group members, Christina, Astrid, Ewa, and Argen for their helps during this project.

I am thankful to Prof. Saverio Bellusci, and his team members, Elie, Vahid, and Kerstin for their assistance.

I would like to thank the organizers and members of the International Max Planck Research School for Heart and Lung Research (IMPRS-HLR), and also the International Giessen Graduate Centre for the Life Sciences (GGL) that provided the opportunity to learn science as well as soft skills in the international environments of these graduate programs.

Finally, I would like to thank my wonderful family for their limitless support.